Simplifying the *Centrolene buckleyi* complex (Amphibia: Anura: Centrolenidae): a taxonomic review and description of two new species (#90745)

First submission

Guidance from your Editor

Please submit by **29 Oct 2023** for the benefit of the authors (and your token reward) .

Structure and Criteria
Please read the 'Structure and Criteria' page for general guidance.

Custom checks
Make sure you include the custom checks shown below, in your review.

Author notes
Have you read the author notes on the guidance page?

Raw data check
Review the raw data.

Image check
Check that figures and images have not been inappropriately manipulated.

If this article is published your review will be made public. You can choose whether to sign your review. If uploading a PDF please remove any identifiable information (if you want to remain anonymous).

Files

Download and review all files from the materials page.

24 Figure file(s)
11 Table file(s)

Custom checks

DNA data checks

- Have you checked the authors data deposition statement?
- Can you access the deposited data?
- Has the data been deposited correctly?
- Is the deposition information noted in the manuscript?

Field study

- Have you checked the authors field study permits?
- Are the field study permits appropriate?

New species checks

- Have you checked our new species policies?
- Do you agree that it is a new species?
- Is it correctly described e.g. meets ICZN standard?

For assistance email peer.review@peerj.com

Structure and Criteria

2

Structure your review

The review form is divided into 5 sections. Please consider these when composing your review:

1. **BASIC REPORTING**
2. **EXPERIMENTAL DESIGN**
3. **VALIDITY OF THE FINDINGS**
4. General comments
5. Confidential notes to the editor

You can also annotate this PDF and upload it as part of your review

When ready submit online.

Editorial Criteria

Use these criteria points to structure your review. The full detailed editorial criteria is on your guidance page.

BASIC REPORTING

- Clear, unambiguous, professional English language used throughout.
- Intro & background to show context. Literature well referenced & relevant.
- Structure conforms to PeerJ standards, discipline norm, or improved for clarity.
- Figures are relevant, high quality, well labelled & described.
- Raw data supplied (see PeerJ policy).

EXPERIMENTAL DESIGN

- Original primary research within Scope of the journal.
- Research question well defined, relevant & meaningful. It is stated how the research fills an identified knowledge gap.
- Rigorous investigation performed to a high technical & ethical standard.
- Methods described with sufficient detail & information to replicate.

VALIDITY OF THE FINDINGS

- Impact and novelty not assessed. *Meaningful* replication encouraged where rationale & benefit to literature is clearly stated.
- All underlying data have been provided; they are robust, statistically sound, & controlled.
- Conclusions are well stated, linked to original research question & limited to supporting results.

Standout reviewing tips

The best reviewers use these techniques

Tip	*Example*
Support criticisms with evidence from the text or from other sources	*Smith et al (J of Methodology, 2005, V3, pp 123) have shown that the analysis you use in Lines 241-250 is not the most appropriate for this situation. Please explain why you used this method.*
Give specific suggestions on how to improve the manuscript	*Your introduction needs more detail. I suggest that you improve the description at lines 57- 86 to provide more justification for your study (specifically, you should expand upon the knowledge gap being filled).*
Comment on language and grammar issues	*The English language should be improved to ensure that an international audience can clearly understand your text. Some examples where the language could be improved include lines 23, 77, 121, 128 – the current phrasing makes comprehension difficult. I suggest you have a colleague who is proficient in English and familiar with the subject matter review your manuscript, or contact a professional editing service.*
Organize by importance of the issues, and number your points	*1. Your most important issue* *2. The next most important item* *3. …* *4. The least important points*
Please provide constructive criticism, and avoid personal opinions	*I thank you for providing the raw data, however your supplemental files need more descriptive metadata identifiers to be useful to future readers. Although your results are compelling, the data analysis should be improved in the following ways: AA, BB, CC*
Comment on strengths (as well as weaknesses) of the manuscript	*I commend the authors for their extensive data set, compiled over many years of detailed fieldwork. In addition, the manuscript is clearly written in professional, unambiguous language. If there is a weakness, it is in the statistical analysis (as I have noted above) which should be improved upon before Acceptance.*

Simplifying the *Centrolene buckleyi* complex (Amphibia: Anura: Centrolenidae): a taxonomic review and description of two new species

Daniela Franco-Mena [Corresp., 1], **Ignacio De la Riva** [2], **Mateo A. Vega-Yánez** [1, 3], **Luis Amador** [4, 5], **Paul Székely** [6, 7, 8], **Diego Batallas** [1, 9], **Diego F. Cisneros-Heredia** [3, 10], **Juan P. Reyes-Puig** [3, 11], **Khristian Venegas-Valencia** [12], **Sandra P. Galeano** [12], **Juan M. Guayasamin** [Corresp. 1]

[1] Laboratorio de Biología Evolutiva, Instituto BIOSFERA, Colegio de Ciencias Biológicas y Ambientales COCIBA, Universidad San Francisco de Quito, Quito, Campus Cumbaya, Pichincha, Ecuador

[2] Department of Biodiversity and Evolutionary Biology, Museo Nacional de Ciencias Naturales-CSIC, Madrid 28006, Spain

[3] Unidad de Investigación, Instituto Nacional de Biodiversidad (INABIO), Quito, Ecuador

[4] Museum of Southwestern Biology and Department of Biology, University of New Mexico, Albuquerque, NM, 87131, United States

[5] Instituto BIOSFERA, Universidad San Francisco de Quito, Quito, Pichincha, Ecuador

[6] Museo de Zoología, Universidad Técnica Particular de Loja, San Cayetano Alto, calle París s/n, 110107, Loja, Ecuador

[7] Laboratorio de Ecología Tropical y Servicios Ecosistémicos (EcoSs-Lab), Facultad de Ciencias Exactas y Naturales, Departamento de Ciencias Biológicas y Agropecuarias , San Cayetano Alto s/n, 110107, Universidad Técnica Particular de Loja, Loja, Ecuador

[8] Research Center of the Department of Natural Sciences, Faculty of Natural and Agricultural Sciences, Al. Universităţii no.1, 900470, Ovidius University Constanţa, Constanța, Romania

[9] Departamento de Biodiversidad, Ecología y Evolución de la Facultad de Ciencias Biológicas, Programa de Doctorado en Biología, Ciudad Universitaria 28040, Universidad Complutense de Madrid, Madrid, Spain

[10] Laboratorio de Zoología Terrestre & Museo de Zoología, Instituto de Biodiversidad Tropical IBIOTROP, Colegio de Ciencias Biológicas y Ambientales, Universidad San Francisco de Quito USFQ, Quito, Ecuador

[11] Fundación Oscar Efrén Reyes, Departamento de Ambiente, Fundación EcoMinga, Baños, Ecuador

[12] Centro de Colecciones y Gestión de Especies, Instituto de Investigación de Recursos Biológicos Alexander von Humboldt, Villa de Leyva, Boyacá, Colombia

Corresponding Authors: Daniela Franco-Mena, Juan M. Guayasamin
Email address: daniellafrancomena@gmail.com, jmguayasamin@usfq.edu.ec

Centrolenidae is a Neotropical family of glassfrogs widely distributed in almost all bioregions of Central and South America, but concentrates its species richness along the Andes. Our knowledge about their phenotypic, genetic diversity, and evolutionary relationships, has increased at an accelerated rate during the last decades and with it, the number of described species. However, notable information gaps still persist, particularly in relation to some complexes of morphologically cryptic species. Recent studies have demonstrated that Buckley's glassfrog, *Centrolene buckleyi*, is a species complex. In this study, we assessed and redefined the species boundaries of *C. buckleyi* under an integrative approach, and formally described two new species discovered within this complex. The new taxa are supported by the following main criteria: (i) diagnosis (morphological traits, vocalizations, osteology, and genetic distances), (ii) monophyly, and (iii) biogeography. Finally, we discuss the importance of geographic barriers in promoting

speciation in the Andes and highlight the need to further evaluate the complex for the Colombian region. Two new species of glassfrogs of the genus *Centrolene* are distributed in the Andes of Ecuador. The first new species is distinguished from all other members of the genus by having a dark green dorsum with minute whitish spots, inclined snout rounded in dorsal profile, relatively medium-sized humeral spine (in adult males), and reduced webbing between fingers; it is smaller than *C. buckleyi* sensu stricto, and also differs significantly from it from morphometric characters. The second new species is differentiated from its congeners by having dorsal skin shagreen with dispersed low warts, sloping snout in profile, relatively small humeral spine (in adult males), and reduced webbing between fingers; it is smaller than *C. buckleyi* sensu stricto but larger than the first new species; this new species also exhibits significant differences with *C. buckleyi* sensu stricto. Furthermore, both new species show skull differences (e.g., shape of frontoparietal fontanelle, squamosal, occipital, and parasphenoides) with *C. buckleyi* sensu stricto. We propose to be considered as Endangered (EN), both new species, due to various factors such as loss of habitat and mining. The distribution of the *C. buckleyi* sensu lato in the Andes of Colombia and Ecuador provides insights into the evolutionary history and diversification of these closely related species. As in many other glassfrogs, speciation in *Centrolene* is mediated by the linearity of the Andes, where habitat continuity is broken by deep river valleys.

Simplifying the *Centrolene buckleyi* complex (Amphibia: Anura: Centrolenidae): A taxonomic review and description of two new species

Daniela Franco-Mena [Corresp.,1], Ignacio de la Riva[2], Mateo A. Vega-Yánez[1,3], Luis Amador[4,5], Paul Székely[6,7,8], Diego Batallas-Revelo[1,9], Diego F. Cisneros-Heredia[3,10], Juan P. Reyes-Puig[3,11], Khristian Venegas-Valencia[12], Sandra P. Galeano[12], Juan M. Guayasamin [Corresp.,1]

[1] Laboratorio de Biología Evolutiva, Instituto BIOSFERA, Colegio de Ciencias Biológicas y Ambientales COCIBA, Universidad San Francisco de Quito, Quito, Campus Cumbaya, Pichincha, Ecuador

[2] Department of Biodiversity and Evolutionary Biology, Museo Nacional de Ciencias Naturales-CSIC, C/ José Gutiérrez Abascal, Madrid 28006, Spain

[3] Unidad de Investigación, Instituto Nacional de Biodiversidad (INABIO), Quito, Ecuador.

[4] Museum of Southwestern Biology and Department of Biology, University of New Mexico, Albuquerque, NM, USA, 87131

[5] Instituto BIOSFERA, Universidad San Francisco de Quito, Quito, Pichincha, Ecuador

[6] Museo de Zoología, Universidad Técnica Particular de Loja, San Cayetano Alto, calle París s/n, 110107, Loja, Ecuador

[7] Laboratorio de Ecología Tropical y Servicios Ecosistémicos (EcoSs-Lab), Facultad de Ciencias Exactas y Naturales, Departamento de Ciencias Biológicas y Agropecuarias, Universidad Técnica Particular de Loja, San Cayetano Alto s/n, 110107, Loja, Ecuador.

[8] Research Center of the Department of Natural Sciences, Faculty of Natural and Agricultural Sciences, Ovidius University Constanţa, Al. Universităţii no.1, 900470, Constanța, Romania

[9] Departamento de Biodiversidad, Ecología y Evolución de la Facultad de Ciencias Biológicas, Programa de Doctorado en Biología, Universidad Complutense de Madrid. Ciudad Universitaria 28040. Madrid, España.

[10] Laboratorio de Zoología Terrestre & Museo de Zoología, Instituto de Biodiversidad Tropical IBIOTROP, Colegio de Ciencias Biológicas y Ambientales, Universidad San Francisco de Quito USFQ, Quito, Ecuador

[11] Fundación EcoMinga; Fundación Oscar Efrén Reyes, Departamento de Ambiente, Baños, Ecuador

[12] Centro de Colecciones y Gestión de Especies. Instituto de Investigación de Recursos Biológicos Alexander von Humboldt, Villa de Leyva, Boyacá, Colombia.

Corresponding Authors:
Daniela Franco-Mena, Juan M. Guayasamin

Email address:

daniellafrancomena@gmail.com , jmguayasamin@usfq.edu.ec

Abstract. Centrolenidae is a Neotropical family of glassfrogs widely distributed in almost all bioregions of Central and South America, but concentrates its species richness along the Andes. Our knowledge about their phenotypic, genetic diversity, and evolutionary relationships, has increased at an accelerated rate during the last decades and with it, the number of described species. However, notable information gaps still persist, particularly in relation to some complexes of morphologically cryptic species. Recent studies have demonstrated that Buckley's glassfrog, *Centrolene buckleyi*, is a species complex. In this study, we assessed and redefined the species boundaries of *C. buckleyi* under an integrative approach, and formally described two new species discovered within this complex. The new taxa are supported by the following main criteria: (i) diagnosis (morphological traits, vocalizations, osteology, and genetic distances), (ii) monophyly, and (iii) biogeography. Finally, we discuss the importance of geographic barriers in promoting speciation in the Andes and highlight the need to further evaluate the complex for the Colombian region. Two new species of glassfrogs of the genus *Centrolene* are distributed in the Andes of Ecuador. The first new species is distinguished from all other members of the genus by having a dark green dorsum with minute whitish spots, inclined snout rounded in dorsal profile, relatively medium-sized humeral spine (in adult males), and reduced webbing between fingers; it is smaller than *C. buckleyi* sensu stricto, and also differs significantly from it from morphometric characters. The second new species is differentiated from its congeners by having dorsal skin shagreen with dispersed low warts, sloping snout in profile, relatively small humeral spine (in adult males), and reduced webbing between fingers; it is smaller than *C. buckleyi* sensu stricto but larger than the first new species; this new species also exhibits significant differences with *C. buckleyi* sensu stricto. Furthermore, both new species show skull differences (e.g., shape of frontoparietal fontanelle, squamosal, occipital, and parasphenoides) with *C. buckleyi* sensu stricto. We propose to be considered as Endangered (EN), both new species, due to various factors such as loss of habitat and mining. The distribution of the *C. buckleyi* sensu lato in the Andes of Colombia and Ecuador provides insights into the evolutionary history and diversification of these closely related species. As in many other glassfrogs, speciation in

Centrolene is mediated by the linearity of the Andes, where habitat continuity is broken by deep river valleys.

Keywords. Andes, Anura, Glassfrogs, New species, Phylogenetic relationships, Taxonomy, Biogeography

Introduction

The formal recognition of species is at the core of the natural sciences and, also, is key for conservation efforts (Mace, 2004; Tsang, 2015). Governments and funding agencies usually allocate resources toward species that are scientifically recognized (Martín-López et al., 2009; Mahoney, 2009; Martin et al., 2018). Also, species defined as endangered benefit from legal frameworks for their persistence in the wild (IUCN, CITES, Endangered Species Act) (Noss et al., 1997; Gregory et al., 2012; Betts et al., 2020; Guayasamin et al., 2021). Under this context, formal recognition of species does not only represent a necessary first step for any study, but should also constitute a priority for biologists in order to facilitate conservation actions.

Glassfrogs and the *Centrolene buckleyi* species complex: The family Centrolenidae Taylor, 1951 contains 164 recognized species (Frost, 2023). The monophyly of the family is supported by molecular characters, morphological, and behavioral traits (Guayasamin et al., 2009; 2020). Centrolenidae is distributed throughout the Neotropics, including Central America, Andes, Amazon Basin, and Brazilian Atlantic Forest (Frost, 2023). Although most Andean glassfrogs have relatively small distributions (Guayasamin et al., 2020), the available information shows that a representative of this group, Centrolene buckleyi (Boulenger, 1882) is apparently an exception. This species has been reported to inhabit montane primary and secondary forests in high tropical Andean zones (1,900–3,300 m), as well as inter-Andean scrubland and Paramo environments of Colombia, Ecuador, and northern Peru (Duellman & Wild 1993; Guayasamin et al., 2006a; Rada & Guayasamin 2008; Guayasamin & Funk 2009; Amador et al., 2018; Guayasamin et al., 2020).

Species with large distributions are good subjects to test for cryptic diversity, especially in topographically and ecologically complex areas such as the Andes. Recent studies have documented morphological, acoustic, and molecular differences within what is currently recognized as the *C. buckleyi* species complex (Guayasamin et al., 2006a; Guayasamin et al., 2008; Amador et al., 2018; Guayasamin et al., 2020). Perhaps the most surprising result is that

the *C. buckleyi* complex is not even monophyletic (Guayasamin et al., 2006b; Amador et al., 2018; Guayasamin et al., 2020) and that vocalizations are strikingly different among some of the populations (Bolívar-G et al., 1999; Guayasamin et al., 2006b; Guayasamin et al., 2020). Although these differences within the *C. buckleyi* complex have been known for a long time, no comprehensive taxonomic analysis has been performed so far. Herein, under an integrative taxonomy umbrella, we present a revision of the *C. buckleyi* complex through a broad population and geographic sampling, redefine *C. buckleyi*, and formally describe two lineages new to science, until now hidden within the complex.

Materials & Methods

Ethics statement. This research was conducted under permits MAE-DNB-CM-2018-0105, MAE-DNB-CM-2015-0016, and MAATE-cmarg-2022-0575, issued by the Ministerio del Ambiente, Agua y Transición Ecológica (MAATE), Ecuador. The study was carried out in accordance with the guidelines for the use of live amphibians and reptiles in field research, compiled by the American Society of Ichthyologists and Herpetologists (Beaupre et al., 2004).

Artificial Intelligence was not used to generate any part of this study. All results are the product of natural intelligence.

Taxonomy and species concept. Glassfrog generic and family names follow the taxonomy proposed by Guayasamin et al. (2009). For recognizing species, we adhere to the conceptual framework developed by Simpson (1961), Wiley (1978), and De Queiroz (2005, 2007). Under this concept, the only necessary property for an entity to be recognized as a species is that it corresponds to a temporal segment of a metapopulation lineage evolving separately from other lineages (De Queiroz 2005, 2007). Independent evolution generates traits that can be used to diagnose the species, such as morphology, monophyly, and vocalizations, among others (De Queiroz 2007; Padial et al., 2010).

Morphological data. Morphological characterization follows Cisneros-Heredia & McDiarmid (2007) and Guayasamin et al. (2009). Webbing nomenclature follows Savage & Heyer (1967), as modified by Guayasamin et al. (2006a). We examined alcohol-preserved specimens from the collection at Centro Jambatu (CJ), Herpetología, Museo de historia natural Gustavo Orcés V., Escuela Politécnica Nacional (MEPN-H), Instituto Nacional de Biodiversidad (INABIO), Museo de Zoología, Universidad Tecnológica Indoamérica (MZUTI), Museo de Zoología, Universidad

Técnica Particular de Loja (MUTPL), Museo de Zoología, Universidad San Francisco de Quito (ZSFQ), in Ecuador; and Colección de Anfibios, Instituto de Investigación de Recursos Biológicos Alexander von Humboldt (IAvH-Am), in Colombia; all examined specimens are listed in Appendix 1. Morphological measurements were taken with Mitutoyo® digital caliper to the nearest 0.1 mm, as described by Guayasamin & Bonaccorso (2004) and Guayasamin et al. (2022), and are as follows: (1) snout–vent length (SVL) = distance from tip of snout to posterior margin of vent; (2) femur length (FEL) = distance from cloaca to knee; (3) tibia length (TL) = length of flexed leg from knee to heel; (4) foot length (FL) = distance from proximal margin of outer metatarsal tubercle; (5) head length (HL) = distance from tip of snout to posterior angle of jaw articulation; (6) head width (HW) = width of head measured at level of jaw articulation; (7) interorbital distance (IOD) = shortest distance between upper eyelids, a measurement that equals to the subjacent frontoparietal bones; (8) eye diameter (ED) = distance between anterior and posterior borders of the eye; (9) tympanum diameter (TD) = distance between anterior and posterior borders of tympanic annulus; (10) arm length (AL) = length of flexed forearm from elbow to proximal edge of Finger I at the level of articulation with arm; (11) hand length (HAL) = distance from proximal edge of Finger I to tip of Finger III; (12) Finger I (FI) = distance from outer margin of hand to tip of Finger I; (13) Finger II (FII) = distance from outer margin of hand to tip of Finger II; (14) width of Finger III (FIII) = maximum width of Finger III measured at distal end; (15) width of Toe III (TIII) = maximum width of Toe III measured at distal end; (16) Internarial distance (IND) = distance between inner edges of the nostrils; and (17) Eye–nostril distance (END) = distance between the anterior edge of the eye and posterior edge of the nostril. With the measurements obtained from male data (female data were scarce) of *Centrolene buckleyi* species complex, we performed a multivariate analysis including Principal Component (PCA), and we performed the Shapiro-Wilk normality test. For data with normal distribution, we used the univariate t-test and for data with non-normal distribution, we used the Wilcoxon-Mann Whitney test (Yánez-Muñoz et al. 2021). All analyses were performed in R Core Team 2022.07.2 (2021).

Throughout the text, the following abbreviations are used for collectors, photo credits and associated information: Diego Batallas-Revelo (DBR), Jaime Culebras (JC), Daniela Franco-Mena (DFM), Juan Manuel Guayasamin (JMG), Amanda Quezada-Riera (AQR), Paul Székely (PS), Mateo Vega-Yánez (MVY), Juan Pablo Reyes-Puig (JPRP), and Jose Vieira (JV).

Phylogenetic relationships. We generated 44 mitochondrial sequences of markers 12S and 16S, from 25 individuals belonging to six species of *Centrolene*. All new sequences were deposited in GenBank (Table 1). For DNA extractions we follow Peñafiel et al. (2019) while amplification and sequencing protocols follow Guayasamin et al. (2008). The newly obtained sequences were compared with those available from Amador et al. (2018) and all other glassfrog genera, downloaded from GenBank (https://www.ncbi.nlm.nih.gov/genbank/) (Appendix 1). Sequence information and GenBank codes of the outgroups are listed in Amador et al. (2018) and Guayasamin et al. (2020). Sequences were aligned using MAFFT v.7 (Multiple Alignment Program for Amino Acid or Nucleotide Sequences: http://mafft.cbrc.jp/alignment/software/), with the G-INS-i strategy (Katoh & Standley, 2013). We used Mesquite 1.12 to visualize the alignment (Maddison & Maddison, 2019). Uncorrected pairwise genetic distances among Centrolene species were calculated with MEGA 11 (Tamura et al., 2021).

Phylogeny was performed using Maximum Likelihood (ML) and Bayesian Inference (BI) methods. To obtain the best nucleotide substitution model, we used Model-Finder under the Bayesian information criterion (BIC) (Kalyaanamoorthy et al., 2017). Maximum likelihood was run in the IQ-TREE 1.5.5 (Nguyen et al., 2015). Node support was assessed via 10,000 ultra-fast bootstrap replicates, a method that shows less bias than other support estimates (Minh et al., 2013). Ultra-fast bootstrapping also leads to a straightforward interpretation of the support values (e.g., support of ≥ 95% should be interpreted as significant; Minh et al., 2013). Bayesian inferences were performed in MrBayes 3.2.7 (Ronquist et al., 2012). We conducted four parallel runs of Markov Chain Monte Carlo (MCMC) for 10,000,000 generations, with sampling every 1,000 iterations and burning of 25%, to estimate the Bayesian tree and Bayesian Posterior Probabilities (BPP). Finally, all trees generated were visualized in iTol v5 (Letunic & Bork, 2021) and edited in Adobe Illustrator 15.0.0 (Adobe Systems Inc.).

Osteology. Osteological images of one specimen of *Centrolene buckleyi* sensu stricto (MZUTI 763) and the holotypes (MZUTI 84, ZSFQ 4418) of the two new species were obtained by using microcomputed tomography (micro-CT) at Museo Nacional de Ciencias Naturales-CSIC (Madrid, Spain). For each scan, we followed the methods described by Lansac et al. (2021). Morphological comparisons and visualization of the micro-CT images were performed with myVGL 3.0.4 (Volume Graphics, Heidelberg, Germany) and we added color to the micro-CT scan images using Adobe Photoshop. The osteology descriptions follow the terminology of

Trueb (1973), Duellman & Trueb (1986), and Guayasamin & Trueb (2007). Cartilage structures were excluded from the osteological descriptions because the settings selected for the micro-CT images do not show the cartilage.

Bioacoustics. Three calls were recorded: (1) *Centrolene elisae* sp. nov. (ZSFQ 5369), from Yanayacu Biological Station (0.6150°S, 77.88189°W; 2,118 m), Napo province, Ecuador, recorded by Daniela Franco-Mena on 11 March 2023, at 23:19 h; (2) *Centrolene marcoreyesi* sp. nov. (MUTPL 271, FUTPL-A 149), from Abra de Zamora (3. 9689°S, 79.1110°W; 2,190 m), Zamora Chinchipe province, Ecuador, recorded by Paul Székely on 29 April 2017; and (3) *Centrolene buckleyi* sensu stricto (MZUTI 0763) from Oyacachi (0.2189°S, 78.044°W; 3,012 m), Napo province, Ecuador, recorded by Italo Tapia on 17 May 2012, at 01:02 h. Call recordings are stored at the Laboratorio de Biología Evolutiva at Universidad San Francisco de Quito (LBE-USFQ) and Fonoteca UTPL (FUTPL). The recordings were obtained with an Olympus LS-11 digital recorder, at a sampling frequency of 44 kHz and 16-bits resolution, and saved in uncompressed WAV format.

The calls were analyzed in Raven 1.6 (K. Lisa Yang Center for Conservation Bioacoustics at the Cornell Lab of Ornithology, 2023), having as settings a Hann window at 99% overlap and 256 samples of DFT size. The parameters analyzed were: Dominant frequency (DF) of the whole call and of each of the elements emitted in the DF; Frequency difference (dfrq), subtracting the dominant frequency of the beginning minus that of the end of the call; Modulation frequency (MF); Number of visible harmonics (NH); Harmonic frequencies, series of values corresponding to multiples of the fundamental frequency (2f0–5f0); Call duration (CD); Inter-call interval (IC); Call rate (CR); Notes per call (NC); Note duration (ND); Duration of first note (N1D); Duration of second note (N2D); Inter-note interval (IN); Note rate (NR); Pulses per note (PN); Pulses/N1 (PN1); Pulses/N2 (PN2); Pulse duration (PD); Inter-pulse interval (IP); and Pulse rate (PR). Definitions, terminology and measurements of the acoustic parameters follow Köhler et al. (2017) and Sueur (2018). The abbreviations used in the units of measurement correspond to: Kilohertz (kHz); milliseconds (ms); seconds (s); per minute (/min); per second (/s); number of specimens/edges/notes/pulses (n). Call type and structure were classified according to Duarte-Marín et al. (2022) and Emmrich et al. (2020). The figures were processed in the R (R Core Team 2022), using Seewave2.2.0 (Sueur et al., 2008) and tune R 1.4.1 (Ligges et al., 2018).

Measures of central tendency (means) and dispersion (maximum, minimum, and standard deviation) were calculated for all the acoustic parameter values analyzed.

Biogeographic history. To reconstruct the ancestral distribution of each node of the 12S–16S calibrated phylogenetic hypothesis of our *Centrolene* data set, we used the R package BioGeoBEARS (BioGeography with Bayesian (and likelihood) Evolutionary Analysis in R Scripts) (Matzke, 2013). Specifically, we ran our biogeographic analysis considering three different models (DEC, DIVALIKE, and BAYAREALIKE) to obtain a probability distribution of the most probable ancestral areas and the diversification of species. For this analysis, we recorded the exact geographical distribution of *Centrolene* species included in the phylogenetic analysis. We coded species distribution according to the Andean Mountain Range sections, northern Andes (Venezuela, Colombia and Ecuador), and central Andes (Peru). We used the Akaike's information criterion corrected (AICc) to select the best fit model. For the analysis, we used a maximum clade credibility (MCC) tree obtained with BEAST v.2.6.6 (Bouckaert et al., 2019) using the temporal calibration scheme outlined by Castroviejo-Fisher et al. (2014). We used a relaxed clock log normal prior linked to both partitions and a calibrated Yule model of speciation as a tree prior. The analysis was run for 7 x 107 generations and were sampled every 5,000 generations. The trace log file was checked for convergence and for ESS values above 200 using Tracer v.1.7.2 (Rambaut et al., 2018). The MCC tree was estimated with Treeanotator (program distributed as part of BEAST) with the sampled trees after discarding the first 20% as burn-in. We used FigTree 1.4.4 (Rambaut, 2014) to visualize the summarized MCC tree.

Results

The Centrolene buckleyi species complex from a phylogenetic perspective. Both methods of phylogenetic reconstruction (ML and BI) inferred similar evolutionary relationships, in particular regarding the lineages that, based on overall morphological similarity, are part of *C. buckleyi* species complex (Fig. 1). The optimal nucleotide substitution model for our dataset according to Model-Finder (lnL = -11309.1953; BIC = 24016.8084) was TIM2+F+I+G4. In general, the Bayesian tree showed higher nodal support and a lower number of collapsed nodes than the ML tree. Since no relevant incongruences were found, we present only the Maximum Likelihood tree, including support values for each node obtained from both ultrafast bootstraps of ML and Bayesian posterior probability (i.e., UFB/BPP) (Fig. 1). The inferred phylogeny, confirms the

placement of all sampled populations in the genus *Centrolene* Jiménez de la Espada, 1872, as defined by Guayasamin et al. (2009).

Our inferred relationships among *Centrolene* species are similar to those reported in previous studies (Guayasamin et al., 2008, 2020; Twomey, Delia & Castroviejo-Fisher, 2014; Amador et al., 2018; Székely et al., 2023b; Cisneros-Heredia et al., 2023), but some novel relationships are revealed because of our increased taxon sampling (Fig. 1). Our phylogenetic analysis shows that *Centrolene buckleyi* represents a species complex as suggested in previous studies (Guayasamin et al., 2006, 2020; Amador et al., 2018), with at least four undescribed species, two of which we formally describe below. Also, we redefined *C. buckleyi* sensu stricto.

Systematics

***Centrolene buckleyi* (Boulenger, 1882)** *sensu stricto*

Hylella buckleyi Boulenger, 1882
Centrolenella buckleyi — Noble, 1920
Hyla purpurea — Nieden, 1923
Cochranella buckleyi — Taylor, 1951
Centrolenella buckleyi — Goin, 1964
Centrolenella buckleyi buckleyi — Rivero, 1968
Centrolenella johnelsi — Cochran and Goin, 1970
Centrolene buckleyi — Ruiz-Carranza and Lynch, 1991
Centrolenella buckleyi — Ayarzagüena, 1992

English common name. Buckley's Glassfrog

Spanish common name. Rana de Cristal de Buckley

Amended definition. *Centrolene buckleyi* is distinguished by: (1) SVL in adult males 26.1─32.5 mm (n = 17), in females 24.2─39.8 (n = 13); (2) in life, dorsum light to dark green with our without scattered darker green patches; upper lip white, usually with a white line extending backwards along the flanks of body; green bones; (3) iris gray-white with thin black reticulation and a horizontal brown stripe; (4) humeral spines, vocal slits and sacs present in adult males; (5)

snout round in dorsal aspect, sloping in lateral profile; (6) webbing absent between Fingers I–III; reduced between outer fingers: III ($2^{1/4}$–3^{-})—(2^{+}–$2^{1/2}$) IV; (7) webbing formula on foot: I ($1^{1/2}$–2^{-})—(2–$2^{1/4}$) II (1^{-}–1^{+})—(2^{+}–$2^{1/2}$) III (1^{+}–$1^{2/3}$)—($2^{1/3}$–3) IV ($2^{2/3}$–3)—($1^{2/3}$–2^{-}) V; (8) ulnar fold low and white, ventrolateral margin of arm white; inner tarsal fold evident; outer tarsal fold absent, external ventrolateral margin of tarsus white; (9) prepollex concealed; in males, nuptial pad Type I; (10) Toe II slightly longer than Toe I.

Diagnosis (modified from Guayasamin et al. 2020). In life, *Centrolene buckleyi* sensu stricto is differentiated from its congeners by having dorsal surfaces light green to dark green (some individuals present scattered olive-green patches), white upper lip, inclined snout in profile, large humeral spine (in adult males), and reduced webbing between fingers (Figs. 2, 3). *Centrolene buckleyi* sensu stricto is larger than *C. elisae* sp. nov. and *C. marcoreyesi* sp. nov. (Fig. 4). Differences between *C. buckleyi* sensu stricto and morphologically similar taxa are summarized in Table 2-3-4, thus, details on the measurements differences are shown in Table 4. Main skull characters to discriminate species are frontoparietal fontanelle, with *C. buckleyi* sensu stricto a posterior border with three slits aligned posteriorly, occipitals projected with condyles reaching the level of exoccipitals; cultriform process of parasphenoid with a blunt anterior border reaching level of neopalatine (Table 6). Relevant genetic distances are shown in Fig. 5 and Table S1. The species that most closely resemble *Centrolene buckleyi* sensu stricto in terms of morphology are *C. altitudinale*, *C. elisae* sp. nov., *C. marcoreyesi* sp. nov. and *C. venezuelense*, traits to differentiate among these species are summarized in Table 2.

Color in life (MZUTI 763, ZSFQ 4420, DHMECN 13828). Dorsal surfaces bright to dark green, sharply demarcated laterally from lower white flanks; some individuals have scattered olive-green spots on the dorsum; throat and most of the venter pale green; parietal peritoneum yellowish white; edge of upper lip white; ventrolateral borders of arms and tarsus white; small, white warts posterior to cloacal opening; bones green; gray–white iris with thin black reticulation and a horizontal brown stripe (Fig. 2).

Color in ethanol. Dorsal surfaces light to dark lavender, lower flanks white, ventral surfaces cream; ventrolateral borders of arms and tarsus white; upper lip white; parietal peritoneum white; all visceral peritoneum clear except for pericardium white.

Variation. Morphometric variation is shown in Table 5. Females larger than males; adult males with vocal slits, exhibit dorsal skin with conspicuous spicules that are absent in females. Color variation is described in the "color in life" section.

Osteology (Figs. 6, 7). The following description is based on an adult male (MZUTI 0763). We present a detailed description of all skeletal elements.

Skull (Fig. 6A-B-C-D). Skull not ornamented or slightly ornamented on occipital, without exostosis or dermal modifications or co-ossification with skin. Maxillary arch complete; alary processes of premaxillae small and with pointed ends; maxilla broadest anteriorly, tapering posteriorly; *pars facialis* broad. Quadratojugal ossified and broad, overlapping anteriorly with maxilla and posteriorly articulated with ventral ramus of squamosal. Two ossified nasals, relatively small, separated from each other, posterolaterally articulated to neopalatine; nasals not articulating with sphenethmoid. Sphenethmoid forming the anterior part of braincase; anterior margin of bony sphenethmoid at level of plane antorbitale, and posterior margin at about anterior third of orbit. In dorsal view, sphenethmoid articulates posterolaterally with paired frontoparietals. Frontoparietals independent, not ornamented, arranged in parallel, posteriorly fused to the occipital. Frontoparietal fontanelle delimited by sphenethmoid anteriorly, frontoparietals laterally, and prootic posteriorly, posterior border present three slits aligned. Occipital fontanelles absent.

Prootics and exoccipitals co-ossified; crista parotica completely ossified. Neopalatine present and in contact with sphenethmoid. Maxillary and premaxillary teeth short and monocuspid. Suspensorium composed of paired pterygoids and squamosals; zygomatic ramus of squamosal short, thick and rounded anterior border, otic ramus slightly posterosuperior oriented. Each pterygoid consists of anterior, medial, and posterior rami. Anterior ramus articulating with posterior end of maxilla; medial ramus coverings the prootic pseudobasal process; posterior ramus oriented towards ventral ramus of the squamosal. Lower jaw composed of paired mentomeckelian bones and dentary. Moderate-sized vomers broadly separated from one another medially, each composed of arcuate bone bordering anterior and medial margins of choana. Prechoanal and postchonal rami thin and unexpanded distally. Slender dentigerous processes extending ventromedially from the union of the pre- and postchoanal processes. Neopalatines unornamented, arcuate, and articulating with lateral margin of sphenethmoid just anterior to the

orbitonasal foramen. Neopalatines narrowly separated from maxilla. Parasphenoid large and broad, anterior end blunt, overlapping sphenethmoid, nearly reaching level of neopalatines; alar processes of parasphenoid relatively short and partially fused to occipital; short posteromedial process present, but distinctly separated from margin of foramen magnum. Columella present, thin. Pterygoid with three branches: anterior ramus curved, oriented anterolaterally toward the maxilla, with which it articulates at approximately midlength of orbit; medial and posterior rami of pterygoid about equal in length; medial ramus in contact with edge of ossified lateral margin of prootic.

Forelimb and hind limb (Fig. 7A-B). The forelimb is composed of humeral bone, radioulna, carpal elements, prepolex, and four digits (I–IV). The hind limb consists of a femur, tibiale, fibula, fibulare (= astragalus), metacarpals, metatarsals, and five digits (I–V). The phalangeal formulae for the hand and foot are standard 2-2-2-3 and 2-2-3-4-3, respectively. Order of finger length: I < II < IV < III, and in toes: I < II < V < III < IV. Metacarpals long and slender; distal end rounded; inner edge of Finger III with dilated medial metacarpal process (Hayes & Starrett 1980). Prepollex well developed, broad and curved, with a rounded distal end. Intercalary element between the last phalanges of all digits; terminal phalanx with T- or Y-shaped end. Carpus is composed of Carpal 1, Element Y, and a large postaxial element assumed to represent a fusion of Carpals 2–4, radiale, and ulnar. Element Y seems to be partially fused with prepollex; prepollex composed of one small bone. Tarsus is composed of three tarsal elements, presumably Tarsal 1 + 2 + 3. Humeral bone with well-developed humeral spine (in males), equivalent to 40–44% of humerus length, oriented at an angle of 35–45° in relation to axis of humeral bone.

Pectoral girdle (Fig. 7C). The pectoral girdle is composed of scapula, suprascapula, zonal area (coracoid, cleithrum, and clavicle) and posteromedial process. Suprascapula completely mineralized, with cleithrum apparent as a slender bone along its leading edge; cleithrum ossified. Clavicles oriented anteromedially, with the medial tips distinctly separated from one another; anterolateral end of the clavicle articulating with scapula.

Vertebral column and pelvic girdle (Fig. 7D). Vertebral column with eight presacral vertebrae; presacrals I and II notably shorter than posterior presacral. All presacrals are non-imbricate except the first, which is partially imbricate. Neural arch of Presacral II bearing a rounded, medial process that articulates with neural arch of Presacral I. Vertebral profile in decreasing

order of overall width of bony parts sacrum > III > IV > II > VI ≅ VII >VIII > V > I. Orientations of transverse processes of Presacrals II, VII, and VIII directed anterolaterally, and those of Presacrals III, IV, V, and VI with clear posterolateral orientation. Sacral diapophyses moderately dilated laterally; leading edge and posterior margin of diapophyses slightly concave. Urostyle long and slender, with bicondylar articulation with the sacrum, and bearing a low dorsal crest throughout its anterior half. Length of urostyle less than combined length of presacral vertebrae. Pelvic girdle composed of ischium, ilium, and pubis. Ilial shafts cylindrical, lacking dorsal crest. Ilia tightly joined with ischia and pubes. Pubis ossified.

Distribution. In Ecuador (Fig. 8), *Centrolene buckleyi* sensu stricto is distributed along north to the central Cordillera Oriental and Cordillera Occidental of the Andes and inhabits Western Montane Forest, Andean Shrub, Páramo, Eastern Montane Forest ecoregions, and pasture at elevations between 2,677–3,416 m (Guayasamin et al., 2020, this study). The individuals reported from Guarumales by Guayasamin et al. (2020) correspond to *C. marcoreyesi* sp. nov. (described below).

Call. Three descriptions of the advertisement call of *Centrolene buckleyi* are available in the literature (Bolívar et al., 1999, Guayasamin et al., 2006a, Guayasamin et al., 2020). Calls recorded of *C. buckleyi sensu stricto* (MZUTI 0763) from Oyacachi consists of the emission of pulsed "Tri" type sounds (sensu Duarte-Marín et al., 2022). The notes as such represent the entire duration of the call since they are emitted alone, and then the average call has a duration of 239–289 (265.13 ± 17.73) ms. Each note is made up of 16–20 (18.4 ± 1.6) pulses, which have an average duration of 5–17 (8.5 ± 1.9) ms. The calls present a modulated frequency ranging from 0.7–2.8 (1.9 ± 0.6) kHz, with an average dominant frequency of 2.8–3.3 (3.1 ± 0.1) kHz; generating between 1–3 harmonics (Table 7, Fig. 9C).

***Centrolene elisae* sp. nov.** (Daniela Franco-Mena, Diego Batallas-Revelo, Mateo A. Vega-Yánez, Juan Pablo Reyes-Puig, Juan M. Guayasamin)

LSID: E9E154BD-3D98-471B-8A41-7F8870CA1572

Centrolene buckleyi—Guayasamin et al. (2006)

Centrolene buckleyi [Ca2]—Amador et al. (2018)

English common name. Elisa's Glassfrog

Spanish common name. Rana de Cristal de Elisa

Holotype. MZUTI 84 (Fig. 10), adult male, from Las Caucheras (0.6133°S, 77.8974°W; 2,187–2,191 m), Napo province, Ecuador, collected by Gisela Bragado and Henry Grifo on 26 August, 2011.

Paratypes. (1 female, 5 males). MZUTI 0083 and MZUTI 0085, adult males, same data as holotype. ZSFQ 4228 (Fig. 11) adult male, from Chamanapamba Reserve (1.4237°S, 78.3932°W; 2,586 m), Tungurahua province, Ecuador, collected by Daniela Franco-Mena, Tasman Rosenfeld, David Brito-Zapata, and Tito Recalde on 23 June, 2021. DHMECN 4800, adult male, from Río Pucayacu, eastern flank of Tungurahua volcano (1.436245°S, 78.409335°W; 2,400msnm), Tungurahua province, Ecuador, Collected by JPRP and Nelson Palacios on 28 April, 2007. ZSFQ 5367 an adult female, ZSFQ 5368, and ZSFQ 5369 adult males (Fig. 11), from Yanayacu Biological Reserve (0.61424°S, 77.8821°W; 2,118 m), Napo province, Ecuador collected by Daniela Franco-Mena, Jose Simbaña and Mateo A. Vega-Yánez on 14 April, 2023.

Generic placement. The new species is placed in the genus *Centrolene* Jiménez de la Espada, 1872, based on molecular phylogenetics (Fig. 1) and morphological data (see below). All species in *Centrolene* (*sensu* Guayasamin et al., 2009) share the following traits: (1) humeral spines present in adult males (except *Centrolene daidalea* Ruiz-Carranza & Lynch (1991) and *C. savagei* Ruiz-Carranza & Lynch (1991)); (2) tri-, tetra-, or pentalobed liver, covered by a transparent hepatic peritoneum; (3) ventral parietal peritoneum translucent posteriorly and white anteriorly; (4) bones varying from green to pale gray in life; and (5) nuptial pads conspicuous in adult males. *Centrolene elisae* presents all the aforementioned traits and its placement within *Centrolene* is unambiguous. Phylogenetic analyses of mitochondrial genes (16S and 12S) also place *C. elisae* in the genus *Centrolene* (Fig. 1).

Definition. Within *Centrolene*, *Centrolene elisae* is distinguished by: (1) SVL in adult males 22.9–25.3 mm (n = 6), in an adult female 27.2 (n = 1); (2) in life, dorsum green, usually with minute whitish spots; anterior half of venter whitish, posterior half translucent; (3) iris gray-white with thin black-brown reticulation and a horizontal brown stripe; (4) humeral spines and vocal slits present in adult males; (5) snout rounded in dorsal profile, inclined in lateral profile; (6) webbing absent between fingers I and II, webbing basal between II and III, outer fingers III

($2^{1/2}$–$2^{2/3}$) – ($2^{1/2}$–2^{+}) IV; (7) webbing on foot: I ($1^{1/2}$–2^{-}) – (2^{+}–$2^{1/3}$) II (1^{+}–$1^{1/3}$) – (2^{+}–$2^{2/3}$) III (1–$1^{1/2}$) – ($2^{1/3}$–$2^{2/3}$) IV ($2^{2/3}$–3^{-}) – ($1^{1/2}$–2)V; (8) ulnar fold low; inner tarsal fold short; outer tarsal fold low; (9) prepollex concealed; nuptial excrescences present, Type-I; (10) Toe I shorter than Toe II.

Diagnosis. *Centrolene elisae* is differentiated from its congeners by having a dark green dorsum with minute whitish spots, white upper lip, inclined snout, rounded in dorsal profile, relatively medium-sized humeral spine (in adult males), and reduced webbing between fingers (Figs. 3, 12). Skull diagnostic characters are expressed in shape of frontoparietal fontanelle, exhibit a regular rounded posterior border; thin occipital condyles not projected that don't reach level of exoccipital, squamosal present a long and sub acuminated zygomatic ramus, cultriformis procces of parasphenoides with sudacuminated anterior border dont reaching level of neopalatines (Table 6). Differences between the new species and morphologically similar taxa are summarized in Table 2-3-4. *Centrolene elisae* is a smaller species in comparison with *C. buckleyi* sensu stricto and *C. marcoreyesi* sp. nov (Fig. 4), also the new species exhibits significant differences with *C. buckleyi* sensu stricto in the following morphometric characters (Table 3-4): AL, ED, END, FEL, FI, FII, FL, HAL HL, HW, IND, IOD, SVL, and TD. On the other hand, *C. elisae* is significantly different from *C. marcoreyesi* in END, FEL, FI, FL, HW, IND, IOD, SVL, and TL. Details on the morphological differences are shown in Table 5 and Fig 4. Genetic distances are available in Fig. 5, Table S1. The species that most closely resemble *Centrolene elisae* in terms of morphology are *C. buckleyi*, *C. marcoreyesi* sp. nov. and *C. venezuelense*, traits to differentiate among these species are summarized in Table 2.

Description of the holotype. Adult male, MZUTI 0084 (Fig. 10); moderate size (SVL = 24,5 mm). Snout rounded in dorsal profile, sloping in lateral profile; upper lip white, loreal region slightly concave; internarial area barely depressed. Eye small (ED 10% of SVL), directed anterolaterally. Tympanic annulus indistinct in its upper portion; tympanic membrane differentiated from skin around the tympanum. Dentigerous processes of vomers lacking teeth; tongue ovoid; vocal slits extending posterolaterally base of tongue to angle of jaws.

Medium-sized humeral spine present, curved. Webbing absent between fingers I and II, webbing basal between II and III, outer fingers III $2^{2/3}$ – 2^{+} IV; disc on third finger larger than those on toes, and shorter than eye diameter, finger discs truncate; subarticular tubercles rounded, and flat,

abundant supernumerary tubercles present over a granular palm; palmar tubercle large, elliptical; thenar tubercle indistinct. Legs slender; heels of adpressed limbs perpendicular to body slightly overlap. Length of tibia 59,4% of SVL; inner metatarsal tubercle large, flat, elliptical; outer metatarsal tubercle indistinct. Subarticular tubercles rounded and flat; supernumerary tubercles present over the granular palm. Webbing on foot: I $1^{1/2}$– 2^{+} II 1^{+}– $2^{-2/3}$ III $1^{+1/}$–$2^{2/3}$ IV 3^{-} – $1^{3/4}$ V; disc on Toe I slightly expanded, all other discs rounded to fairly truncate, pointed papillae on discs absent. Skin on dorsal surfaces of head, body, and lateral surface of head and flanks shagreen, covered with minute spinules and spots; throat smooth; venter and lower flanks areolate; cloacal opening directed posteriorly at the upper level of thighs; subcloacal area granular.

Measurements (in mm) of the holotype (MZUTI 0084). SVL = 24.5, FEL = 13.2, TL = 14.6, FL = 12.0, HL = 5.6, HW = 7.0, IOD = 2.8, ED = 2.5, TD = 0.7, AL = 5.2, HAL = 8.5, FI = 3.9, FII = 5.4, FII = 1.5, TIII = 1.4, IND = 1.8, END = 1.5.

Measurements (in mm) of type series. Meristic variation of the type series is summarized in Table 5.

Color in life. Dorsal surfaces dark green with small to minute white spots; upper flanks sharply demarcated laterally from lower white flanks; throat and most of the venter pale green; parietal peritoneum yellowish white; whitish-yellow labial line present; ventrolateral borders of arms and tarsus white; small, white spots posterior to cloacal opening corresponding to pericloacal warts; bones green; copper–white and gray iris with thin black reticulation and a horizontal brown stripe. Digits and disks green and yellowish interdigital webbing (ZSFQ 5367, ZSFQ 5369, ZSFQ 4428; Fig. 11).

Color in ethanol. Dorsal surfaces of body lavender to grayish lavender with few to numerous minute white dots; white upper lip. Dorsal surfaces of limbs cream to light lavender, with or without minute cream spots. Pericardium white, other visceral peritoneum clear. Cloacal ornamentation and ulnar and tarsal folds with a thin layer of iridophores. Melanophores present from dorsal surfaces of fingers; toes with melanophores restricted to Toe V or, rarely, Toe IV (Fig. 3, 10).

Variation. Morphometric variation is shown in Table 5. The only known female is larger than the males. One male (ZSFQ 4428) had a slightly darker dorsal coloration, and more dorsal spicules than other individuals (Fig. 11).

Osteology. The following description of osteological features applies to the holotype (MZUTI 0084) of *Centrolene elisae* (Figs. 13, 14).

Skull. Skull (Fig. 13) not ornamented or slightly ornamented on occipital, without exostosis or dermal modifications or co-ossification with skin. Maxillary arch complete; alary processes of premaxillae small and with pointed ends; maxilla with conspicuous pars facilis on anterior end, tapering posteriorly. Quadratojugal ossified, overlapping anteriorly with maxilla and posteriorly articulated with ventral ramus of squamosal. Two ossified nasals, relatively small, broadly separated from each other, posterolaterally articulated to neopalatines; nasals nearly articulating with sphenethmoid. Sphenethmoid forming the anterior part of braincase; anterior margin of bony sphenethmoid lying at level of plane antorbitale, its posterior margin at about level of anterior third of orbit. In dorsal view, sphenethmoid articulating posterolaterally with paired frontoparietals. Frontoparietals not ornamented, arranged in parallel, posteriorly fused to the prootic + exoccipital. Posteriorly there is the frontoparietal, prootic and exoccipital are external, they do not articulate to the fontanelle. Frontopareital fontanelle with a regular rounded posterior border. Occipital fontanelles absent. Prootics and exoccipitals fused; crista parotica completely ossified. Neopalatine present ventrally overlapping sphenethmoid. Maxillary and premaxillary teeth short and monocuspid. Suspensorium composed of paired pterygoids and squamosals. Each pterygoid consisting of anterior, medial, and posterior rami. Anterior ramus articulating with posterior end of maxilla; medial ramus covering the prootic pseudobasal process; posterior ramus oriented towards ventral ramus of squamosal; zygomatic ramus of squamosal long with subacuminated anterior border, otic ramus oriented posteriorly. Moderate-sized vomers broadly separated from one another medially, each composed of arcuate bone bordering anterior and medial margins of choana. Prechoanal and postchonal rami thin and unexpanded distally. Slender dentigerous processes extending ventromedially from the union of the pre- and postchoanal processes. Neopalatines unornamented, arcuate, and articulated with the lateral margin of sphenethmoid just anterior to the orbitonasal foramen. Each neopalatine narrowly separated from maxilla. Parasphenoid large and broad, anterior end subacuminated overlapping sphenethmoid,

nearly reaching level of neopalatines; alary processes of parasphenoid relatively short; posteromedial process short, but distinctly separated from margin of foramen magnum. Columella present, thin. Pterygoid with three branches: a curved anterior ramus oriented anterolaterally toward the maxilla, with which it articulates at approximately midlength of orbit; medial and posterior rami of pterygoid about equal in length, medial ramus in contact with edge of ossified lateral margin of the prootic. Lower jaw composed of mentomeckelian bone; dorsal portion of mentomeckelian bone fused to dentary.

Forelimb and hind limb. Forelimb (Fig. 14A) composed of humeral bone, humeral spine, radioulna, carpal elements, prepollex, and four digits (I–V). Hind limb (Fig. 14B) consisting of a femur, tibiale, fibula, fibulare (= astragalus), metacarpals, metatarsals, and five digits (I–V). Phalangeal formulae for hand and foot standard—2-2-3-3 and 2-2-3-4-3. Order of fingers length: I < II < IV < III, that of toes: I < II < V < III < IV. Metacarpals long and slender; distal end rounded; inner edge of Finger III with dilated medial metacarpal process (Hayes & Starrett 1980). Intercalary element between the last phalanges of all digits; terminal phalanx with T- or Y-shaped end. Carpus is composed of Carpal 1, a large postaxial element assumed to represent a fusion of Carpals 2–4, radiale, ulnare, and Element Y. Prepollex well-developed, broad, and curved, with a pointed distal end. Tarsus composed of three elements, presumably Tarsal 1 + 2 + 3. Humeral bone with well-developed, curved, humeral spine (in males), equivalent to 40–44% of humerus length, oriented at an angle of 35–45° in relation to axis of humerus.

Pectoral girdle. Pectoral girdle (Fig. 14C) composed of scapula, suprascapula, zonal area (coracoid, cleithrum, and clavicle), and posteromedial process. Suprascapula completely mineralized, with cleithrum apparent as a slender bone along its leading edge; cleithrum ossified. Clavicles oriented anteromedially, with medial tips distinctly separated from one another; anterolateral end of clavicle articulating with scapula.

Vertebral column and pelvic girdle. Vertebral column (Fig. 14D) with eight presacral vertebrae; Presacrals I and II notably shorter than posterior presacrals. All presacrals non-imbricate except the first, which is partially imbricate. Neural arch of Presacral II bearing a rounded, medial process that articulates with neural arch of Presacral I. Transverse processes present in all vertebrae, except Presacral I. Vertebral profile in decreasing order of overall width of bony parts: sacrum > III > IV > II > VI ≅ VII ≅VIII > V > I. Orientations of transverse

processes of Presacrals III, VII, and VIII lateral to slightly posterolateral, those of Presacrals II and VIII directed anterolaterally, and those of Presacrals IV and V with clear posterolateral orientation. Sacral diapophyses moderately dilated laterally; leading edge and posterior margin of diapophyses slightly concave. Urostyle long and slender, with bicondylar articulation with the sacrum, bearing a low dorsal crest throughout its anterior half. Length of urostyle shorter than combined length of presacral vertebrae. Pelvic girdle (Fig. 14D) composed of ischium, ilium, and pubis. Ilial shafts cylindrical, lacking dorsal crest. Ilia tightly joined with ischia and pubes. Pubis ossified.

Natural history. *Centrolene elisae* is a nocturnal species. All individuals were found on the upper surfaces of leaves of vegetation along small streams (Fig. 15). At Las Caucheras six individuals were found in a paddock near a small stream and a river on the leaves of shrubs and ferns, approximately 20 to 250 cm above ground level; five individuals (MZUTI 83–85, ZSFQ 5368, 69) were calling. At Rio Pucayacu, a calling male DHMECN 4800, was found at 2 meters in bushes leafs above the stream during volcanic eruptions of Tungurahua. At Chamanapamba Reserve, one individual (ZSFQ 4228) was calling, perched on a fern leaf 230 cm above ground level, near a small stream. The streams where the species was recorded were between 1–1.50 meters wide, in primary and secondary forest. At Yanayacu Biological Station, intensive inventories for 3 years (2002–2004) resulted in only three individuals of *C. elisae*, suggesting that this species is quite rare (Guayasamin et al., 2006a), also near Yanayacu reserve, the area for cattle ranching and agriculture continues growing, threatening the surrounding forests and streams of the habitat of *C. elisae*. At Chamanapamba reserve *C. elisae* is syntopic with *Nymphargus* sp., *Hyloscirtus sethmacfarlanei*, *Pristimantis marcoreyesi*, *Pristimantis* aff. *gladiator* (Carolina Reyes-Puig and JRP pers. comm., Reyes-Puig et al. 2022a).

Eggs. At Chamanapamba reserve we found three egg clutches with embryos at Gosner Stage 22 (Fig. 16A, B). The three egg clutches were attached to the upper side of a leaf at ~170 cm above the small stream. The first clutch contained 24 embryos, and the second clutch contained 47 embryos; an adult male (ZSFQ 4428) was observed near the eggs.

Call. The advertisement call (sensu Wells 2007) consists of the emission of pulsed "Tri" type sounds (*sensu* Duarte-Marín et al., 2022). Calls are emitted every 13.7–15 s. Each call has an

average duration of 162–215 (195.3 ± 29) ms and is composed of two pulsed notes. The first note has an average duration of 82–113 (101.3 ± 16.9) ms and is formed by 7–9 (7.7 ± 1.2) pulses. The second note is shorter and has an average duration of 31–38 (35.3 ± 3.8) ms and consists of 2 pulses. The time between notes is 50–70 (59.7 ± 10) ms. The calls present a modulated frequency ranging from 3.1–3.2 kHz, with an average dominant frequency of 3.5–3.8 (3.6 ± 0.1) kHz; generating between 1–4 partial harmonics (Table 7, Fig. 9A).

Centrolene elisae differs structurally by the emission of a second note of short duration, consisting of two pulses. It should be noted that this structural pattern is also present in the announcement song of *C. condor* described by Almendáriz and Batallas (2012). *C. buckleyi* presents a longer duration in its calls (considering that the note is the equivalent of the call), pulses and intervals. Finally, the dominant frequency is higher in *C. elisae*, with a higher frequency modulation (considering only the frequency difference, discarding from this criterion the duration of the call as a modulation factor) in *C. buckleyi.* Also, the call of *C. venezuelense* (Rivero, 1968) is formed by four notes, regularly spaced, while in *C. elisae* it is formed by two notes.

Distribution. *Centrolene elisae* is endemic to the cloud forests of the eastern Cordillera of the Ecuadorian Andes (Fig. 8). The species has been documented from four localities: Las Caucheras, Yanayacu Biological Station (Napo Province), Chamanapamba Reserve, and Rio Pucayaku in Nelson Palacios Reserve at the eastern flank of Tungurahua volcano (Tungurahua Province), at elevations between 2,100–2,586 m.

Conservation status. We followed IUCN criteria to assess the current extinction risk of the species (Gärdenfors et al., 2001). Two localities of *Centrolene elisae*, are within private protected areas. Threats are related to land use change as a general pattern in the Tropical Andes (Gaglio et al. 2017). We propose *C. elisae* to be considered as Endangered (EN) B1.b(ii)c, with an estimated extent of occurrence < 5000 Km^2.

Evolutionary relationships. The gene sampling of our study indicates that, *Centrolene elisae* forms part of a clade with an unresolved polytomy with *C. venezuelense,* a potential new species from Colombia (*C.* cf. *venezuelense*; IAvH-Am-17401, 17403, 17407, 17410), and another one from northern Ecuador (*Centrolene* sp.; ZSFQ 2134) (Fig.1).

Etymology. The species epithet "*elisae*" is a noun in genitive case, with the Latin suffix "e" (ICZN 31.1.2). We are pleased to dedicate the species to Elisa Bonaccorso (Fig. 17), in recognition for her contributions to bird systematics and biogeography (Bonaccorso 2009; Bonaccorso et al., 2006; Bonaccorso et al., 2011; Sornoza-Molina et al., 2018), conservation biology (Lessman et al., 2014, 2016; Bonaccorso et al., 2021), batrachology (Bonaccorso et al., 2003; Guayasamin & Bonaccorso, 2004), and her passionate commitment to the formation of the next generation of scientists.

Remarks. *Centrolene elisae* (MZUTI 83–85) corresponds to the species cited as "*Centrolene buckleyi* [Ca2]" by Amador et al. (2018) and *C. buckleyi* in Guayasamin et al. (2006).

***Centrolene marcoreyesi* sp. nov.** (Daniela Franco-Mena, Paul Székely, Jaime Culebras, Diego Batallas-Revelo, Juan Pablo Reyes-Puig, Juan M. Guayasamin)

LSID: FC59A40D-6F9C-45BF-A6FE-280FA20BC2D1

Centrolene buckleyi [Ca1]—Amador et al. (2018)

English common name. Marco Reyes Glassfrog

Spanish common name. Rana de Cristal de Marco Reyes

Holotype. ZSFQ 4418 (Fig. 18), adult male from Estación Científica San Francisco (3.971667°S, -79.079167°W; 1,840 m), Zamora Chinchipe province, Ecuador, collected by Marco Reyes-Puig and Sebastián Valverde on 15 February, 2012.

Paratypes. (6 males). ZSFQ 4417 adult male, same data as the holotype; MUTPL 271, 272, adult males, from Abra de Zamora (3.9689°S, 79.1110°W; 2,190 m) (Fig. 19), Zamora Chinchipe province, Ecuador, collected by Paul Székely and Diana Székely on 29 April, 2017; CJ 11364, adult male, from Guarumales (3.94049°S, -78.986891°W; 2,070 m), Zamora Chinchipe province, Ecuador, collected by Jaime Culebras, Santiago Hualpa, Daniel Hualpa, and Darwin Núñez on 27 February, 2020; CJ 11564, adult male, from Guarumales (3.93491°S, -78.99956°W; 2,008 m), Zamora Chinchipe province, Ecuador, collected by Jaime Culebras and Darwin Nuñez on 22 February, 2021; CJ 12631, adult male from Guarumales (3.93825°S, -79.00525°W; 2,109 m), Zamora Chinchipe province, Ecuador, collected by Jaime Culebras, Daniel Hualpa and Santiago Hualpa on 15 April 2022.

Generic placement. The new species is placed in the genus *Centrolene* Jiménez de la Espada, 1872, based on morphological and genetic data. All species in *Centrolene* (*sensu* Guayasamin et al., 2009) share the following traits: (1) humeral spines present in adult males (except in *Centrolene daidalea* and *C. savagei*); (2) tri-, tetra-, or pentalobed liver, covered by a transparent hepatic peritoneum; (3) ventral parietal peritoneum transparent/translucent posteriorly and white anteriorly; (4) bones varying from green to pale gray in life; and (5) nuptial pads conspicuous (males). *Centrolene marcoreyesi* presents all the aforementioned traits and its placement within *Centrolene* is unambiguous. Phylogenetic analyses of mitochondrial genes (16S and 12S) also place *C. marcoreyesi* in the genus *Centrolene* (Fig. 1).

Definition. Within *Centrolene*, *Centrolene marcoreyesi* is defined by the following set of traits: (1) SVL in adult males 24.5–27.0 mm (n = 6), unknown in females; (2) in life, dorsum shagreen usually with low whitish spots; anterior two-thirds of venter whitish, posterior third translucent; (3) in life, iris white-lavender with fine brown reticulations; (4) humeral spines, vocal sac and slits present in adult males; (5) snout rounded in dorsal profile, sloping in lateral profile; (6) webbing absent between inner finger and Finger II, reduced to moderate between outer fingers: III ($2^{1/3}$–$2^{3/4}$) – ($2^{1/4}$–$2^{2/3}$) IV; (7) webbing on feet: I ($1^{1/2}$–$1^{2/3}$) – (2^{-}–2) II (1^{+}–$1^{1/4}$) – ($2^{1/4}$–2^{+}) III ($1^{1/2}$–$1^{2/3}$) – ($2^{1/3}$–$2^{1/2}$) IV (2^{+}–$2^{1/2}$) – ($1^{2/3}$–3^{-}) V; (8) inner and outer ulnar and tarsal folds conspicuous; (9) concealed prepollex; nuptial excrescences present, Type-I; (10) Toe I shorter than Toe II.

Diagnosis. *Centrolene marcoreyesi* is differentiated from its congeners by having dorsal skin shagreen with light dispersed low warts, yellowish-white upper lip, sloping snout in lateral profile, relatively small humeral spine (in adult males), and reduced webbing between fingers (Fig. 3). *Centrolene marcoreyesi* is smaller than *C. buckleyi* sensu stricto and larger than *C. elisae* (Fig. 4); also, the new species exhibits significant differences *C. buckleyi* sensu stricto in the following morphometric characters (Table 3–4): AL, ED, FII, FL, HL, IND, and SVL. Additionally, *C. marcoreyesi* is significantly different from *C. elisae* in END, FEL, FI, FL, HW, IND, IOD, SVL, and TL. Details on the morphological differences are shown in Table 5 and Fig. 4. Main diagnostic skull characters are shape of frontoparietal fontanelle, and in *C. marcoreyesi* it presents an irregular posterior border, occipital condyles are slightly projected posteriorly but don't reach level of exoccipital; squamosal present short zygomatic ramus with a claw shape

anterior border; cultriform process of parasphenoides present anterior border rounded don't reach level of neopalatines (Table 6). Genetic distances are available in Fig. 5 and Table S1. The species that most closely resemble *Centrolene marcoreyesi* in terms of morphology are *C. buckleyi* sensu stricto and *C. elisae* traits to differentiate among these species are summarized in Table 2.

Description of holotype. Adult male, ZSFQ 4418, of moderate size (SVL = 25.9 mm) (Fig. 18). Snout rounded in dorsal profile, sloping in lateral profile; upper lip white, loreal region slightly concave; internarial area barely depressed. Eye small (eye diameter = 10% of SVL), directed anterolaterally. Tympanic annulus differentiated, but obscured in its upper portion by the supratympanic fold; tympanic membrane differentiated, clearly thinner than skin found around the tympanum. Dentigerous processes of vomers lacking teeth; tongue ovoid, with notched posterior border; vocal slits extending posterolaterally from the base of the tongue to angle of jaws. Humeral spine present, relatively small, curved, and pointy at its distal end. Webbing absent between Fingers I–III, reduced between outer fingers: III $2^{2/3}$—$2^{1/2}$ IV; disc on third finger larger than those on toes, and smaller than eye diameter; finger discs truncate; subarticular tubercles rounded; abundant supernumerary tubercles on palm; palmar tubercle large, elliptical; thenar tubercle indistinct. Legs slender; heels overlapping when adpressed perpendicularly to the body. Length of tibia 59.8 % of SVL; inner metatarsal tubercle large, flat, elliptical; outer metatarsal tubercle indistinct. Subarticular tubercles rounded and flat; numerous supernumerary tubercles on granular palms. Webbing on feet: I $1^{2/3}$ – 2^{+} II $1^{1/4}$ – $2^{1/4}$ III ($1^{1/2}$–$1^{2/3}$) – ($2^{1/3}$–$2^{1/2}$) IV (2^{+}–$2^{1/2}$) – ($1^{2/3}$–3^{-}) V; all disc toes slightly expanded; discs lacking pointed projections (papillae). Inner and outer ulnar and tarsal folds conspicuous.

Measurements (in mm) of the holotype (ZSFQ 4418). SVL = 25.9, FEL = 13.7, TL = 15.5, FL = 13.8, HL = 6.2, HW = 7.6, IOD = 2.9, ED = 2.7, TD = 0.9, AL = 5.1, HAL = 9.7, F1 = 5.3, FII length = 6.2, FIII = 1.7, TIII = 1.2, IND = 2.1, END = 1.8.

Measurements (in mm) of the type series. Meristic variation of the type series is summarized in Table 5.

Color in life. Description based on color photographs of MUTPL 271 (Fig. 19). Dorsal surfaces of body, arms, and limbs green with numerous whitish spots of various sizes. Yellowish-white upper lip; anterior two-thirds of venter yellowish white, posterior third translucent. Fingers, toes,

683 and membranes yellowish green. Bones green. Iris white with a slight lavender tone, with fine
684 brown reticulations.

685 **Color in ethanol.** Dorsum lavender, with yellowish-white dots distributed along the dorsum.
686 Some individuals (CJ 11364, 11564, 12631) present a grayish-lavender dorsum with white spots;
687 white upper lip. Anterior one third to two-thirds of the parietal peritonium white, hepatic
688 peritoneal translucid venter yellowish cream, posterior third translucent.

689 **Variation.** Morphometric variation is shown in Table 4. One male (ZSFQ 4428) had a slightly
690 darker dorsal coloration, and more dorsal spicules than other individuals (Fig. 10). Individuals
691 from the type locality in the Estación Científica San Francisco (ZSFQ 4417, 18) exhibit a more
692 reduced webbing between Fingers III and IV than the rest specimens represented in the type
693 series.

694 **Osteology.** The following description of osteological features is based on the holotype (ZSFQ
695 4418) of *Centrolene marcoreyesi* (Figs. 20, 21).

696 **Skull.** Skull (Fig. 20A, B, C, D) unornamented, without dermal modifications or cossification
697 with the skin. Maxillary arch complete; alary process of the premaxilla of moderate size, with
698 pointed distal end. Pars facialis of maxilla expanded anteriorly, attenuating posteriorly.
699 Quadratojugal ossified, overlapping anteriorly with maxilla and posteriorly articulated with
700 angulosplenial. Two ossified nasals, broad and well developed, separated from each other, not
701 articulating to the palatal bar and almost in contact with the sphenethmoid. Sphenethmoid large,
702 but not contacting nasals. Paired frontoparietals not ornamented, arranged in parallel, posteriorly
703 fused to prootic + exoccipitals. Frontoparietal fontanelle delimited by sphenethmoid anteriorly,
704 frontoparietals laterally, irregular posterior border. Occipital condyles thin, slightly projected
705 don't reach level of the exoccipital. Occipital fontanelles absent. Prootics and exoccipitals fused;
706 crista parotica completely ossified. Neopalatine present, ventrally overlapping sphenethmoid.
707 Maxillary and premaxillary teeth short and monocuspid. Suspensorium composed of paired
708 pterygoids and squamosals, zygomatic ramus of squamosal is short and present a claw shape
709 anterior border, otic ramus is oriented posterosuperior. Each pterygoid consists of anterior,
710 medial, and posterior rami; anterior ramus articulating with posterior end of maxilla, medial
711 ramus coverings the prootic pseudobasal process, and posterior ramus oriented towards ventral
712 ramus of squamosal. Moderate-sized vomers broadly separated from one another medially. Each

composed of arcuate bone bordering anterior and medial margins of choana. Prechoanal and postchoanal rami thin and unexpanded distally. Slender dentigerous processes extending ventromedially from the union of the pre- and postchoanal processes. Neopalatines unornamented, arcuate, and articulating with the lateral margin of sphenethmoid just anterior to the orbitonasal foramen. Each neopalatine narrowly separated from maxilla. Parasphenoid large and broad, anterior ends slightly rounded and overlapping sphenethmoid, nearly reaching level of neopalatines; alary processes of parasphenoid relatively short; posteromedial process short, but distinctly separated from margin of foramen magnum. Columella present, thin. Pterygoid with three branches: a curved anterior ramus oriented anterolaterally toward the maxilla, with which it articulates at approximately midlength of orbit; medial and posterior rami of pterygoid about equal in length; medial ramus in contact with edge of ossified lateral margin of the prootic. Lower jaw composed of mentomeckelian bone; dorsal portion of mentomeckelian bone fused to dentary.

Forelimb and hind limb. The forelimb (Fig. 21A) is composed of humeral bone, humeral spine, radioulna, carpal elements, prepollex, and four digits (I–V). The hind limb (Fig. 21B) consists of femur, tibiale, fibula, fibulare (= astragalus), metacarpals, metatarsals, and five digits (I–V). The phalangeal formulae for the hand and foot are standard—2-2-3-3 and 2-2-3-4-3. Order of finger length: I < II < IV < III, that of toes: I < II < V < III < IV. Metacarpals long and slender; distal end rounded; inner edge of Finger III with dilated medial metacarpal process (Hayes & Starrett 1980). Intercalary element between the last phalanges of all digits; terminal phalanx with T- or Y-shaped end. Carpus composed of Carpal 1, a large postaxial element assumed to represent a fusion of Carpals 2–4, radiale, ulnare, and Element Y. Prepollex well-developed, broad, and curved, with pointed distal end. Tarsus composed of three elements, presumably Tarsal 1 + 2 + 3. Humeral bone with a small, curved, humeral spine (in males), equivalent to 30–35% of humerus length, oriented at an angle of 35–45° in relation to axis of humerus.

Pectoral girdle. Composed of scapula, suprascapula, zonal area (coracoid, cleithrum, and clavicle), and posteromedial process. Suprascapula completely mineralized, with cleithrum apparent as a slender bone along its leading edge; cleithrum ossified. Clavicles oriented anteromedially, with the medial tips distinctly separated from one another; anterolateral end of clavicle articulating with scapula (Fig. 21C).

743 **Vertebral column and pelvic girdle.** Vertebral column (Fig. 21D) with eight presacral
744 vertebrae; Presacrals I and II notably shorter than posterior presacral. All presacrals are non-
745 imbricate except the first, which seems partially fused with Presacral II. Neural arch of Presacral
746 II bearings a rounded, medial process that articulates with neural arch of Presacral I. Transverse
747 processes present in all vertebrae, except Presacral I. Vertebral profile in decreasing order of
748 overall width of bony parts: sacrum > III > IV ≅ V ≅ VI ≅VII ≅ VIII > II > I. Orientations of
749 transverse processes of Presacrals II, III, and VII lateral; IV, V, and VI posterolateral, those of
750 Presacrals VIII directed anterolaterally. Sacral diapophyses moderately dilated laterally; leading
751 edge and posterior margin of diapophyses slightly concave. Urostyle long and slender, with
752 bicondylar articulation with the sacrum, and bearing low dorsal crest throughout its anterior half.
753 Length of urostyle less than combined length of presacral vertebrae. Pelvic girdle (Fig. 21D)
754 composed of ischium, ilium, and pubis. Ilial shafts cylindrical, lacking dorsal crest. Ilia tightly
755 joined with ischia and pubes. Pubis ossified.

756 **Natural history.** The holotype ZSFQ 4418 was collected at night in a small stream, on
757 herbaceous vegetation. In Abra de Zamora (Fig. 22A-B), several individuals were calling near
758 small streams in an evergreen upper montane forest ecosystem (Homeier et al. 2008). The
759 encountered males were calling on the upper surfaces of leaves, at about 1 m from the water
760 surface (Fig. 22B). In Parque Nacional Podocarpus several males were observed calling from
761 about 2 m on leaves over fast flowing streams. At Guarumales (Fig. 22C) four individuals (CJ
762 10139, 10140, 10158, 10305) were found calling near a river, approximately 150 to 350 cm
763 above ground level; two individuals (CJ 11366, 11372) were found on leaves, about 100–200 cm
764 above ground level; the two other individuals were observed on fern leaves. A male (CJ 11564)
765 was observed calling nearby a clutch with 19 eggs (one of them dead; Fig. 23). On 15 April,
766 2022, a male (CJ 11564) was observed calling from a fern leaf at 150 cm above ground level; the
767 streams where the species is present are variable in width, between 2 to 8 m. Males were found
768 in primary and secondary forests and on the edge of pastures. At Abra de Zamora *C. marcoreyesi*
769 was sympatric with *Gastrotheca testudinea* and in Guarumales with *Nymphargus cariticomatus*,
770 *N. posadae*, *N. cochranae,* and *Hyalinobatrachium* sp.

771 **Call.** The call consists of one or two "Tri" type pulsed notes (*sensu* Duarte-Marín et al., 2022).
772 The notes as such represent the entire duration of the call since they are emitted alone, however,

there may be emissions with two consecutive notes, and then the average call has a duration of 52–1807 (971.6 ± 589.5) ms. Each note has an average duration of 52–85 (65.4 ± 9.5) ms and is made up of 7–10 (8.2 ± 1.1) pulses, which have an average duration of 2–11 (6.5 ± 1.2) ms. The calls present an average modulated frequency of 2.3–9.8 (6.2 ± 2.3) kHz, with an average dominant frequency of 3.1–3.6 (3.3 ± 0.1) kHz; generating between 1–3 partial harmonics (Table 7, Fig. 9B).

Centrolene marcoreyesi differs structurally by the notes as such represent the entire duration of the call since they are emitted alone. It should be noted that this structural pattern is also present in the announcement song of *C. buckleyi* sensu stricto. *C. buckleyi* sensu stricto presents a longer duration in its calls (considering that the note is the equivalent of the call), pulses and intervals. Finally, the dominant frequency is higher in *C. marcoreyesi*, with a higher frequency modulation (considering only the frequency difference, discarding from this criterion the duration of the song as a modulation factor) in *C. buckleyi* sensu stricto.

Distribution. *Centrolene marcoreyesi* is endemic to the eastern slopes of the southern Ecuadorian Andes (Fig. 8), where it is known from four localities within the Zamora Chinchipe Province: Estación Científica San Francisco, Abra de Zamora, Parque Nacional Podocarpus and Guarumales, at an altitudinal range of 1,840–2,190 m.

Conservation status. We followed IUCN criteria to assess the current extinction risk of this species (Gärdenfors et al. 2001). Even if some of the known localities of *Centrolene marcoreyesi* are inside protected areas, and as such benefit from conservation measures, this species is threatened by degradation of its habitats, especially due to cattle farming, introduction of invasive exotic species and illegal and legal mining. Thus, we propose *C. marcoreyesi* to be considered as Endangered (EN) B1 a,b(i,iii) with an estimated extent of occurrence < 100 km^2.

Evolutionary relationships. The gene sampling of our study indicates that *Centrolene marcoreyesi* is sister to *C. sabini* (Fig.1).

Etymology. The species epithet "*marcoreyesi*" is a noun in genitive case, with the Latin suffix "i" (ICZN 31.1.2). With this species, we honor Marco M. Reyes-Puig (Fig. 17), a notable herpetologist from the herpetology division of the Museo Ecuatoriano de Ciencias Naturales (now Instituto Nacional de Biodiversidad, INABIO). Marco was the original collector of this new species on a field campaign to Zamora Chinchipe, with this recognition we recall him and

his work and we emphasize the memory that unites us as his brother (JPRP), sister (CRP), and friends.

Remarks. *Centrolene marcoreyesi* (ZSFQ 4417 [MRy 547], ZSFQ 4418 [Mry 548]) corresponds to the species cited as "*Centrolene buckleyi* [Ca1]" by Amador et al. (2018).

Biogeographic history of the new species. The Dispersal-Vicariance biogeographical model (DIVALIKE, as implemented in BioGeoBEARS) was found to have the best fit to the ancestral area reconstruction for our *Centrolene* species (AICc weight: 0.98; Table 8), suggesting that vicariance events were fundamental at the moment of establishing the current distribution of lineages. The most common recent ancestor (MRCA) of our calibrated *Centrolene* species tree probably originates in the northern Andes of Ecuador at ~ 7 Ma (late Miocene, 95% HPD: 5.9–7.9 Ma) (Fig. 24). This MRCA split into two main clades, a clade with just northern Andean species that includes *C. buckleyi* sensu stricto, and another clade with northern and central Andean species that includes the two new species described here *C. elisae* and *C. marcoreyesi*. The deepest node of the second clade diverged shortly after at 5.7 Ma (late Miocene to early Pliocene, 95% HPD: 4.3–7.2 Ma) and the ancestors of this clade were supposed to be also originated in the Ecuadorian north Andes. In relation to the new species, the MRCA of *C. marcoreyesi* and its sister species *C. sabini* diverged at ~ 1.5 Ma (95% HPD: 0.2–3.1 Ma) during the Pleistocene ad it was distributed in both north and central Andes at the time. On the other hand, *C. elisae* and its sister species C. cf. elisae originated from an MRCA distributed only in the northern Andes and that diverged almost at the same time as *C. marcoreyesi* in the south, at ~ 1.2 Ma (95% HPD: 0.4–2.2 Ma).

Discussion

Centrolene buckleyi was recognized as a species complex based on acoustic and phylogenetic data (Guayasamin et al., 2006, Guayasamin et al., 2008, Amador et al., 2018, Guayasamin et al., 2020). Here we redefine *C. buckleyi* sensu stricto and describe two new species based on phylogenetics, morphological, genetic, acoustic, and osteological evidence. We highlight that the two new species are not sister to *C. buckleyi* sensu stricto, and that they exhibit a combination of traits that support their validity (Tables 5, 6). As seen in other cryptic groups, availability of skull and osteological characters proved to be useful. In the *C. buckleyi* sensu stricto, the shape of frontoparietal fontanelle, shape of occipital condyles and its relation with level of exoccipital,

shape, size and orientation of zygomatic and otic ramus in squamosals, and shape of anterior border of cultriforms process in parasphenoides, are key diagnostic features, although we note that intraspecific variation requires further study. Also, since vocalizations are a key mechanism for species identification (Wells & Schwartz 2007), finding non-overlapping differences among closely related taxa reinforces the hypothesis that the lineages are, indeed, evolving independently (e.g., *Centrolene buckleyi* sensu stricto and *C. elisae*); thus, even in somehow morphologically cryptic species, calls tend to exhibit more disparities, resulting in useful traits for species identification (Escalona et al. 2019). We also note that the call characteristics in glassfrogs are partially modulated by environmental constraints (e.g., vegetation density, temperature; see Mendoza-Henao et al. 2023).

Biogeography. The radiation of numerous South American amphibians is heavily influenced by the topographic complexity of the Andes that facilitates allopatric speciation (Lynch & Duellman 1997; Coloma et al., 2012; Páez-Moscoso & Guayasamin 2012; Castroviejo-Fisher et al., 2014; Guayasamin et al. 2020). Based on the speciation timing and diversification rate of amphibians in the tropical Andes, there are two clades that relatively turn out to be the youngest: Telmatobiidae with an age of ~ 22 million years and Centrolenidae about 25–44 million years (Hutter et al., 2017, Guayasamin et al., 2020). The latter clade has strong relationships between diversification rates and elevational changes within their distribution ranges, suggesting that their speciation processes are in part determined by rapid orogenesis in the Andes (Hutter et al., 2017; Graham 2009; Parra et al., 2009; Garzione et al., 2014), in addition to allopatric partitioning through niche conservatism (Hutter et al., 2013). The genus *Centrolene,* specifically, has been accumulating richness in today's mid-elevation habitats, long before the Andes reached their current elevations (Hutter et al., 2013). However, the highest radiation in *Centrolene* species is recent, with numerous species originating during the late Miocene and Pliocene. These speciation events coincide with periods of rapid mountain uplift, that affects mainly the Northeastern Andean Cordilleras (Antonelli et al., 2009; Kellog et al., 2019), where the new species are distributed.

Centrolene marcoreyesi and its sister species, *C. sabini,* are distributed on the eastern slopes of the Andes, but separated by the Huancabamba Depression, which has also influenced the diversification of other Andean groups (Vuilleumier 1969, 1984; Duellman 1979; Fjeldså et al.

1999; Winger & Bates 2015; Torres-Carvajal et al., 2020; Venegas et al., 2021). This depression, a low-elevation, arid valley, likely represents a formidable barrier for cloud forest species, adapted to constant humidity and cold climate (Hutter et al., 2013). The huge gap between the distribution of these two species suggests that other species of *Centrolene* might remain undiscovered along the eastern Andes of Peru.

These matches between geological and speciation events supports our vicariant model obtained with the ancestral range estimation analyses (Fig. 23). Therefore, the distribution of the *Centrolene buckleyi* sensu lato in the Andes of Colombia and Ecuador provides insights into the evolutionary history and diversification of these closely related species. As in many other glassfrogs (Hutter et al., 2013; Castroviejo-Fisher et al., 2014; Guayasamin et al., 2020), speciation in *Centrolene* is mediated by the linearity of the Andes, where habitat continuity is broken by deep river valleys (Remsen 1984; Graves 1988; Guayasamin et al., 2020). The consequence of such a scenario is the presence of allopatric sister taxa, inhabiting very similar environments (i.e., niche conservatism) (Hutter et al., 2013).

The new species, *Centrolene elisae*, also fits the linearity + fragmentation scenario (Guayasamin et al., 2020). All species closely related to *C. elisae* occur on the eastern Andean mountain chain, and represent latitudinal replacements of each other (Fig. 6). The two new species described herein have a similar phylogeographic pattern since both species have geographically distant genetic neighbors: *C. elisae* to the north of the Andes has a species gap as does *C. marcoreyesi* to the south. This suggests that there are still populations to be discovered, especially within areas of challenging access such as the Llanganates and Sangay National Parks.

Pending taxonomic issues in Colombia. We highlight the case of the *Centrolene buckleyi* sensu lato in Colombia, as we consider that a thorough review is required in order to better understand species delimitations and relationships within the complex. Our study includes phylogenetic analysis of one population from the municipality of Tocancipá, Department of Cundinamarca, and an additional population from the Páramo de Chingaza, Department of Cundinamarca, both located in the Eastern Andean mountains near Bogotá. As mentioned before, we found a close relation of these populations with *C. venezuelense* and *C. elisae.* Although the presence of a polytomy does not yet allow to define the relation among these three species, the external and internal morphologic analysis of *C. elisae*, as well as its vocalizations, allows differentiating it

from *C. venezuelense* and the Colombian populations. But, in the case of the Colombian populations and *C. venezuelense* -it is most closely related species based on the phylogenetic analysis conducted-, the relation remains uncertain, as we do not count with enough evidence to delimit them as different species.

Some limitations prevent us from identifying if entities present at the Eastern Andes of Colombia should be considered as a different taxon. The lack of osteological attributes for Colombian populations and inaccessibility of type material of *C. venezuelense* for comparison, are some of them. Señaris and Ayarzaguena (2005) provided morphological, osteological, and call descriptions for *C. venezuelense*. However, high variation in some of the character states shown, such as, form and presence of ulnar and tarsal folds and coloration of the dorsum and eye, made it difficult to identify differences with the Colombian populations here evaluated. As for call attributes, we found variation in the frequency and duration of the calls recorded for the Colombian populations (not shown) and those published for *C. venezuelense* that could indicate taxonomic independence. However, given the close phylogenetic relation found in the analyses of these two entities, and the operational difficulties to morphologically differentiate them, we highlight the need to develop a further revision of the type material and new material of *C. venezuelense* in order to readjust its diagnosis if needed. We also suggest collecting acoustic information from the type locality of the species associated with voucher specimens, a consideration not included in Señaris and Ayarzaguena (2005). Taking these steps will allow more robust comparisons of *C. venezuelense* with other entities within the *Centrolene buckleyi* sensu lato including the Colombian populations.

Our findings suggest that populations of *C. buckleyi* present in the department of Cundinamarca are closely related to *C. venezuelense*, and show some evidence that could indicate taxonomic independence within the complex. However, expanding the sampling of Colombian populations present in other areas of the Eastern Andes is required, in order to determine whether populations found there are an extension of the distribution of *C. venezuelense,* or if they correspond to an independent taxonomic entity. Having this in mind, we suggest that these Colombian populations to be treated as *C.* cf. *venezuelense*, until further research is conducted. Also, we emphasize that given the taxonomic complexity of *Centrolene buckleyi*, its presence in the three Andean mountains ranges in Colombia (Cochran & Goin, 1970; Ardila & Acosta, 2000; Lynch, 2001;

Bernal et al. 2005; Amador et al. 2018; Guayasamin et al. 2020), and the influence these have on amphibian speciation events (see: Lynch & Duellman 1997; Coloma et al., 2012; Páez-Moscoso & Guayasamin 2012; Castroviejo-Fisher et al., 2014; Guayasamin et al. 2020), we are likely facing a broad scenario of cryptic diversity, in which the species richness of the country is being underestimated. This scenario opens the doors to an important case of taxonomic uncertainty that deserves to be reviewed in depth for the entire country in order to continue clarifying relations within the *C. buckleyi* sensu lato.

Conservation. *Centrolene elisae* has been found in several private reserves (Chamanapamba Reserve, Yanayacu Biological Station, San Isidro Reserve), which have been a key to preserving the forest on the Amazonian slopes of the Andes. We note the particularly high amphibian diversity and endemism that has been recently documented from EcoMinga reserves near the Llanganates and Sangay National Parks (see Yánez-Muñoz et al., 2010; Reyes-Puig et al., 2010; Páez-Moscoso et al., 2011; Reyes-Puig & Yánez-Muñoz 2012; Reyes-Puig et al., 2013, 2014, 2015, 2019, 2022a, 2022b). Thus, the upper Pastaza river basin emerges as a priority area for conservation.

For the other species described in this work, *C. marcoreyesi*, even considering that some populations are located inside Parque Nacional Podocarpus (one of Ecuador's largest national parks) and the Key Biodiversity Area Abra de Zamora, the species faces several threats here. The main identified threats are the loss and degradation of habitats due to cattle farming, the introduction of exotic species (Rainbow Trout, *Oncorhynchus mykiss*) and forest fires (Székely et al., 2020). To make matters worse, the spread of the illegal mining activities in Parque Nacional Podocarpus (Villa et al., 2022) and the increase of the mining concessions in southern Ecuador (Roy et al., 2018) threaten the survival of the species even in protected areas.

Abra de Zamora is a Key Biodiversity Area of unique importance for biodiversity due to the presence of many restricted range amphibian species and a center of amphibian diversification (Székely et al., 2020). Since 1938 until recently, 14 species of anurans were described from this relatively small area (e.g. Parker, 1938; Lynch, 1979; Trueb, 1979; Székely et al., 2020; Székely et al., 2023a) and others are waiting for the formal description (PS pers. comm.). From 2020, Abra de Zamora counts with a conservation action plan for amphibians (Ordóñez-Delgado et al., 2020), and several conservation projects were implemented by the EcoSs Lab group from the

Universidad Técnica Particular de Loja in collaboration with Naturaleza y Cultura Internacional NGO, with the main purpose of safeguarding the unique ecosystems found here.

The other population of *C. marcoreyesi*, from Guarumales, is not properly protected, even though it is located in the Sangay-Podocarpus connectivity corridor. This corridor was created with the aim of protecting over 567,000 ha of high-elevation paramo grasslands, cloud forest ecosystems, and a chain of lakes and wetlands, through a participatory model of management for conservation with the direct involvement of local governments (Sánchez-Nivicela, 2022). However, the main threat that affects this species here is probably the habitat destruction due to the expansion of the agricultural/cattle raising frontier.

Conclusions

We provide morphological, phylogenetic, osteological, and acoustic evidence that supports the validity of two new species, *Centrolene elisae* and *C. marcoreyesi,* formerly confused with *C. buckleyi*. Our phylogenetic hypothesis suggests that *C. elisae* is sister to *C. venezuelense,* and that *C. marcoreyesi* is the sister species of *C. sabini*. Speciation is driven by the linearity of the Andes and disruption by river valleys. Finally, for *C. elisae,* we propose the Endangered (EN) B1.b(ii)c IUCN category, with an estimated extent of occurrence < 5000 Km^2; and *C. marcoreyesi* is threatened by habitat degradation because of cattle farming and mining, and we propose this species to be considered as Endangered (EN) B1 a,b(i,iii) with an estimated extent of occurrence < 100 Km^2.

Acknowledgements

We are grateful to the people who provided specimens and tissues under their care for this study: Luis Coloma, Andrea Terán (Centro Jambatu), Mario H. Yánez-Muñoz, Miguel Urgilés (Instituto Nacional de Biodiversidad), Gabriela Maldonado, Mónica Páez (Museo de Zoología Universidad, Tecnológica Indoamérica), Emilia Peñaherrera, David Brito, Carolina Reyes-Puig (Museo de Zoología, Universidad San Francisco de Quito), Mónica Guerra, Diego Almeida (Colección de Herpetología, Museo de Historia Natural “Gustavo Orcés V.” (MEPN-H), Escuela Politécnica Nacional), Juan C. Sánchez-Nivicela and Sebastián Valverde. Cristina Paradela from the CT-Scan service of the Museo Nacional de Ciencias Naturales (MNCN), obtained the images for the osteological studies. Special thanks to Fernando Rojas-Runjaic for his accurate review

comments and for the English review throughout the manuscript, and to Marco Rada for reading an early version of the manuscript and providing some suggestions. Technical support in the laboratory was provided by Gabriela Gavilanes (LBE), and Mailyn Gonzalez and Eduardo Tovar Luque (Instituto Humboldt). DFM is grateful to Fundación Carolina and Universidad Rey Juan Carlos (URJC). Special thanks to Tito Recalde and Javier Robayo for their help during logistics and fieldwork (Chamanapamba reserve, EcoMinga Foundation), José Simbaña (Yanayacu Biological Station), Jose Vieira, Amanda Quezada (photographs). The Ecuadorian Ministerio del Ambiente provided research and collection permits (No. MAE-DNB-CM-2018-0105 and MAATE-cmarg-2022-0575). Colombian samples were collected under the project “Ecoreservas" conducted by the Instituto de Investigación de Recursos Biológicos Alexander von Humboldt, Ecopetrol, CENIT and Bicentenario (No. 22-077).

References

Almendáriz A, Batallas D. 2012. Nuevos datos sobre la distribución, historia natural y el canto de *Centrolene condor* Cisneros-Heredia y Morales-Mite 2008 (Amphibia: Anura: Centrolenidae). *Revista Politécnica* 30:42–53. http://bibdigital.epn.edu.ec/handle/15000/5052

Amador L, Parada A, D’Elía G, Guayasamin JM. 2018. Uncovering hidden specific diversity of Andean glassfrogs of the *Centrolene buckleyi* species complex (Anura: Centrolenidae). *PeerJ* 6: e5856. https://doi.org/10.7717/peerj.5856

Antonelli A, Nylander JAA, Persson C, Sanmartín I. 2009. Tracing the impact of the Andean uplift on Neotropical plant evolution. *Proceedings of the National Academy of Sciences* 106(24): 9749–9754. https://doi.org/10.1073/pnas.0811421106

Ardila MC, Acosta AR. 2000. Anfibios. En: Rangel-Ch. J. O. 2000. Colombia: diversidad biótica III. La región de vida paramuna. Universidad Nacional de Colombia. Bogotá. https://repositorio.unal.edu.co/handle/unal/81936

Ayarzagüena J. 1992. Los centrolenidos de la Guayana Venezolana. Publicaciones de la Asociación de Amigos de Doñana. Sevilla 1: 1–46.

Beaupre SJ, Jacobson ER, Lillywhite HB, Zamudio K. 2004. *Guidelines for use of live amphibians and reptiles in field and laboratory research.* American Society of Ichthyologists and Herpetologists, Lawrence, 43 pp.

https://www.fullerton.edu/doresearch/resource_library/policies/IACUC_GuidelinesforUseof AmphibsReptiles%202004.pdf

Bernal MH, Páez CA, Vejarano MA. 2005. Composición y distribución de los anfibios de la cuenca del río Coello (Tolima), Colombia. *Actualidades Biológicas* 27 (82): 87-92. https://doi.org/10.17533/udea.acbi.329432

Betts J, Young RP, Hilton-Taylor C, Hoffmann M, Rodríguez JP, Stuart SN, Milner-Gulland EJ. 2020. A framework for evaluating the impact of the IUCN Red List of threatened species. *Conservation Biology* 34(3): 632–643. https://doi.org/10.1111/cobi.13454

Bolívar-G W, Grant T, Osorio LA. 1999. Combat behavior in *Centrolene buckleyi* and other centrolenid frogs. *Alytes* 16 (3–4): 77–83. https://www.researchgate.net/profile/Wilmar-Bolivar-2/publication/256544287_Combat_behavior_in_Centrolene_buckleyi_and_other_centrolenid_frogs/links/544e4a1c0cf2bca5ce90330e/Combat-behavior-in-Centrolene-buckleyi-and-other-centrolenid-frogs.pdf

Bonaccorso E, Guayasamin JM, Mendez D, Speare R. 2003. Chytridiomycosis as a possible cause of population declines in *Atelopus cruciger* (Anura: Bufonidae). *Herpetological Review* 34: 331–334. https://researchonline.jcu.edu.au/6376/

Guayasamin JM, Bonaccorso E. 2004. A new species of glass frog (Centrolenidae: *Cochranella*) from the lowlands of northwestern Ecuador, with comments on the *Cochranella granulosa* group. *Herpetologica* 60: 85–94. https://doi.org/10.1655/03-74

Bonaccorso E, Koch I, Peterson AT. 2006. Pleistocene fragmentation of Amazon species' ranges. *Diversity and distributions* 12(2): 157–164. https://doi.org/10.1111/j.1366-9516.2005.00212.x

Bonaccorso E. 2009. Historical biogeography and speciation in the Neotropical highlands: molecular phylogenetics of the jay genus *Cyanolyca*. *Molecular Phylogenetics and Evolution* 50(3): 618–632. https://doi.org/10.1016/j.ympev.2008.12.012

Bonaccorso E, Guayasamin JM, Peterson AT, Navarro-Sigüenza AG. 2011. Molecular phylogeny and systematics of Neotropical toucanets in the genus *Aulacorhynchus* (Aves, Ramphastidae). *Zoologica Scripta* 40(4): 336–349. https://doi.org/10.1111/j.1463-6409.2011.00475.x

1041 Bonaccorso E, Ordóñez-Garza N, Pazmiño DA, Hearn A, Páez-Rosas D, Cruz S, Guayasamin
1042 JM. 2021. International fisheries threaten globally endangered sharks in the Eastern Tropical
1043 Pacific Ocean: the case of the Fu Yuan Yu Leng 999 reefer vessel seized within the
1044 Galápagos Marine Reserve. *Scientific Reports* 11(1): 1–11. https://doi.org/10.1038/s41598-
1045 021-94126-3
1046 Bouckaert R, Vaughan TG, Barido-Sottani J, Duchêne S, Fourment M, Gavryushkina A, et al.
1047 2019. BEAST 2.5: An advanced software platform for Bayesian evolutionary analysis. *PLoS*
1048 *Computational Biology* 15(4): e1006650. https://doi.org/10.1371/journal.pcbi.1006650
1049 Boulenger GA. 1882. *Catalogue of the Batrachia Salientias. Ecaudata in the Collection of the*
1050 *British Museum*. Second Edition. London: Taylor and Francis.
1051 https://doi.org/10.5962/bhl.title.8307
1052 Cadle JE, McDiarmid RW. 1990. "Two new species of *Centrolenella* (Anura: Centrolenidae)
1053 from northwestern Peru". *Proceedings of the Biological Society of Washington* 103(3): 746–
1054 768. https://repository.si.edu/handle/10088/4497?show=full
1055 Castroviejo-Fisher S, Guayasamin JM, Gonzalez-Voyer A, Vilà C. 2014. Neotropical
1056 diversification seen through glassfrogs. *Journal of Biogeography* 41(1): 66–80.
1057 http://dx.doi.org/10.1111/jbi.12208
1058 Catenazzi A, Von May R, Lehr E, Gagliardi–Urrutia G, Guayasamin JM. 2012. A new, high–
1059 elevation glassfrog (Anura: Centrolenidae) from Manu National Park, southern Peru. *Zootaxa*
1060 3388(1): 56–68. https://doi.org/10.11646/zootaxa.3388.1.5
1061 Cisneros-Heredia DF, Mcdiarmid RW. 2007. Revision of the characters of Centrolenidae
1062 (Amphibia: Anura: Athesphatanura), with comments on its taxonomy and the description of
1063 new taxa of glassfrogs. *Zootaxa* 1572: 82. https://doi.org/10.11646/zootaxa.1572.1.1
1064 Cisneros-Heredia DF, Morales-Mite M. 2008. A new species of glassfrog from the elfin forests
1065 of the Cordillera del Cóndor, southeastern Ecuador. *Herpetozoa* 21(1/2): 49–56.
1066 https://www.zobodat.at/pdf/HER_21_1_2_0049-0056.pdf
1067 Cisneros-Heredia DF, Yánez-Muñoz MH, Sánchez-Nivicela JC, Ron SR. 2023. Two new
1068 syntopic species of glassfrogs (Amphibia, Centrolenidae, *Centrolene*) from the southwestern
1069 Andes of Ecuador. *PeerJ* 11:e15195. https://doi.org/10.7717/peerj.15195
1070 Cochran DM, Goin XJ. 1970. *Frogs of Colombia.* Bulletin of the United States National
1071 Museum. Washington G.P.O 1907-1971. 288: 1–655. https://doi.org/10.5962/bhl.part.6346

1072 Coloma LA, Carvajal-Endara S, Dueñas JF, Paredes-Recalde A, Morales-Mite M, Almeida-
1073 Reinoso D, Tapia E, Hutter CR, Toral E, Guayasamin JM. 2012. Molecular phylogenetics of
1074 stream treefrogs of the *Hyloscirtus larinopygion* group (Anura: Hylidae), and description of
1075 two new species from Ecuador. *Zootaxa* 3364: 1–78.
1076 https://doi.org/10.11646/zootaxa.3364.1.
1077 de Queiroz K. 2005. *Ernst Mayr and the modern concept of species*. Proceedings of the National
1078 Academy of Sciences USA 102: 600–6607. https://doi.org/10.1073/pnas.0502030102
1079 de Queiroz K. 2007. Species concepts and species delimitation. *Systematic Biology* 56: 879–886.
1080 https://doi.org/10.1080/10635150701701083
1081 Dodson CH. 2003. Why are there so many orchid species. *Lankesteriana* 7: 99–103.
1082 https://doi.org/10.15517/lank.v3i2.23028
1083 Duarte-Marín S, Rada M, Rivera-Correa M, Caorsi V, Barona E, González-Duran G, Vargas-
1084 Salinas F. 2022. Tic, Tii and Trii calls: Advertisement call descriptions for eight glass frogs
1085 from Colombia and analysis of the structure of auditory signals in Centrolenidae.
1086 *Bioacoustics* 32(2): 143–180. https://doi.org/10.1080/09524622.2022.2077833
1087 Duellman WE. 1979. *The herpetofauna of the Andes: Patterns of distribution, origins,*
1088 *differentiation, and present communities Pp. 371–459, in Duellman W.E. (Ed.), The South*
1089 *American Herpetofauna: Its Origin, Evolution, and Dispersal*. Monographs of the Museum
1090 of Natural History. The University of Kansas, Lawrence.
1091 https://doi.org/10.5962/bhl.title.3207
1092 Duellman WE. 1981. *"Three new species of centrolenid frogs from the Pacific versant of*
1093 *Ecuador and Colombia".* Occasional papers of the Museum of Natural History, the
1094 University of Kansas 88: 1–9. https://biostor.org/reference/20792
1095 Duellman WE, Burrowes PA. 1989. New species of frogs, *Centrolenella*, from the Pacific
1096 versant of Ecuador and southern Colombia (No. 59 UNI). 132: 1–14.
1097 https://biostor.org/reference/211
1098 Duellman WE, Schulte R. 1993. *New species of centrolenid frogs from northern Peru*. Museum
1099 of Natural History, the University of Kansas.155: 1–33. https://biostor.org/reference/220
1100 Duellman ED, Trueb L. 1986. *Biology of amphibians*. MacGraw-Hill Inc. Nueva York, EUA.

1101 Duellman WE, Wild ER. 1993. *Anuran Amphibians from the Cordillera de Huancabama,*
1102 *Northern Peru: Systematics, Ecology, and Biogeography*. Museum of Natural History, the
1103 University of Kansas. https://biostor.org/reference/221
1104 Emmrich M, Vences M, Ernst R, Köhler J, Barej MF, Glaw F, Jansen M, Rödel MO. 2020. A
1105 guild classification system proposed for anuran advertisement calls. *Zoosystematics and*
1106 *Evolution* 96(2): 515–525. https://doi.org/10.3897/zse.96.38770
1107 Escalona MD, Ivo Simões P, Gonzalez-Voyer A, Castroviejo-Fisher S. 2019. Neotropical frogs
1108 and mating songs: The evolution of advertisement calls in glassfrogs. *Journal of*
1109 *Evolutionary Biology* 32: 63–176. https://doi.org/10.1111/jeb.13406
1110 Fjeldså J, Lambin E, Mertens B. 1999. Correlation between endemism and local ecoclimatic
1111 stability documented by comparing Andean bird distributions and remotely sensed land
1112 surface data. *Ecography* 22(1): 63–78. https://doi.org/10.1111/j.1600-0587.1999.tb00455.x
1113 Franco-Mena D, Guayasamin JM, Andrade-Brito D, Yánez-Muñoz MH, Rojas-Runjaic FJM.
1114 2023. Unveiling the evolutionary relationships and the high cryptic diversity in Andean
1115 rainfrogs (Craugastoridae: *Pristimantis myersi* group). *PeerJ* 11:e14715
1116 https://doi.org/10.7717/peerj.14715
1117 Frost DR. 2023. *Amphibian Species of the World: An Online Reference*. Version 6.1 (19 of
1118 March 2023). Electronic Database accessible at
1119 https://amphibiansoftheworld.amnh.org/index.php. American Museum of Natural History,
1120 New York, USA. doi.org/10.5531/db.vz.0001
1121 Gaglio M, Aschonitis VG, Mancuso MM, Reyes Puig JP, Moscoso F, Castaldelli G, Fano EA.
1122 2017. Changes in land use and ecosystem services in tropical forest areas: a case study in
1123 Andes mountains of Ecuador. *International Journal of Biodiversity Science, Ecosystem*
1124 *Services & Management* 13(1): 264–279. https://doi.org/10.1080/21513732.2017.1345980
1125 Gärdenfors U, Hilton-Taylor C, Mace GM, Rodriguez JP. 2001. The application of IUCN Red
1126 List criteria at regional levels. *Conservation biology* 15(5): 1206–1212.
1127 https://doi.org/10.1111/j.1523-1739.2001.00112.x
1128 Garzione CN, Auerbach DJ, Smith JJS, Rosario JJ, Passey BH, Jordan TE, Eiler JM. 2014.
1129 Clumped isotope evidence for diachronous surface cooling of the Altiplano and pulsed
1130 surface uplift of the Central Andes. *Earth and Planetary Science Letters* 393: 173–181.
1131 https://doi.org/10.1016/j.epsl.2014.02.029

1132 Gentry AH. 1982. *Patterns of neotropical plant species diversity.* Evolutionary biology Springer,
1133 Boston, MA 1– 84. DOI: 10.1007/978-1-4615-6968-8_1
1134 Goin, CJ. 1964. Distribution and synonymy of *Centrolenella fleischmanni* in northern South
1135 America. *Herpetologica* 20: 1–8. http://www.jstor.org/stable/3890875
1136 Graham A. 2009. The Andes: a geological overview from a biological perspective. *Annals of the*
1137 *Missouri Botanical Garden* 96(3): 371–385. https://doi.org/10.3417/2007146
1138 Graves GR. 1988. Linearity of geographic range and its possible effect on the population
1139 structure of Andean birds. *Auk* 105(1): 47–52. https://doi.org/10.1093/auk/105.1.47
1140 Gregory R, Long G, Colligan M, Geiger JG, Laser M. 2012. When experts disagree (and better
1141 science won't help much): using structured deliberations to support endangered species
1142 recovery planning. *Journal of Environmental Management* 105: 30–43.
1143 https://doi.org/10.1016/j.jenvman.2012.03.001
1144 Guayasamin JM, Bonaccorso E. 2004. A new species of glass frog (Centrolenidae: *Cochranella*)
1145 from the lowlands of northwestern Ecuador, with comments on the *Cochranella granulosa*
1146 group. *Herpetologica* 60: 485–494. https://doi.org/10.1655/03-74
1147 Guayasamin JM, Bustamante MR, Almeida-Reinoso D, Funk WC. 2006a. Glass frogs
1148 (Centrolenidae) of Yanayacu Biological Station, Ecuador, with the description of a new
1149 species and comments on centrolenid systematics. *Zoological Journal of the Linnean Society*
1150 147: 489–513. https://doi.org/10.1111/j.1096-3642.2006.00223.x
1151 Guayasamin JM, Cisneros-Heredia DF, Yánez-Muñoz MH, Bustamante MR. 2006b. Notes on
1152 geographic distribution. Amphibia, Centrolenidae, *Centrolene ilex, Centrolene litorale,*
1153 *Centrolene medemi, Cochranella albomaculata, Cochranella ametarsia*: Range extensions
1154 and new country records. *Check List* 2: 24–25. ISSN: 1809-127X
1155 Guayasamin JM, Trueb L. 2007. A new species of glassfrog (Anura: Centrolenidae) from the
1156 lowlands of northwestern Ecuador, with comments on centrolenid osteology. *Zootaxa* 1447:
1157 27–45. https://doi.org/10.11646/zootaxa.1447.1.2
1158 Guayasamin JM, Castroviejo-Fisher S, Ayarzagüena, J, Trueb L, Vilà C. 2008. Phylogenetic
1159 relationships of glassfrogs (Centrolenidae) based on mitochondrial and nuclear genes.
1160 *Molecular Phylogenetic Evolution* 48: 574–595. https://doi.org/10.1016/j.ympev.2008.04.012

1161 Guayasamin JM, Castroviejo-Fisher S, Trueb L, Ayarzagüena J, Rada M, Vilá C. 2009.
1162 Phylogenetic systematics of glassfrogs (Amphibia: Centrolenidae) and their sister taxon
1163 *Allophryne ruthveni*. *Zootaxa* 2100: 1–97. https://doi.org/10.11646/zootaxa.2100.1.1
1164 Guayasamin JM, Funk WC. 2009. The amphibian community at Yanayacu Biological Station,
1165 Ecuador, with a comparison of vertical microhabitat use among *Pristimantis* species and the
1166 description of a new species of the *Pristimantis myersi* group. *Zootaxa* 2220(2009): 41–66.
1167 https://doi.org/10.11646/zootaxa.2220.1.2
1168 Guayasamin JM, Cisneros-Heredia DF, Maynard RJ, Lynch RL, Culebras J, Hamilton PS. 2017.
1169 A marvelous new glassfrog (Centrolenidae, *Hyalinobatrachium*) from Amazonian Ecuador.
1170 *ZooKeys* 673: 1–20. https://doi.org/10.3897/zookeys.673.12108
1171 Guayasamin JM, Cisneros-Heredia DF, McDiarmid RW, Peña P, Hutter CR. 2020. Glassfrogs of
1172 Ecuador: diversity, evolution, and conservation. *Diversity* 12: 222.
1173 https://doi.org/10.3390/d12060222
1174 Guayasamin JM, Vandegrift R, Policha T, Encalada AC, Greene N, Ríos-Touma B, Roy BA.
1175 2021. Biodiversity conservation: local and global consequences of the application of "rights
1176 of nature" by Ecuador. *Neotropical Biodiversity* 7(1): 541–545.
1177 https://doi.org/10.1080/23766808.2021.2006550
1178 Guayasamin JM, Brunner RM, Valencia-Aguilar A, Franco-Mena D, Ringler E, Armijos AM,
1179 Culebras J. 2022. Two new glassfrogs (Centrolenidae: *Hyalinobatrachium*) from Ecuador,
1180 with comments on the endangered biodiversity of the Andes. *PeerJ* 10: e13109.
1181 https://doi.org/10.7717/peerj.13109
1182 Hayes MP, Starrett PH. 1980. Notes on a collection of centrolenid frogs from the Colombian
1183 Chocó. *Bulletin of the Southern California Academy of Sciences* 79: 89–96.
1184 https://biostor.org/reference/101954
1185 Homeier J, Werner FA, Gradstein SR, Breckle S, Richter M. 2008. *Potential vegetation and*
1186 *floristic composition of Andean forests in South Ecuador, with a focus on the RBSF*. In: Beck
1187 E, Bendix J, Kottke I, Makeschin F, Mosandl R, editors. Gradients in a tropical mountain
1188 ecosystem of Ecuador Ecological Studies, no. 198. Berlin/Heidelberg: Springer pp. 87–100.
1189 DOI: 10.1007/978-3-540-73526-7_10

1190 Hutter CR, Guayasamin JM, Wiens JJ. 2013. Explaining Andean megadiversity: The
1191 evolutionary and ecological causes of glassfrog elevational richness patterns. *Biology Letters*
1192 16: 1135–1144. https://doi.org/10.1111/ele.12148
1193 Hutter CR, Lambert SM, Wiens JJ. 2017. Rapid diversification and time explain amphibian
1194 richness at different scales in the Tropical Andes, Earth's most biodiverse hotspot. *The*
1195 *American Naturalist* 190(6): 828–843. https://doi.org/10.1086/694319
1196 International Union for Conservation of Nature. 2019. *Guidelines for using the IUCN red list*
1197 *categories and criteria: version 14*. Standards and Petitions Subcommittee of the
1198 International Union for the Conservation of Nature (accessed 12 January 2021)
1199 ICZN. 1999. *International Code of Zoological Nomenclature*. Fourth Edition: adopted by the
1200 International Union of Biological Sciences. The International Trust for Zoological
1201 Nomenclature. London, U.K. Available from: https://www.iczn.org/. ISBN 0 85301 006 4
1202 Jiménez de la Espada M. 1872. *Nuevos batrácios Americanos*. Anales de la Sociedad Española
1203 de Historia Natural. Madrid 1: 85–88. https://biostor.org/reference/20815
1204 Jost L. 2004. Explosive local radiation of the genus *Teagueia* (Orchidaceae) in the upper Pastaza
1205 watershed of Ecuador. *Lyonia* 7: 41–47. https://doi.org/10.15517/lank.v17i2.30159
1206 Kalyaanamoorthy S, Minh BQ, Wong TK, von Haeseler A, Jermiin LS. 2017. ModelFinder: fast
1207 model selection for accurate phylogenetic estimates. *Nature Methods* 14: 587–589.
1208 https://doi.org/10.1038/nmeth.4285
1209 K. Lisa Yang Center for Conservation Bioacoustics at the Cornell Lab of Ornithology. (2023).
1210 Raven Pro: Interactive Sound Analysis Software (Version 1.6.5). Computer software. The
1211 Cornell Lab of Ornithology. Ithaca, EE.UU. Available from
1212 https://ravensoundsoftware.com/.
1213 Katoh K, Standley DM. 2013. MAFFT multiple sequence alignment software version 7:
1214 improvements in performance and usability. *Molecular Biology and Evolution* 30: 772–780.
1215 https://doi.org/10.1093/molbev/mst010
1216 Kellogg JN, Franco Camelio GB, Mora-Páez H. 2019. *Chapter 4 - Cenozoic tectonic evolution of*
1217 *the North Andes with constraints from volcanic ages, seismic reflection, and satellite*
1218 *geodesy*. In Horton BK, Folguera A (Eds), Andean Tectonics (pp. 69–102). Elsevier.

1219 Köehler J, Jansen M, Rodriguez A, Kok PJ, Toledo LF, Emmrich M, Vences, M. 2017. The use
1220 of bioacoustics in anuran taxonomy: theory, terminology, methods and recommendations for
1221 best practice. *Zootaxa* 4251(1): 1–124. https://doi.org/10.11646/zootaxa.4251.1.1
1222 Lansac C, Aguayo R, De la Riva I. 2021. An assessment of the taxonomic validity of three
1223 species of marsupial frogs (Anura: Hemiphractidae: *Gastrotheca*) from the Yungas of
1224 Bolivia based on external morphology and cranial osteology. *Zootaxa* 50682: 211–239.
1225 https://doi.org/10.11646/zootaxa.5068.2.3
1226 Lees AC, Pimm SL. 2015. Species, extinct before we know them?. *Current Biology* 25(5):
1227 R177–R180. https://doi.org/10.1016/j.cub.2014.12.017
1228 Letunic I, Bork P. 2021. Interactive Tree Of Life (iTOL) v5: an online tool for phylogenetic tree
1229 display and annotation. *Nucleic acids research* 49(W1), W293–W296.
1230 https://doi.org/10.1093/nar/gkab301
1231 Lessmann J, Munoz J, Bonaccorso E. 2014. Maximizing species conservation in continental
1232 Ecuador: A case of systematic conservation planning for biodiverse regions. *Ecology and*
1233 *Evolution* 4(12): 2410–2422. https://doi.org/10.1002/ece3.1102
1234 Lessmann J, Fajardo J, Muñoz J, Bonaccorso E. 2016. Large expansion of oil industry in the
1235 Ecuadorian Amazon: biodiversity vulnerability and conservation alternatives. *Ecology and*
1236 *evolution* 6(14): 4997–5012. https://doi.org/10.1002/ece3.2099
1237 Ligges U, Krey S, Mersmann O, Schnackenberg S. 2018. tuneR: analysis of music and speech.
1238 See https://CRAN. R-project. org/package= tuneR.
1239 Lynch JD. 1979. *Leptodactylid frogs of the genus Eleutherodactylus from the Andes of southern*
1240 *Ecuador*. Misc Publ Univ Kans Mus Nat Hist. 66: 1–62.
1241 https://doi.org/10.5962/bhl.title.16268
1242 Lynch JD. 2001. A small amphibian fauna from a previously unexplored Paramo of the
1243 Cordillera Occidental in western Colombia. *Journal of Herpetology* 221-231.
1244 Lynch JD, Duellman WE. 1997. *Frogs of the genus Eleutherodactylus in western Ecuador.*
1245 *Systematics, ecology, and biogeography*. Special Publication. Natural History Museum,
1246 University of Kansas 23: 1–236. https://doi.org/10.5962/bhl.title.7951
1247 Mace GM. 2004. The role of taxonomy in species conservation. Philosophical Transactions of
1248 the Royal Society of London. Series B: *Biological Sciences* 359(1444): 711-719.
1249 https://doi.org/10.1098/rstb.2003.1454

1250 Maddison W, Maddison WP. 2019. Mesquite: a modular system for evolutionary analysis.
1251 version 3.61. Available at: http://mesquiteproject.org.
1252 Mahoney J. 2009. What Determines the Level of Funding for an Endangered Species?. *Major*
1253 *Themes in Economics*11(1), 17–33.
1254 Madriñán S, Cortés AJ, Richardson JE. 2013. Páramo is the world's fastest evolving and coolest
1255 biodiversity hotspot. *Frontiers in genetics* 4: 192. https://doi.org/10.3389/fgene.2013.00192
1256 Martin TG, Kehoe L, Mantyka-Pringle C, Chades I, Wilson S, Bloom RG, Smith PA. 2018.
1257 Prioritizing recovery funding to maximize conservation of endangered species. *Conservation*
1258 *Letters* 11(6): e12604. https://doi.org/10.1111/conl.12604
1259 Martín-López B, Montes C, Ramírez L, Benayas J. 2009. What drives policy decision-making
1260 related to species conservation?. *Biological Conservation* 142(7): 1370-1380.
1261 https://doi.org/10.1016/j.biocon.2009.01.030
1262 Mahoney J. 2009. What Determines the Level of Funding for an Endangered Species?. Major
1263 *Themes in Economics* 11(1): 17–33. Available at:
1264 https://scholarworks.uni.edu/mtie/vol11/iss1/4
1265 Matzke NJ. 2013. Probabilistic historical biogeography: new models for founder-event
1266 speciation, imperfect detection, and fossils allow improved accuracy and model-testing.
1267 *Frontiers of Biogeography* 5(4). http://dx.doi.org/10.21425/F5FBG19694
1268 Mendoza-Henao AM, KR Zamudio, JM Guayasamin, M Escalona, G Parra-Oleas. 2023.
1269 Environmental rather than character displacement explain call evolution in glassfrogs.
1270 *Evolution* 77: 355–369. https://doi.org/10.1093/evolut/qpac041
1271 Minh BQ, Nguyen M, von Haeseler A. 2013. Ultrafast approximation for phylogenetic bootstrap.
1272 *Molecular Biology and Evolution* 30: 1188–1195. https://doi.org/10.1093/molbev/mst024
1273 Nieden F. 1923. Amphibia: Anura I.: Subordo Aglossa und Phaneroglossa, Sectio 1 Arcifera.
1274 Das Tierreich 46: xxxii + 584.
1275 Noble GK. 1920. *Two new batrachians from Colombia. Bulletin of the American Museum of*
1276 *Natural History*. 42: 441–44. http://digitallibrary.amnh.org/handle/2246/1917
1277 Noss RF, O'Connell M, Murphy DD. 1997. The science of conservation planning: habitat
1278 conservation under the Endangered Species Act. Island Press.

1279 Nguyen LT, Schmidt HA, von Haeseler A, Minh BQ. 2015. IQ-TREE: A fast and effective
1280 ftochastic flgorithm for estimating maximum-likelihood phylogenies. *Molecular Biology and*
1281 *Evolution* 32(1): 268–274. https://doi.org/10.1093/molbev/msu300
1282 Ordóñez-Delgado L, Székely P, Székely D, Serrano F, Armijos-Ojeda D. 2020. Plan de Acción
1283 para la Conservación de los Anfibios del Abra de Zamora. Universidad Técnica Particular de
1284 Loja and Naturaleza & Cultura Internacional, Ecuador.
1285 Padial JM, Miralles A, De la Riva I, Vences M. 2010. The integrative future of taxonomy.
1286 *Frontiers in Zoology* 7: 1–14. https://doi.org/10.1186/1742-9994-7-16
1287 Páez-Moscoso DJ, Guayasamin JM, Yánez-Muñoz M. 2011. A new species of Andean toad
1288 (Bufonidae, *Osornophryne*) discovered using molecular and morphological data, with a
1289 taxonomic key for the genus. *ZooKeys* 108: 73. https://doi.org/10.3897/zookeys.108.1129
1290 Páez-Moscoso DJ, Guayasamin JM. 2012. Species limits in the Andean toad genus
1291 *Osornophryne* (Bufonidae). *Molecular Phylogenetics and Evolution* 65(3): 805–822.
1292 https://doi.org/10.1016/j.ympev.2012.08.001
1293 Parker HW. 1938. *The vertical distribution of some reptiles and amphibians in southern*
1294 *Ecuador*. Ann Mag Nat Hist. 2: 438–450.Parra M, Mora A, Sobel ER, Strecker MR,
1295 González R. 2009. Episodic orogenic front migration in the northern Andes: Constraints from
1296 low-temperature thermochronology in the Eastern Cordillera, Colombia. *Tectonics* 28(4): 1–
1297 27. https://doi.org/10.1029/2008TC002423
1298 Parra M, Mora A, Sobel ER, Strecker MR, González R. 2009. Episodic orogenic front migration
1299 in the northern Andes: Constraints from low-temperature thermochronology in the Eastern
1300 Cordillera, Colombia. *Tectonics* 28(4): 1–27. https://doi.org/10.1029/2008TC002423
1301 Peñafiel N, Flores DM, Rivero De Aguilar J, Guayasamin JM, Bonaccorso E. 2019. A cost-
1302 effective protocol for total DNA isolation from animal tissue. *Neotropical Biodiversity* 5: 69–
1303 74. https://doi.org/10.1080/23766808.2019.1706387
1304 Pérez-Escobar OA, Chomicki G, Condamine FL, Karremans AP, Bogarín D, Matzke NJ,
1305 Antonelli A. 2017. Recent origin and rapid speciation of Neotropical orchids in the world's
1306 richest plant biodiversity hotspot. *New Phytologist* 215: 891–905.
1307 https://doi.org/10.1111/nph.14629
1308 Polato NR, Gill BA, Shah AA, Gray MM, Casner KL, Barthelet A, Zamudio KR. 2018. *Narrow*
1309 *thermal tolerance and low dispersal drive higher speciation in tropical mountains*.

Proceedings of the National Academy of Sciences 115: 12471–12476. https://doi.org/10.1073/pnas.1809326115

Rada M, Guayasamin JM. 2008. Redescripción de *Cochranella megista* (Rivero, 1985) y ampliación de la distribución de nueve ranas de cristal (Anura: Centrolenidae) en Colombia. *Papéis Avulsos de Zoologia* 48: 89–101. https://doi.org/10.1590/S0031-10492008001200001

Rambaut A. 2014. FigTree v1.4.2. A graphical viewer of phylogenetic trees. http://tree.bio.ed.ac.uk/software/figtree/

Rambaut A, Drummond AJ, Xie D, Baele G, Suchard MA. 2018. Posterior summarisation in Bayesian phylogenetics using Tracer 1.7. *Systematic Biology* syy032. doi:10.1093/sysbio/syy032

RStudio Team. 2022. RStudio: Integrated Development Environment for R. RStudio, PBC, Boston, MA URL http://www.rstudio.com/.

Remsen JV. 1984. High incidence of "leapfrog" pattern of geographic variation in Andean birds: Implications for the speciation process. *Science* 224: 171–173. https://doi.org/10.1126/science.224.4645.171

Reyes-Puig JP, Yánez-Muñoz MH, Cisneros-Heredia DF, Ramírez-Jaramillo SR. 2010. Una nueva especie de rana *Pristimantis* (Terrarana: Strabomantidae) de los bosques nublados de la cuenca alta del río Pastaza, Ecuador. *ACI Avances en Ciencias e Ingenierías* 2: 3. https://doi.org/10.18272/aci.v2i3.48

Reyes-Puig JP, Yánez-Muñoz MH. 2012. Una nueva especie de *Pristimantis* (Anura: Craugastoridae) del corredor ecológico llangantes-sangay, Andes de Ecuador. *Papéis Avulsos de Zoologia* 52: 81–91. https://doi.org/10.1590/S0031-10492012000600001

Reyes-Puig MM, Reyes-Puig JP, Yánez-Muñoz MH. 2013. Ranas terrestres del género *Pristimantis* (Anura: Craugastoridae) de la Reserva Ecológica Río Zúñag, Tungurahua, Ecuador: Lista anotada y descripción de una especie nueva. *ACI Avances en Ciencias e Ingenierías* 5: 2. https://doi.org/10.18272/aci.v5i2.133

Reyes-Puig JP, Reyes-Puig C, Ramírez-Jaramillo SR. 2014. Tres nuevas especies de ranas terrestres *Pristimantis* (Anura: Craugastoridae) de la cuenca alta del Río Pastaza, Ecuador. ACI Avances en Ciencias e Ingenierías 6: 2. https://doi.org/10.18272/aci.v6i2.179

Reyes-Puig JP, Reyes-Puig CP, Pérez-Lara MB, Yánez-Muñoz MH. 2015. Dos nuevas especies de ranas *Pristimantis* (Craugastoridae) de la cordillera de los Sacha Llanganatis, vertiente

oriental de los Andes de Ecuador. *ACI Avances en Ciencias e Ingenierías* 7: 2. https://doi.org/10.18272/aci.v7i2.258

Reyes-Puig JP, Reyes-Puig C, Ron S, Ortega JA, Guayasamin JM, Goodrum M, Yánez-Muñoz MH. 2019. A new species of terrestrial frog of the genus *Noblella* Barbour, 1930 (Amphibia: Strabomantidae) from the Llanganates-Sangay Ecological Corridor, Tungurahua, Ecuador. *PeerJ* 7: e7405. https://doi.org/10.7717/peerj.7405

Reyes-Puig JP, Reyes-Puig C, Franco-Mena D, Jost L, Yánez-Muñoz MH. 2022a. Strong differentiation between amphibian communities on two adjacent mountains in the Upper Rio Pastaza watershed of Ecuador, with descriptions of two new species of terrestrial frogs. *ZooKeys* 1081: 35. https://doi.org/10.3897/zookeys.1081.71488

Reyes-Puig JP, Recalde D, Recalde F, Koch C, Guayasamin JM, Cisneros-Heredia DF, Yánez-Muñoz MH. 2022b. A spectacular new species of *Hyloscirtus* (Anura: Hylidae) from the Cordillera de Los Llanganates in the eastern Andes of Ecuador. PeerJ 10: e14066. https://doi.org/10.7717/peerj.14066

Rivero JA. 1968. Los centrolenidos de Venezuela (Amphibia, Salientia). Memoria. Sociedad de Ciencias Naturales La Salle. Caracas 28: 301–334. https://doi.org/10.2988/0097-0298(2005)13[9:A]2.0.CO;2

Ronquist F, Teslenko M, Van Der Mark P, Ayres DL, Darling A, Höhna S, Huelsenbeck JP. 2012. MrBayes 3.2: efficient Bayesian phylogenetic inference and model choice across a large model space. *Systematic biology* 61(3): 539–542. https://doi.org/10.1093/sysbio/sys029

Roy BA, Zorrilla M, Endara L, Thomas DC, Vandegrift R, Rubenstein JM, Read M. 2018. New mining concessions could severely decrease biodiversity and ecosystem services in Ecuador. *Tropical Conservation Science* 11: 1940082918780427. https://doi.org/10.1177/19400829187804

Ruiz-Carranza PM, Lynch JD. 1991. Ranas Centrolenidae de Colombia II. Nuevas especies de *Centrolene* de la Cordillera Oriental y Sierra Nevada de Santa Marta. *Lozania* 58: 1–26. ISSN/ISBN: 0085-2899

Ruiz-Carranza PM, Ardila-Robayo MC, Lynch JD. 1996. Lista actualizada de la fauna de Amphibia de Colombia. *Revista de la Academia Colombiana de Ciencias Exactas, Físicas y Naturales* 20(77): 365-415. ISSN 0370-3908

1371 Sánchez-Nivicela JC. 2022. *Anfibios y reptiles del corredor de conectividad Sangay-*
1372 *Podocarpus*. Naturaleza y Cultura Internacional. Cuenca-Ecuador. 252 pp.
1373 Savage JM, Heyer WR. 1967. Variation and distribution in the tree-frog genus *Phyllomedusa* in
1374 Costa Rica, central America: With 6 figures. *Studies on Neotropical Fauna and Environment*
1375 5: 111–131. https://doi.org/10.1080/01650526709360400
1376 Señaris JC, Ayarzagüena, J. 2005. *Revisión Taxonómica de la Familia Centrolenidae (Amphibia:*
1377 *Anura) en Venezuela*. Sevilla: Publicaciones del Comité Español del Programa Hombre y
1378 Biosfera – Red IberoMaB de la UNESCO. 337 p.
1379 Sueur J, Aubin T, Simonis C. 2008. Seewave: a free modular tool for sound analysis and
1380 synthesis. *Bioacoustics* 18: 213–226. https://doi.org/10.1080/09524622.2008.9753600
1381 Sueur J. 2018. Sound analysis and synthesis with R (p. 637). Cham: Springer.
1382 Simpson GG. 1961. *Principles of animal taxonomy*. Principles of Animal Taxonomy. Columbia
1383 University Press. https://doi.org/10.1126/science.133.3464.1589
1384 Sornoza-Molina F, Freile JF, Nilsson J, Krabbe N, Bonaccorso E. 2018. A striking, critically
1385 endangered, new species of hillstar (Trochilidae: *Oreotrochilus*) from the southwestern
1386 Andes of Ecuador. *Auk*: *Ornithological Advances* 135(4): 1146–1171.
1387 https://doi.org/10.1642/AUK-18-58.1
1388 Székely P, Eguiguren JS, Ordóñez-Delgado L, Armijos-Ojeda D, Székely D. 2020. Fifty years
1389 after: A taxonomic revision of the amphibian species from the Ecuadorian biodiversity
1390 hotspot Abra de Zamora, with description of two new *Pristimantis* species. *PLOS One* 15(9).
1391 e0238306 http://dx.doi.org/10.1371/journal.pone.0238306
1392 Székely P, Székely D, Armijos-Ojeda D, Hualpa-Vega S, Vörös J. 2023a. Molecular and
1393 Morphological Assessment of Rain Frogs in the *Pristimantis orestes* Species Group
1394 (Amphibia: Anura: Strabomantidae) with the Description of Three New Cryptic Species from
1395 Southern Ecuador. *Herpetological Monographs* 37(1): 41–69.
1396 https://doi.org/10.1655/HERPMONOGRAPHS-D-22-00002
1397 Székely P, Córdova-Díaz M, Hualpa-Vega D, Hualpa-Vega S, Székely D. 2023b. A new
1398 glassfrog species of the genus *Centrolene* (Amphibia, Anura, Centrolenidae) from Cordillera
1399 del Cóndor, southern Ecuador. *ZooKeys* 1149. https://doi.org/10.3897/zookeys.1149.96134

1400 Taylor EH. 1951. Two new genera and a new family of tropical American frogs. Dos nuevos
1401 géneros y una familia nueva de ranas del trópico americano. *Proceedings of the Biological*
1402 *Society of Washington* 64: 33–40. https://biostor.org/reference/65690
1403 Tamura K, Stecher G, Kumar S. 2021. MEGA 11: Molecular Evolutionary Genetics Analysis
1404 Version 11. *Molecular Biology and Evolution* https://doi.org/10.1093/molbev/msab120.
1405 Team RC. 2018. R: A language and environment for statistical computing. 2014. R Foundation
1406 for Statistical Computing: Vienna, Austria. Available from: http://www.R-project.org
1407 Torres-Carvajal O, Venegas PJ, Sales Nunes PM. 2020. Description and phylogeny of a new
1408 species of Andean lizard (Gymnophthalmidae: Cercosaurinae) from the Huancabamba
1409 Depression. *South American Journal of Herpetology* 18(1): 13.
1410 https://doi.org/10.2994/SAJH-D-18-00069.1
1411 Trueb L. 1973. *Bones, frogs, and evolution*. Evolutionary biology of the anurans: contemporary
1412 research on major problems 65–132.
1413 Trueb L. 1979. Leptodactylid frogs of the genus *Telmatobius* in Ecuador with the description of
1414 a new species. *Copeia* 1979: 714–733. https://doi.org/10.2307/1443882
1415 Tsang SM. 2015. Quantifying the bat bushmeat trade in North Sulawesi, Indonesia, with
1416 suggestions for conservation action. *Global Ecology and Conservation* 3: 324-330.
1417 https://doi.org/10.1016/j.gecco.2015.01.003
1418 Twomey E, Delia J, Castroviejo-Fisher S. 2014. A review of Northern Peruvian glassfrogs
1419 (Centrolenidae), with the description of four new remarkable species. *Zootaxa* 3851:1–87.
1420 https://doi.org/10.11646/zootaxa.3851.1.1
1421 Venegas PJ, García-Ayachi LA, Ormeño J, Bullard S, Catenazzi A, Motta AP. 2021. Two new
1422 species of terrestrial-breeding frogs (Anura: Brachycephaloidea) from Cordillera de Colán,
1423 Peru. *Neotropical Biodiversity* 7(1): 279–296.
1424 https://doi.org/10.1080/23766808.2021.1953894
1425 Villa J, Aguilar C, Villacís S, Finer M, Josse C. 2022. Minería ilegal de oro en el Parque
1426 Nacional Podocarpus, Ecuador. Monitoring of the Andean Amazon Project (MAAP): 172.
1427 Available at: https://maaproject.org/2023/mineria-podocarpus-ecuador/ (accessed 19 August
1428 2023).
1429 Vuilleumier F. 1969. Pleistocene speciation in birds living in the high Andes. *Nature* 223:1179–
1430 1180. https://doi.org/10.1038/2231179a0

Vuilleumier F. 1969. Pleistocene speciation in birds living in the high Andes. *Nature* 223(5211):1179-1180. https://doi.org/10.1038/2231179a0

Vuilleumier F. 1984. Zoogeography of Andean birds: Two major barriers; and speciation and taxonomy of the Diglossa carbonaria superspecies. *National Geographic Society Research Reports* 16: 713–731.

Wells KD, Schwartz JJ. 2007. *The behavioral ecology of anuran communication*. In P. M. Narins, A. S. Feng, R. R. Fay & A. N. Popper (Eds.), Hearing and sound communication in amphibians (pp. 44–86). Springer. DOI: 10.1007/978-0-387-47796-1_3

Wiley EO. 1978. The evolutionary species concept reconsidered. *Systematic zoology* 27(1): 17–26. https://doi.org/10.2307/2412809

Winger BM, Bates JM. 2015. The tempo of trait divergence in geographic isolation: Avian speciation across the Marañon Valley of Peru. *Evolution* 69(3): 772–787. https://doi.org/10.1111/evo.12607

Yánez-Muñoz MH, Cisneros-Heredia DF, Reyes-Puig JP. 2010. Una nueva especie de rana terrestre *Pristimantis* (Anura: Terrarana: Strabomantidae) de la cuenca alta del Río Pastaza, Ecuador. *ACI Avances en Ciencias e Ingenierías* 2: 3. https://doi.org/10.18272/aci.v2i3.48

Yánez-Muñoz MH, Reyes-Puig JP, Batallas-Revelo D, Broaddus C, Urgilés-Merchán M, Cisneros-Heredia DF, Guayasamin JM. 2021. A new Andean treefrog (Amphibia: *Hyloscirtus bogotensis* group) from Ecuador: an example of community involvement for conservation. *PeerJ* 9:e11914. doi: 10.7717/peerj.11914.

Table 1(on next page)

Species, vouchers and GenBank accession numbers for newly generated DNA sequences (12S–16S) used in genetic analyses and locality.

Acronyms are CJ = Centro Jambatu, DHMECN = División de Herpetología, Museo Ecuatoriano de Ciencias Naturales, MUTPL = Museo de Zoología, Universidad Técnica Particular de Loja, ZSFQ = Museo de Zoología Universidad San Francisco de Quito; IAvH-Am = Colección de Anfibios, Instituto de Investigación de Recursos Biológicos Alexander von Humboldt.

1

Species	Museum Number	12S	16S
Centrolene buckleyi	DHMECN 867	–	OR479083
Centrolene buckleyi	*DHMECN 13828*	OR479108	OR479085
Centrolene buckleyi	DHMECN 14180	–	OR479086
Centrolene buckleyi	ZSFQ 4420	OR479107	OR479084
Centrolene buckleyi	ZSFQ 4421	OR479109	OR479087
Centrolene buckleyi	ZSFQ 5366	OR479112	OR479090
Centrolene buckleyi	CJ 1055	OR479115	OR479093
Centrolene buckleyi	CJ 2171	OR479110	OR479088
Centrolene buckleyi	CJ 9789	OR479114	OR479092
Centrolene buckleyi	CJ 4292	OR479113	OR479091
Centrolene buckleyi	CJ 11305	OR479111	OR479089
Centrolene elisae sp. nov.	ZSFQ 4228	OR479117	OR479099
Centrolene cf. *elisae*	ZSFQ 2134	OR479116	OR479098
Centrolene marcoreyesi sp. nov.	CJ 11364	OR479121	OR479097
Centrolene marcoreyesi sp. nov.	CJ 11564	OR479118	OR479094
Centrolene marcoreyesi sp. nov.	CJ 12631	OR479120	OR479096
Centrolene marcoreyesi sp. nov.	MUTPL 271	OR479119	OR479095
Centrolene cf. *venezuelense*	IAvH-Am-17401	OR479122	OR479100
Centrolene cf. *venezuelense*	IAvH-Am-17403	OR479124	OR479102
Centrolene cf. *venezuelense*	IAvH-Am-17407	OR479125	OR479103
Centrolene cf. *venezuelense*	IAvH-Am-17410	OR479123	OR479101
Centrolene sp.	ZSFQ 621	OR479128	OR479106
Centrolene sp.	ZSFQ 4422	OR479126	OR479104
Centrolene sp.	ZSFQ 4423	OR479127	OR479105

2

Table 2(on next page)

Differences between the new species and morphologically similar taxa within *Centrolene*. Distribution

1

Species	Distribution	SVL in adult males (mm)	Snout (lateral view)	Texture of dorsal skin (males)	Dorsal coloration (in life)	Source
C. altitudinalis	Venezuela: Andes, Estado Mérida, 1,975–2,400 m.	21.5–24.5 (n= 12)	Round to slightly sloping	Shagreen with small spicules	Uniform dark green dorsum with white or cream dots	Señaris & Ayarzagüena (2005)
C. ballux	Ecuador, Colombia: Pacific slopes of Andes, 1,780–2,340 m.	19.2–23.3 (n= 25)	Bluntly rounded	Shagreen	Green dorsum with small light spots	Duellman & Burrowes (1989); Guayasamin et al., 2020
C. buckleyi sensu stricto	Ecuador: central and northern Andes.Cordillera Oriental and Cordillera Occidental; 2,573–3,416 m.	25.0–34.7 (n= 20)	Slightly sloping to sloping	Shagreen with or without small warts	Bright to dark green; some individuals have scattered olive-green spots on the dorsum	Guayasamin et al., 2020; Culebras et al., 2023, unpublished data; This study.
C. camposi	Ecuador: Southwestern slopes of the Cordillera Occidental of the Andes; 2,950 m.	29.1–31.2 (n = 2)	Sloping	Shagreen with dispersed low and rounded warts (microspicules and spicules present)	Uniform green dorsum with light green warts	Cisneros-Heredia et al. 2023
C. condor	Ecuador: Eastern Montane Forest ecoregion; 1,737–2,920 m.	23.7–28.6 (n=7)	Subacuminated	Shagreen with low warts and abundant spicules	Green with many small yellowish–white flecks and dark bluish-black/brown flecks	Almendariz & Batallas-Revelo, 2011; Cisneros-Heredia & Morales (2008)

					and punctuations	
***C. elisae* sp. nov.**	Ecuador: eastern versant of central and northern Andes; 2,118–2,586 m.	22.0–25.3 (n= 5)	Rounded	Shagreen covered with minute spinules and spots	Dark green with small to minute white spots.	This study
C. ericsmithi	Ecuador: Southwestern slopes of the Cordillera Occidental of the Andes; 2,950 m.	27.3 (n = 1)	Rounded	Shagreen with dispersed spicules, and covered by microspicules	Bright green dorsum, white tubercles	Cisneros-Heredia et al. 2023
C. heloderma	Ecuador: Montane forests; 1,850–2.575 m	26.8–31.5 (n= 17)	Sloping	Pustular	Green with green to bluish white warts	Duellman (1981); Guayasamin et al., 2020
C. hesperia	Perú: Pacific slope of the Cordillera Central; 1.500–1,800 m.	23.0–27.3 (*n*= 54)	Slightly sloping	Shagreen with spinules	Dorsal life leaf green with green spicules	Cadle & McDiarmid (1990)
C. huilense	Ecuador: Amazonian slope of the Andes; 2,100–2,190 m.	23.6–26.7 (*n*= 7)	Sloping	Shagreen with spinules	Green with dark green to dark lavender spots and smaller white spots	Ruiz-Carranza et al., (1996); Guayasamin et al., 2020
C. lynchi	Ecuador:Pacific slope of the Cordillera Occidental of the Andes; 1,140–1,852 m.	23.3–26.5 mm (n=22)	Round	Shagreen with spinules	Dull green with minute yellowish–white warts.	Duellman & Burrowes (1989); Guayasamin et al., 2020
C.	Ecuador: Eastern	24.5–	Sloping	Shagreen with	Green, with	This study

***marcoreyesi* sp. nov.**	slopes of the southern Andes; 2,008–2,923 m.	27.0 (n = 6)		dispersed low warts	whitish spots	
C. muelleri	Peru: Huallaga and Marañón drainages in the southern; 1,830–2,050 m.	23.5	Slightly sloping	Finely shagreen with dorsolateral rows of warts	Green with dark greenish-black spots and pale-yellow tubercles	Duellman & Schulte (1993); Guayasamin et al., 2020
C. notosticta	Colombia: Western slope of the Eastern Andes; 1,661–2,440 m.	19.4–22.7 (n= 31)	Blunt	Shagreen with spinules	Green with small yellow spots	Ruiz-Carranza & Lynch (1991)
C. sabini	Peru: Kosñipata valley; 2,750–2,800 m.	29.6–31.2 (n = 5)	Obtuse	Skin on dorsal surfaces of head and body spiculate; skin on dorsal surfaces of limbs smooth.	Green with yellowish-green spots and patches	Catenazzi et al., 2012
C. venezuelense	Venezuela: Andean mountains; 2,400–3,050 m.	23.4–33.8 (n = 15)	Rounded	Dorsum with smooth to finely granular skin, with spicules of different sizes.	Light green, with small cream-colored spots.	Señaris & Ayarzagüena (2005)
C. zarza	Ecuador: Southern montane forest; 1,434–1,480 m.	23.2–26.2 (n = 5)	Sloping	Shagreen with elevated, and some enameled, warts	Light green with many white or whitish spots and flecks	Székely et al., 2023b

2

Table 3(on next page)

Shapiro–Wilk normality test for morphometrics measurements of *Centrolene buckleyi* sensu stricto, *C. elisae* sp. nov., and *C. marcoreyesi* sp. nov. Please show the significant level

1

Character	*Centrolene buckleyi* sensu stricto	*Centrolene elisae* sp. nov	*Centrolene marcoreyesi* sp. nov
	p-value (α 0.05)	p-value (α 0.05)	p-value (α 0.05)
AL	0.7601	0.4928	0.3503
ED	0.2757	0.4135	0.4072
END	0.6777	0.6406	0.5217
FEL	0.0584*	0.0487*	0.4529
FI	0.6546	0.8007	0.8945
FII	0.6637	0.5117	0.3838
FIII	0.0227*	0.5378	0.7561
FL	0.6039	0.1049	0.5378
HAL	0.5504	0.7344	0.3083
HL	0.9986	0.3092	0.9909
HW	0.7600	0.3742	0.2909
IND	0.6198	0.3589	0.8837
IOD	0.2670	0.1521	0.0570*
SVL	0.0104*	0.6814	0.1697
TD	0.8429	0.0229*	0.4057
TIII	0.5593	0.5627	0.7332
TL	0.0376*	0.3838	0.2748

2

3

4

5

Table 4(on next page)

Comparisons and significance of morphometric characters of species of *Centrolene buckleyi* complex.

Asterisks show the degree of significance; A = univariate t-test; and B = Wilcoxon-Mann Whitney test.

1

Character	*Centrolene buckleyi* sensu stricto *Centrolene elisae* sp. nov.		*Centrolene buckleyi* sensu stricto *Centrolene marcoreyesi* sp. nov.		*Centrolene elisae* sp. nov. *Centrolene marcoreyesi* sp. nov.	
	A	**B**	**A**	**B**	**A**	**B**
	p-value (α 0.05)	p-value (α 0.05)	p-value (α 0.05)	p-value (α 0.05)	p-value (α 0.05)	p-value (α 0.05)
AL	0.00200*	-	0.00147*	-	0.9303	-
ED	0.00063*	-	0.03865*	-	0.5301	-
END	0.00052*	-	0.2563	-	0.00630*	
FEL	-	0.00291*	-	0.1274	-	0.05128*
FI	0.00028*	-	0.9678	-	0.00128*	-
FII	0.00217*	-	0.01578*	-	0.0831	-
FIII	-	0.1414	-	0.00536	0.1628	-
FL	1.43e-06*	-	0.00762*	-	0.00023*	-
HAL	0.05734*	-	0.3157	-	0.134	-
HL	0.00018*	-	0.01005*	-	0.2702	-
HW	1.78e-10*	-	0.3981	-	0.01896*	-
IND	0.00075*	-	0.04132*	-	0.04162*	-
IOD	0.00172*	-	0.1241	-	-	0.02214*
SVL	-	1.98e-05*	-	0.00470*	0.00842*	-

TD	-	0.00364*	0.0776	-	-	0.5672
TIII	0.4733	-	0.1444	-	0.2623	-
TL	-	0.0928	-	0.4089	0.00076*	-

2

Table 5(on next page)

Morphological measurement of *Centrolene buckleyi* sensu stricto*, C. elisae* sp. nov., and *C. marcoreyesi* sp. nov.

	C. buckleyi		*C. elisae* sp. nov		*C. marcoreyesi* sp. nov
	Machos (n = 17)	**Hembras (n = 13)**	**Machos (n=6)**	**Hembras (n=1)**	**Machos (n=6)**
SVL	26.1–32.5 (27.9 ± 1.5)	24.2–39.8 (28.7 ± 4.3)	22.9–25.3 (24.3 ± 0.8)	27.2	24.5–27.0 (25.9 ± 1.0)
FEL	14.0–16.9 (15.1 ± 1.0)	13.3–19.6 (15.2 ± 1.9)	13.1–14.7 (13.5 ± 0.6)	15.3	13.7–15.1 (14.3 ± 0.6)
TL	14.3–18.3 (15.6 ± 1.2)	13.7 –18.6 (15.5 ± 1.5)	13.9 –15.1 (14.6 ± 0.4)	16.4	15.3–15.8 (15.6 ± 0.2)
FL	12.4–15.9 (14.2 ± 1.0)	12.7–19.3 (14.3 ± 1.8)	11.8–12.9 (12.2 ± 0.4)	13.8	13.0–13.8 (13.4 ± 0.3)
HL	5.7–7.6 (6.7 ± 0.5)	5.3–8.2 (6.8 ± 08)	5.5–6.1 (5.9 ± 0.3)	6.9	5.8–6.7 (6.2 ± 0.3)
HW	7.0 –9.7 (8.2 ± 0.6)	6.8–10.7 (8.2 ± 1.1)	6.9–7.9 (7.4 ± 0.4)	8.1	7.6–8.4 (8.0 ± 0.3)
IOD	2.7–3.7 (3.1 ± 0.3)	2.6– 4.0 (3.1 ± 0.4)	2.3–2.9 (2.7 ± 0.2)	3.3	2.4–3.2 (2.9 ± 0.2)
ED	2.2 –3.2 (2.8 ± 0.3)	2.3–3.8 (2.9 ± 0.4)	2.4–2.6 (2.5 ± 0.1)	2.9	2.1–2.8 (2.5 ± 0.2)
TD	0.7–1.2 (1.0 ± 0.1)	0.4–1.3 (0.9 ± 0.2)	0.5–0.8 (0.7 ± 0.1)	0.9	0.4–0.9 (0.7 ± 0.2)
AL	4.9–7.0 (5.8 ± 0.5)	5.1–7.1 (5.9 ± 0.7)	4.5–5.5 (5.0 ± 0.4)	5.6	4.3–5.7 (5.0 ± 0.4)
HAL	8.5–11.8 (9.9 ± 0.9)	8.2–13.9 (9.8 ± 1.5)	8.5–9.9 (9.3 ± 0.4)	10.0	9.5–10.1 (9.7 ± 0.2)
FI	3.8–5.9 (4.8 ± 0.6)	3.5–7.1 (4.8 ± 0.9)	3.6–4.4 (4.0 ± 0.3)	4.8	4.2–5.4 (4.9 ± 0.4)
FII	5.4–7.5 (6.5 ± 0.6)	4.6–8.1 (6.1 ± 0.9)	5.3–6.2 (5.7 ± 0.3)	6.1	5.8–6.2 (6.0 ± 0.2)
FIII	1.6–3.0 (1.9 ± 0.4)	1.1–2.2 (1.8 ± 0.3)	1.5–1.9 (1.6 ± 0.2)	1.8	0.8–1.7 (1.3 ± 0.3)
TIII	1.3–1.9 (1.5 ± 0.3)	1.0–2.0 (1.5 ± 0.3)	1.4–1.6 (1.5 ± 0.1)	1.6	1.1–1.6 (1.3 ± 0.1)
IND	1.8–2.8 (2.2 ± 0.2)	1.6–3.0 (2.2 ± 0.4)	1.6–2.1 (1.8 ± 0.1)	2.3	1.7–2.2 (2.0 ± 0.1)
END	1.6–2.2 (1.9 ± 0.2)	1.5–2.2 (1.9 ± 0.3)	1.5–1.8 (1.6 ± 0.1)	1.9	1.7–2.0 (1.8 ± 0.1)

1
2

Table 6(on next page)

Main skull characters of *Centrolene buckleyi* sensu stricto and new species.

1
2

Species	Frontoparietal fontanelle shape	Occipital	Squamosal	Parasphenoides
Centrolene buckleyi sensu stricto	posterior border with three aligned slits	condyles broad projected reach level of exoccipital	zygomatic ramus short thick and rounded	cultriform process with blunt anterior border that reach level of neopalatine
Centrolene elisae sp. nov.	posterior border regular and rounded	condyles thin not projected don't reach level of exoccipital posteriorly	zygomatic ramus long and sub acuminated	cultriform process with subacuminated anterior border dont reach level of neopalatine
Centrolene marcoreyesi sp. nov.	posterior border irregular	condyles thin slightly projected don't reach level of exoccipital	zygomatic ramus short and clawed shape	cultriform process with rounded anterior border dont reach level of neopalatine

Table 7 (on next page)

Spectral and temporal values of the calls of *Centrolene buckleyi* sensu stricto (MZUTI 0763), *Centrolene elisae* sp. nov. (ZSFQ 5369), and *Centrolene marcoreyesi* sp. nov. (MUTPL 271, FUTPL-A 149). how many calls do you record for each species?

1

Parameters	*Centrolene buckleyi* sensu stricto	*Centrolene elisae* sp. nov.	*Centrolene marcoreyesi* sp. nov.
	n=1/8/–/147	**n=1/4/6/29**	**n=2/13/23/191**
CD (ms)	239–289 (265.1 ± 17.7)	162–215 (195.3 ± 3)	52–1807 (971.6 ± 589.5)
IC (s)	19.6–71.3 (41.3 ± 17.3)	13.7–15	15.2–67.5 (33.9 ± 13.6)
CR (/min)	0.8–3 (1.7 ± 0.7)	3.9–4.3	0.9–3.7 (2 ± 0.7)
NC	1	2	1–2 (1.8 ± 0.4)
ND (ms)	–	31–113 (68.3 ± 37.8)	52–85 (65.4 ± 9.5)
N1D (ms)	–	82–113 (101.3 ± 16.9)	–
N2D (ms)	–	31–38 (35.3 ± 3.8)	–
IN (ms)	–	50–70 (59.7 ± 10)	816–1690 (1112.9 ± 327.3)
NR (/s)	–	5.6–7.6 (6.3 ±1.1)	0.6–1.1 (0.9 ± 0.2)
PN	16–20 (18.4 ± 1.6)	2–9 (4.8 ± 3.2)	7–10 (8.2 ± 1.1)
PN1	–	7–9 (7.7 ± 1.2)	–
PN2	–	2	–
PD (ms)	5–17 (8.5 ± 1.9)	4–9 (6.7 ± 1.4)	2–11 (6.5 ± 1.2)
IP (ms)	1–17 (6.4 ± 2.1)	2–11 (6.3 ± 2)	1–6 (2.3 ± 1)
PR (/s)	41.7–142.9 (68.5 ± 13)	58.8–125 (79.6 ± 17.8)	45.45–200 (124.7 ± 19.7)
DF (kHz)	2.8–3.3 (3.09 ± 0.1)	3.5–3.8 (3.6 ± 0.1)	3.1–3.6 (3.3 ± 0.1)
dfrq (kHz)	0.2–0.7 (0.5 ± 0.2)	0.4	0.2–0.5 (0.4 ± 0.1)
FM (kHz)	0.7–2.8 (1.9 ± 0.6)	3.1–3.2	2.3–9.8 (6.2 ± 2.3)
NH	1–3	1–4	1–3
2*f*0 (kHz)	5.5–6.6 (6.2 ± 0.2)	7–7.8 (7.2 ± 0.3)	6.2–7.3 (6.6 ± 0.2)
*3f*0 (kHz)	8.4–9.8 (9.2 ± 0.3)	10.2–11.5 (10.8 ± 0.4)	9.3–10.3 (9.9 ± 0.3)
*4f*0 (kHz)	11.2–13.1 (12.4 ± 0.4)	13.6–15.7 (14.4 ± 0.7)	12.4–13.8 (13.1 ± 0.4)
*5f*0 (kHz)	–	17.1–19 (18.3 ± 0.8)	–

What you mean?

2
3

Table 8(on next page)

Comparison of biogeographic models tested with BioGeoBEARS for *Centrolene* species in our dataset.

Model abbreviations: BAYAREALIKE, Bayesian inference of historical biogeography for many discrete areas (with likelihood interpretation); DEC, Dispersal-Extinction-Cladogenesis; DIVALIKE, Dispersal-Vicariance Analysis (with likelihood interpretation). Ln*L*, Log-likelihood score; d, dispersal; e, extinction; AICc, standard correction to Akaike's Information Criterion.

1
2
3

Model	Ln*L*	d	e	AICc
BAYAREALIKE	- 49.7905	0.1092	0.2640	104.3312
DEC	-42.5888	0.0983	0.0379	89.9276
DIVALIKE	-38.3840	0.0891	7.1341e-09	81.5181

4

Figure 1

Phylogenetic relationships of species in the genus *Centrolene*, inferred under Maximum Likelihood criterion and based on a concatenated dataset of mitochondrial genes (12S + 16S).

Node support is expressed in Bootstrap values (%), followed by Bayesian posterior probabilities; missing values indicate support below 60 (bootstrap) or 0.6 (posterior probability). Each terminal includes the following information: species name, voucher number, and locality. New sequences generated in this study are in blue. Photographs of *C. buckleyi* sensu stricto by JMG, *C. elisae* sp. nov. by DFM and *C. marcoreyesi.* sp. nov. by PS.

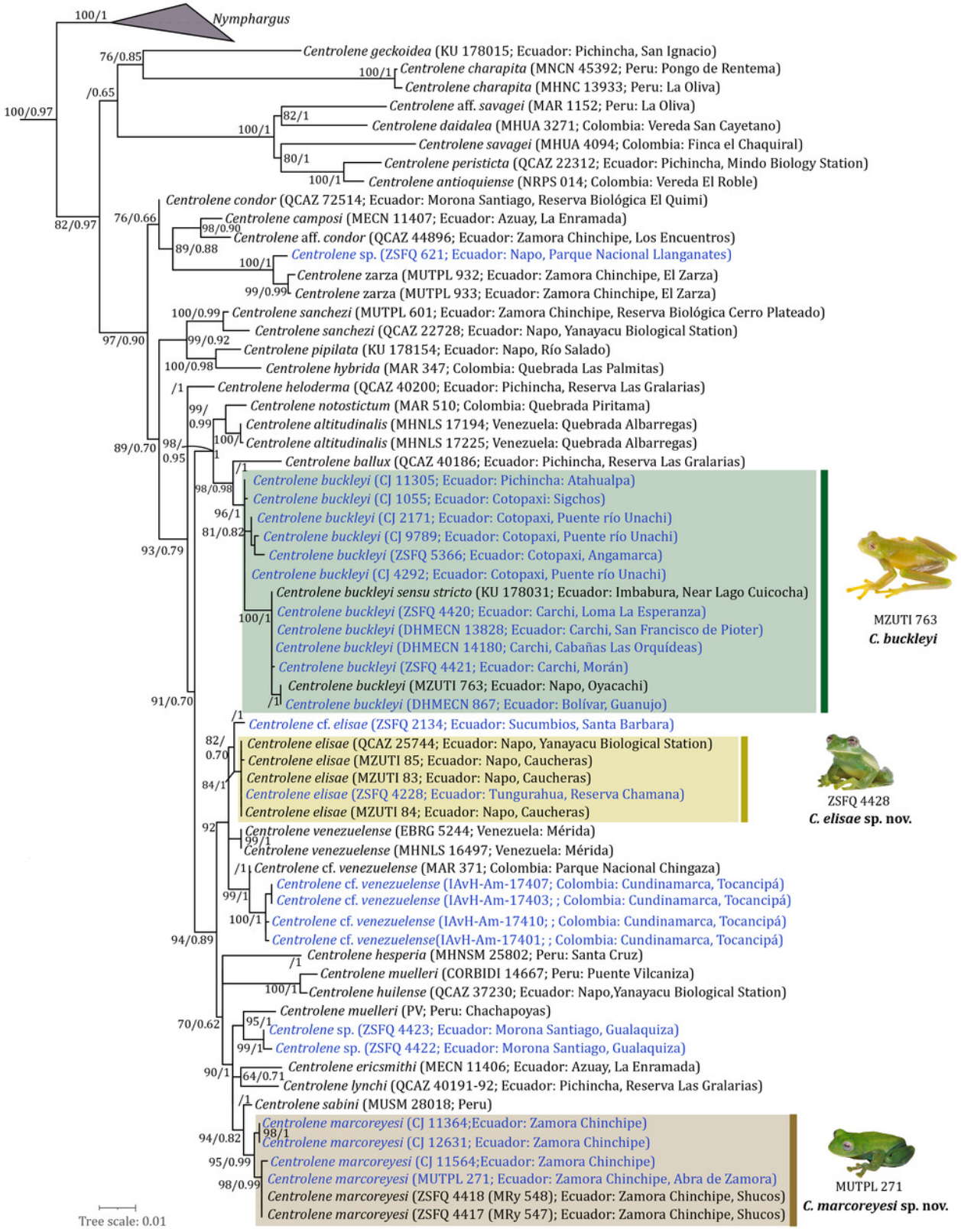
Nymphargus
Centrolene geckoidea (KU 178015; Ecuador: Pichincha, San Ignacio)
Centrolene charapita (MNCN 45392; Peru: Pongo de Rentema)
Centrolene charapita (MHNC 13933; Peru: La Oliva)
Centrolene aff. savagei (MAR 1152; Peru: La Oliva)
Centrolene daidalea (MHUA 3271; Colombia: Vereda San Cayetano)
Centrolene savagei (MHUA 4094; Colombia: Finca el Chaquiral)
Centrolene peristicta (QCAZ 22312; Ecuador: Pichincha, Mindo Biology Station)
Centrolene antioquiense (NRPS 014; Colombia: Vereda El Roble)
Centrolene condor (QCAZ 72514; Ecuador: Morona Santiago, Reserva Biológica El Quimi)
Centrolene camposi (MECN 11407; Ecuador: Azuay, La Enramada)
Centrolene aff. condor (QCAZ 44896; Ecuador: Zamora Chinchipe, Los Encuentros)
Centrolene sp. (ZSFQ 621; Ecuador: Napo, Parque Nacional Llanganates)
Centrolene zarza (MUTPL 932; Ecuador: Zamora Chinchipe, El Zarza)
Centrolene zarza (MUTPL 933; Ecuador: Zamora Chinchipe, El Zarza)
Centrolene sanchezi (MUTPL 601; Ecuador: Zamora Chinchipe, Reserva Biológica Cerro Plateado)
Centrolene sanchezi (QCAZ 22728; Ecuador: Napo, Yanayacu Biological Station)
Centrolene pipilata (KU 178154; Ecuador: Napo, Río Salado)
Centrolene hybrida (MAR 347; Colombia: Quebrada Las Palmitas)
Centrolene heloderma (QCAZ 40200; Ecuador: Pichincha, Reserva Las Gralarias)
Centrolene notostictum (MAR 510; Colombia: Quebrada Piritama)
Centrolene altitudinalis (MHNLS 17194; Venezuela: Quebrada Albarregas)
Centrolene altitudinalis (MHNLS 17225; Venezuela: Quebrada Albarregas)
Centrolene ballux (QCAZ 40186; Ecuador: Pichincha, Reserva Las Gralarias)
Centrolene buckleyi (CJ 11305; Ecuador: Pichincha: Atahualpa)
Centrolene buckleyi (CJ 1055; Ecuador: Cotopaxi: Sigchos)
Centrolene buckleyi (CJ 2171; Ecuador: Cotopaxi, Puente río Unachi)
Centrolene buckleyi (CJ 9789; Ecuador: Cotopaxi, Puente río Unachi)
Centrolene buckleyi (ZSFQ 5366; Ecuador: Cotopaxi, Angamarca)
Centrolene buckleyi (CJ 4292; Ecuador: Cotopaxi, Puente río Unachi)
Centrolene buckleyi sensu stricto (KU 178031; Ecuador: Imbabura, Near Lago Cuicocha)
Centrolene buckleyi (ZSFQ 4420; Ecuador: Carchi, Loma La Esperanza)
Centrolene buckleyi (DHMECN 13828; Ecuador: Carchi, San Francisco de Pioter)
Centrolene buckleyi (DHMECN 14180; Carchi, Cabañas Las Orquídeas)
Centrolene buckleyi (ZSFQ 4421; Ecuador: Carchi, Morán)
Centrolene buckleyi (MZUTI 763; Ecuador: Napo, Oyacachi)
Centrolene buckleyi (DHMECN 867; Ecuador: Bolívar, Guanujo)
MZUTI 763
C. buckleyi
Centrolene cf. elisae (ZSFQ 2134; Ecuador: Sucumbios, Santa Barbara)
Centrolene elisae (QCAZ 25744; Ecuador: Napo, Yanayacu Biological Station)
Centrolene elisae (MZUTI 85; Ecuador: Napo, Caucheras)
Centrolene elisae (MZUTI 83; Ecuador: Napo, Caucheras)
Centrolene elisae (ZSFQ 4228; Ecuador: Tungurahua, Reserva Chamana)
Centrolene elisae (MZUTI 84; Ecuador: Napo, Caucheras)
ZSFQ 4428
C. elisae sp. nov.
Centrolene venezuelense (EBRG 5244; Venezuela: Mérida)
Centrolene venezuelense (MHNLS 16497; Venezuela: Mérida)
Centrolene cf. venezuelense (MAR 371; Colombia: Parque Nacional Chingaza)
Centrolene cf. venezuelense (IAvH-Am-17407; Colombia: Cundinamarca, Tocancipá)
Centrolene cf. venezuelense (IAvH-Am-17403; ; Colombia: Cundinamarca, Tocancipá)
Centrolene cf. venezuelense (IAvH-Am-17410; ; Colombia: Cundinamarca, Tocancipá)
Centrolene cf. venezuelense(IAvH-Am-17401; ; Colombia: Cundinamarca, Tocancipá)
Centrolene hesperia (MHNSM 25802; Peru: Santa Cruz)
Centrolene muelleri (CORBIDI 14667; Peru: Puente Vilcaniza)
Centrolene huilense (QCAZ 37230; Ecuador: Napo,Yanayacu Biological Station)
Centrolene muelleri (PV; Peru: Chachapoyas)
Centrolene sp. (ZSFQ 4423; Ecuador: Morona Santiago, Gualaquiza)
Centrolene sp. (ZSFQ 4422; Ecuador: Morona Santiago, Gualaquiza)
Centrolene ericsmithi (MECN 11406; Ecuador: Azuay, La Enramada)
Centrolene lynchi (QCAZ 40191-92; Ecuador: Pichincha, Reserva Las Gralarias)
Centrolene sabini (MUSM 28018; Peru)
Centrolene marcoreyesi (CJ 11364;Ecuador: Zamora Chinchipe)
Centrolene marcoreyesi (CJ 12631; Ecuador: Zamora Chinchipe)
Centrolene marcoreyesi (CJ 11564;Ecuador: Zamora Chinchipe)
Centrolene marcoreyesi (MUTPL 271; Ecuador: Zamora Chinchipe, Abra de Zamora)
Centrolene marcoreyesi (ZSFQ 4418 (MRy 548); Ecuador: Zamora Chinchipe, Shucos)
Centrolene marcoreyesi (ZSFQ 4417 (MRy 547); Ecuador: Zamora Chinchipe, Shucos)
MUTPL 271
C. marcoreyesi sp. nov.
Tree scale: 0.01

Figure 2

Centrolene buckleyi sensu stricto in life, adult males, MZUTI 763 (A–B); ZSFQ 4420 (C–D) and DHMECN 13828 (E–F).

Photographs A–B by JMG; C–D–E–F by DBR.

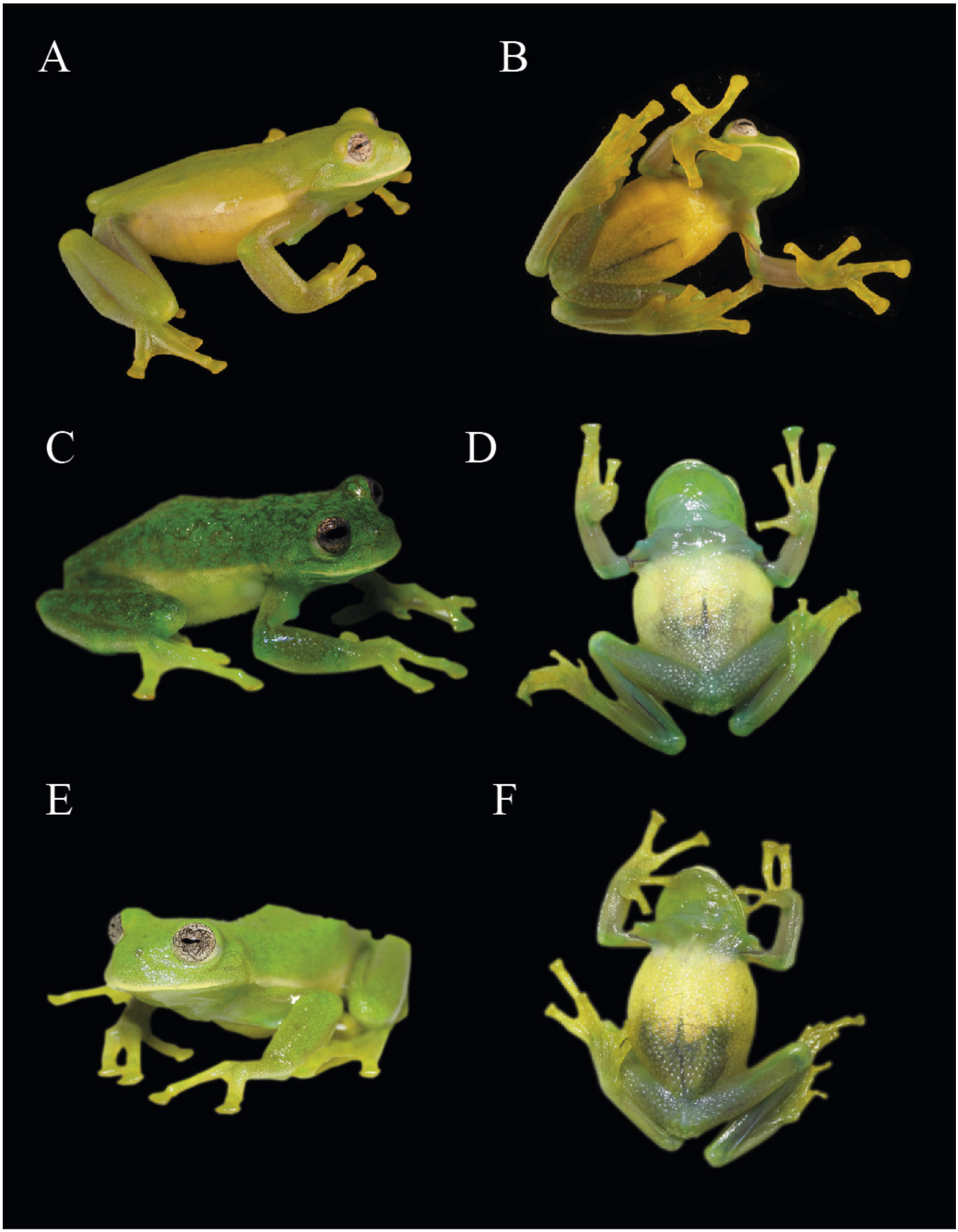
A
B
C
D
E
F

Figure 3

Comparison of species previously confused with *Centrolene buckleyi,* in ethanol.

From left to right: Head in dorsal view, head in lateral view, body in dorsal view, hand in ventral view, and foot in ventral view. (A)*Centrolene buckleyi* sensu stricto, male, MZUTI 0763; (B)*C. elisae*sp. nov., male holotype MZUTI-084; (C)*C. marcoreyesi* sp. nov. male holotype, ZSFQ 4418. Photographs by DFM (A, B, C).

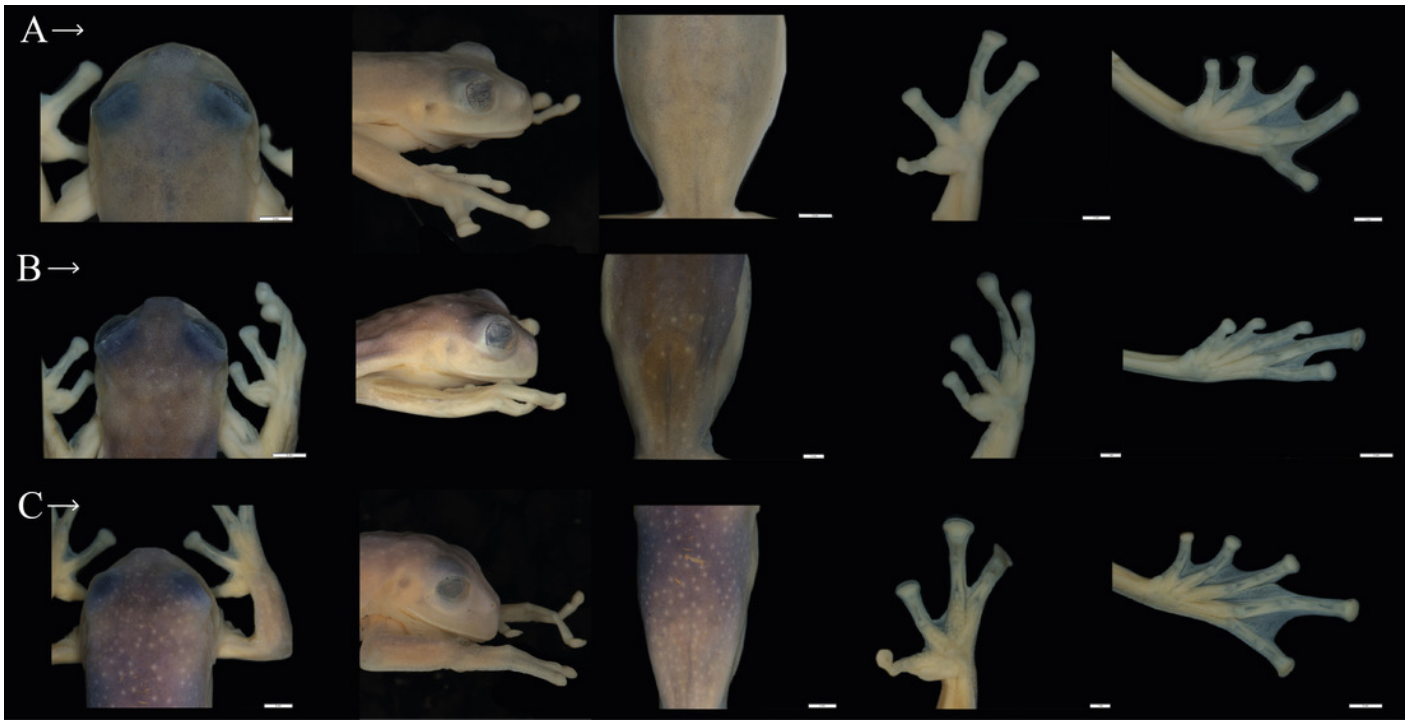

Figure 4

Principal component analysis from morphometric variables of *Centrolene buckleyi* sensu stricto, *C. elisae* sp. nov. and *C. marcoreyesi* sp. nov.

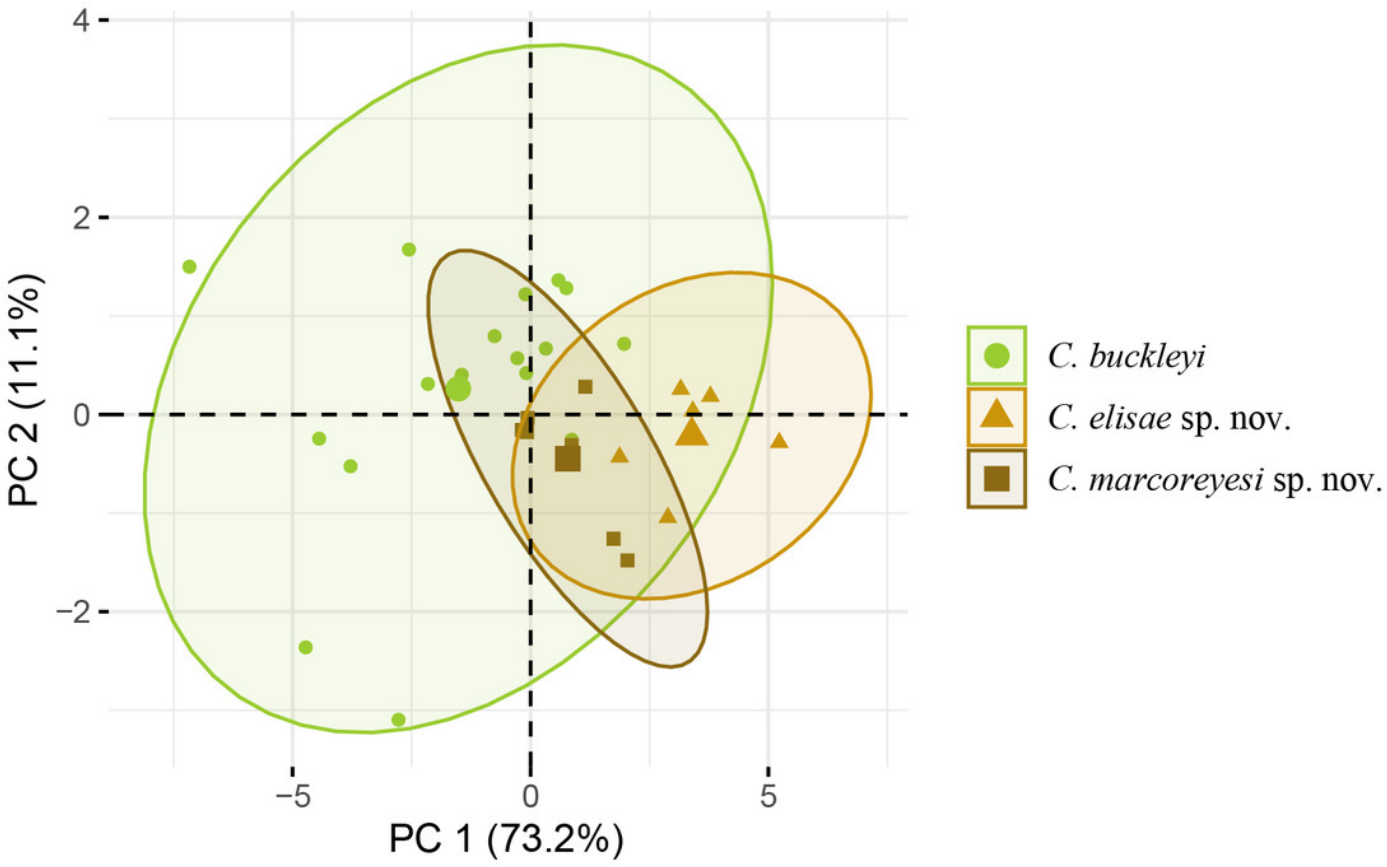

Figure 5

Estimates of evolutionary divergence over sequence pairs between *Centrolene* species.

Genetic p-distances for the 16S mtDNA gene (under the diagonal) and 12S mtDNA gene between *Centrolene* species.

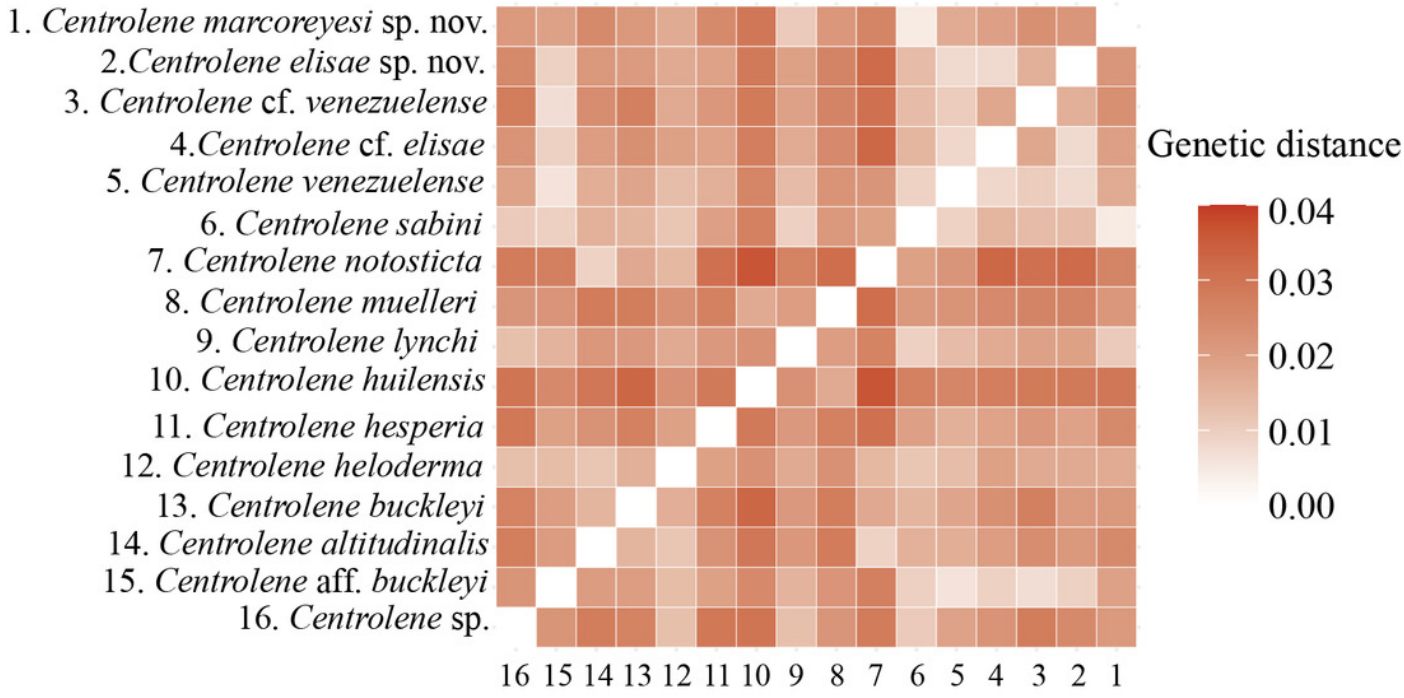

Figure 6

Cranial osteology of *Centrolene buckleyi* sensu stricto, adult male (MZUTI 0763).

(A) Dorsal view. (B) Ventral view. (C) Frontal view. (D) Lateral view. Labels: AP = alary process of premaxilla; AS = angulosplenial; COL = columella; D = dental; EXO = exoccipital; FP = frontoparietal; MMK = mentomeckelian bone; MX = maxilla; NA = nasal; NPL = neopalatine; OC = occipital condyle; PM = premaxilla; PO = prootic; PS = parasphenoid; PT = pterygoid; QJ = quadratojugal; SQ = squamosal; SE = sphenethmoid; SM = septomaxilla; V = vomer. Images prepared by DFM.

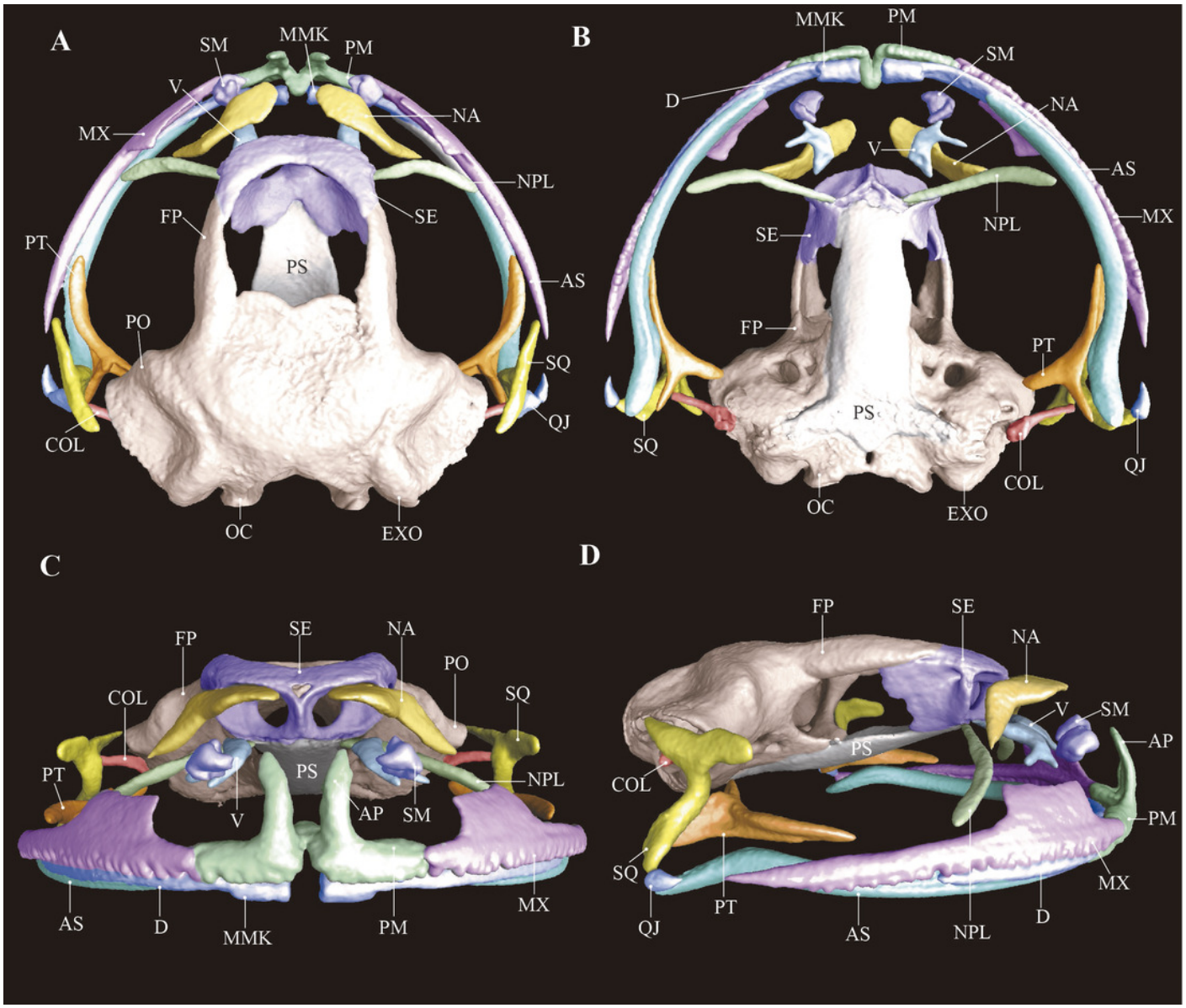
A
SM
MMK
PM
V
MX
NA
NPL
SE
FP
PT
PS
AS
PO
SQ
QJ
COL
OC
EXO
B
MMK
PM
SM
D
NA
V
AS
NPL
MX
SE
FP
PT
PS
SQ
COL
QJ
OC
EXO
C
FP
SE
NA
PO
SQ
COL
PT
PS
NPL
V
AP
SM
AS
D
MMK
PM
MX
D
FP
SE
NA
V
SM
AP
PS
COL
PM
SQ
MX
PT
D
QJ
AS
NPL

Figure 7

Post-cranial osteology of *Centrolene buckleyi* sensu stricto*,* adult male, MZUTI-0763.

(A) Forearm in ventral view. (B) Hindlimb in ventral view. (C) Pectoral girdle in ventral view. (D) Vertebral column and pelvic girdle in dorsal view. Labels: C3+C4+C5 = carpals; FB = fibulare; FM = femur; HM = humeral bone; HS = humeral spine; IE = intercalary element; MP = metacarpal process; MTC = metacarpales; MTT = metatarsals; PL = phalanges; PP = prepolex; RD = radiale; RU = radioulna; TIB = tibiale; T-SP = T-shaped phalange; T1, T2, T3 = tarsals; UL = ulnare; Y = Element Y; CC = coracoid; CLE = cleithrum; CV = clavicle; IC = ischium; IL = ilium; P–V = presacral vertebrae; PTP = posteromedial process; PUB = pubis; SC–SPS = scapula and suprascapular; S–D = sacral diapophysis; UR = urostyle. Images prepared by DFM.

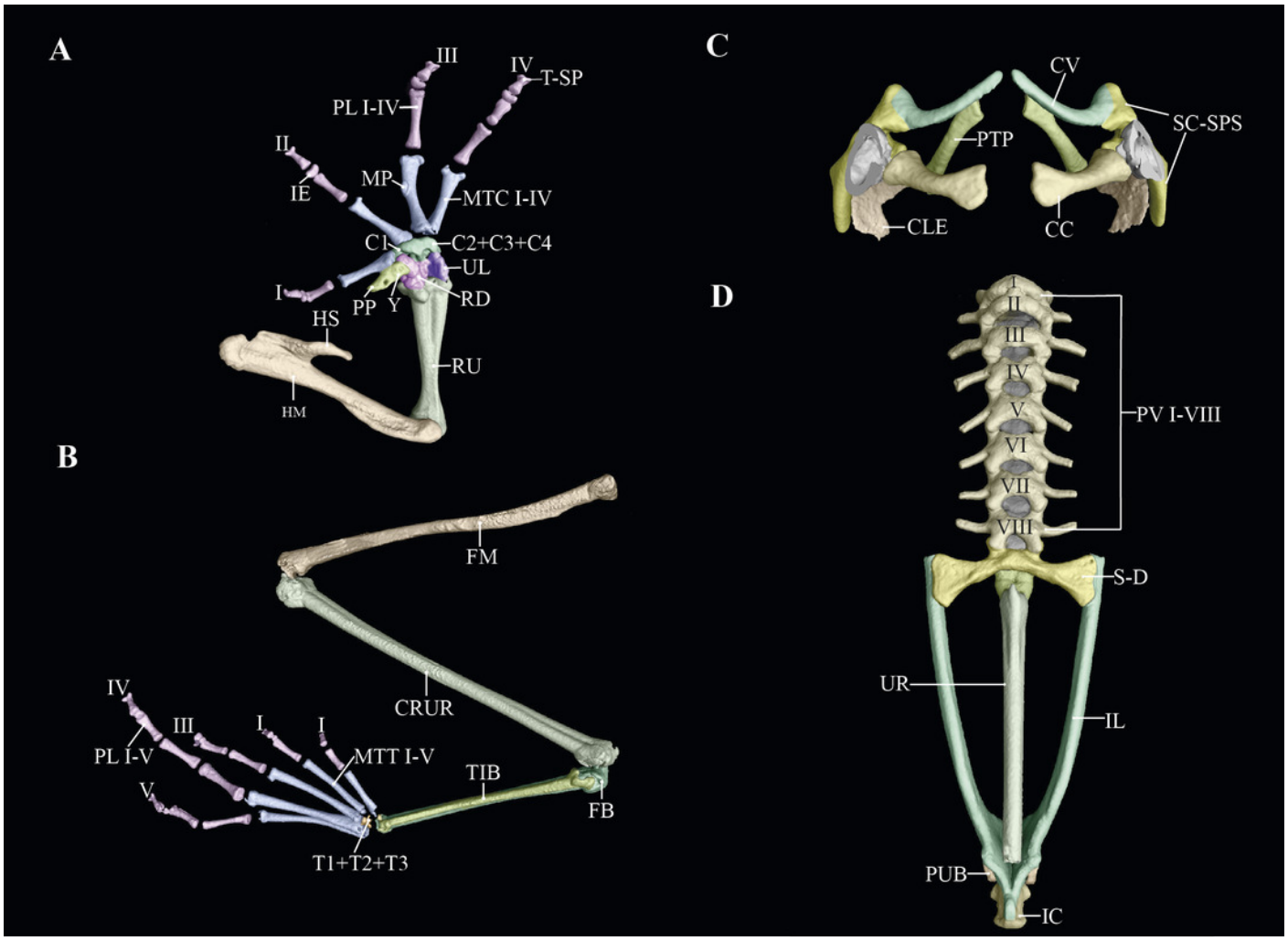
A
III
IV
T-SP
PL I-IV
II
IE
MP
MTC I-IV
C1
C2+C3+C4
UL
I
PP
Y
RD
HS
RU
HM
B
FM
CRUR
IV
III
I
I
PL I-V
MTT I-V
V
TIB
FB
T1+T2+T3
C
CV
SC-SPS
PTP
CLE
CC
D
I
II
III
IV
V
VI
VII
VIII
PV I-VIII
S-D
UR
IL
PUB
IC

Figure 8

Phylogeny and distribution of *Centrolene*, highlighting lineages closely related to *Centrolene buckleyi*, including the two new species described herein.

Collapsed clades and outgroups not shown (see Fig. 1 for complete tree). Circles = localities of specimens used for the phylogenetic analyses; Triangle = occurrence of *C. lemniscata,* a species morphologically similar to *C. buckleyi,* but for which there are no molecular sequences available. In the phylogenetic tree the highlighted species correspond to colors of circles on the map.

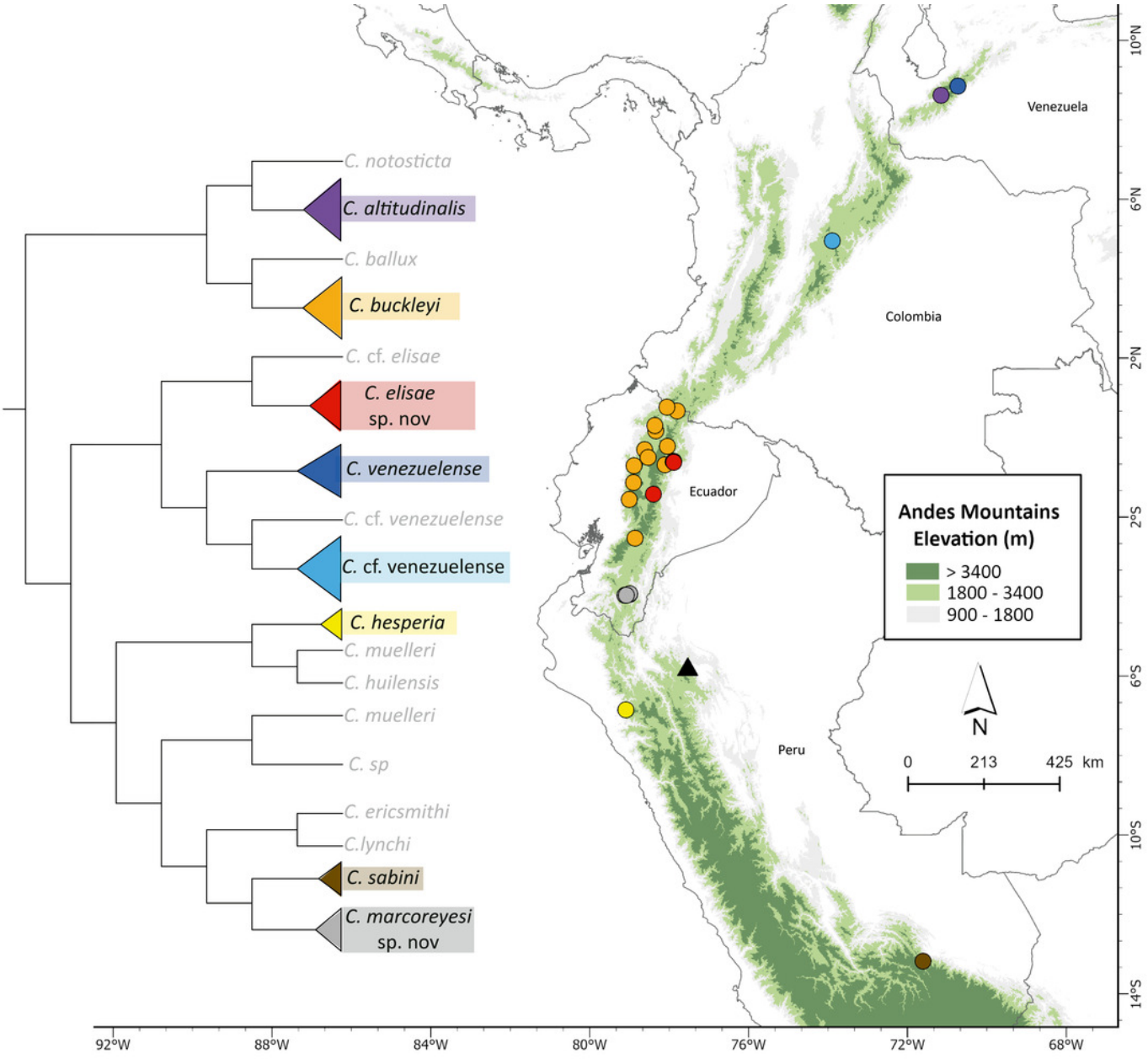
C. notosticta
C. altitudinalis
C. ballux
C. buckleyi
C. cf. elisae
C. elisae
sp. nov
C. venezuelense
C. cf. venezuelense
C. cf. venezuelense
C. hesperia
C. muelleri
C. huilensis
C. muelleri
C. sp
C. ericsmithi
C.lynchi
C. sabini
C. marcoreyesi
sp. nov
Venezuela
Colombia
Ecuador
Peru
Andes Mountains
Elevation (m)
> 3400
1800 - 3400
900 - 1800
N
0
213
425 km
10°N
6°N
2°N
2°S
6°S
10°S
14°S
92°W
88°W
84°W
80°W
76°W
72°W
68°W

Figure 9

Oscillograms and spectrograms of the advertisement calls of three species of *Centrolene* with a multipulsed "Tri" type structure.

(A) *Centrolene elisae* sp. nov. (ZSFQ 5369), (B) *Centrolene marcoreyesi* sp. nov. (MUTPL 271), and (C) *Centrolene buckleyi* sensu stricto (MZUTI 763)

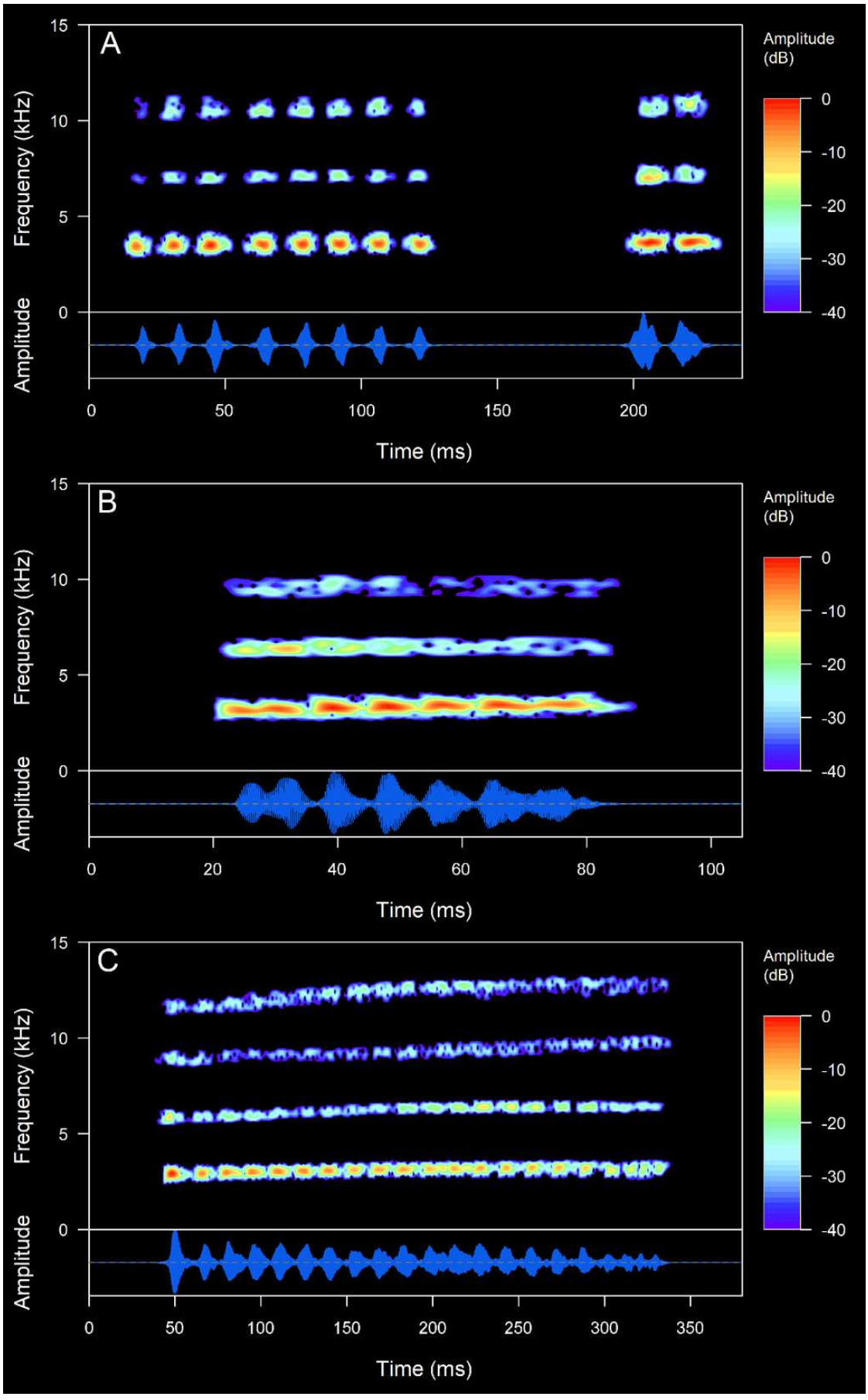
A
B
C
Frequency (kHz)
Amplitude
Time (ms)
Amplitude (dB)
0
-10
-20
-30
-40

Figure 10

Dorsal and ventral views of the preserved holotype of *Centrolene elisae* sp. nov., adult male, MZUTI 0084.

Photographs by JV.

Figure 11

Centrolene elisae sp. nov. in life (paratypes): adult female, ZSFQ 5367 (A–B); adult male, ZSFQ 5369 (C–D) and an adult male, ZSFQ 4428 (E–F).

Photographs A–D by MVY; (E, F) by DFM.

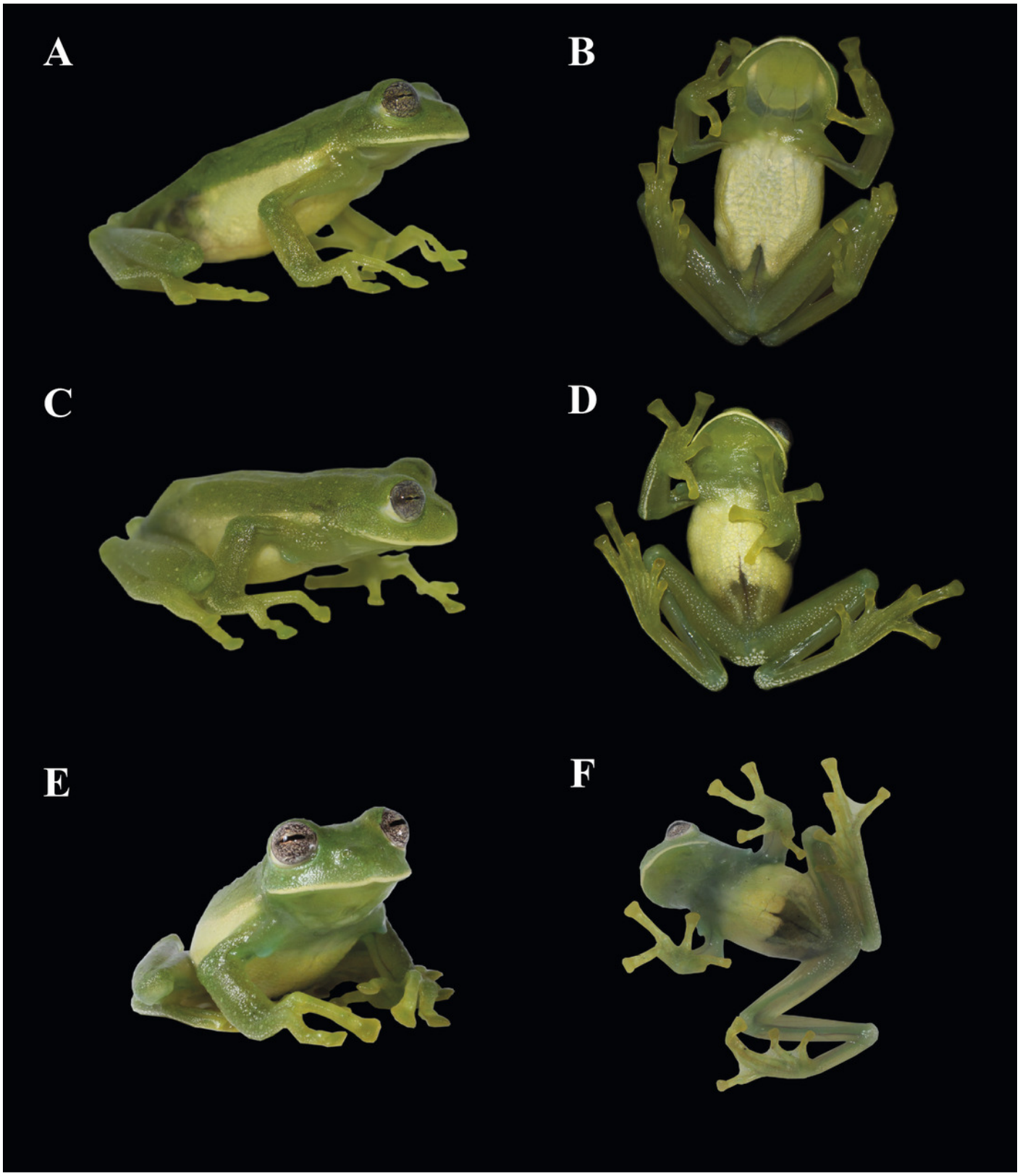
A
B
C
D
E
F

Figure 12

Centrolene elisae sp. nov., adult male, QCAZ 22388.

(A) Head in dorsal view. (B) Head in lateral view; note inclined snout. (C) Hand in ventral view; note absence of webbing between Fingers III and IV. (D) Foot in ventral view. Scale bar = 2 mm. Drawings by JMG (modified from Guayasamin et al. 2006).

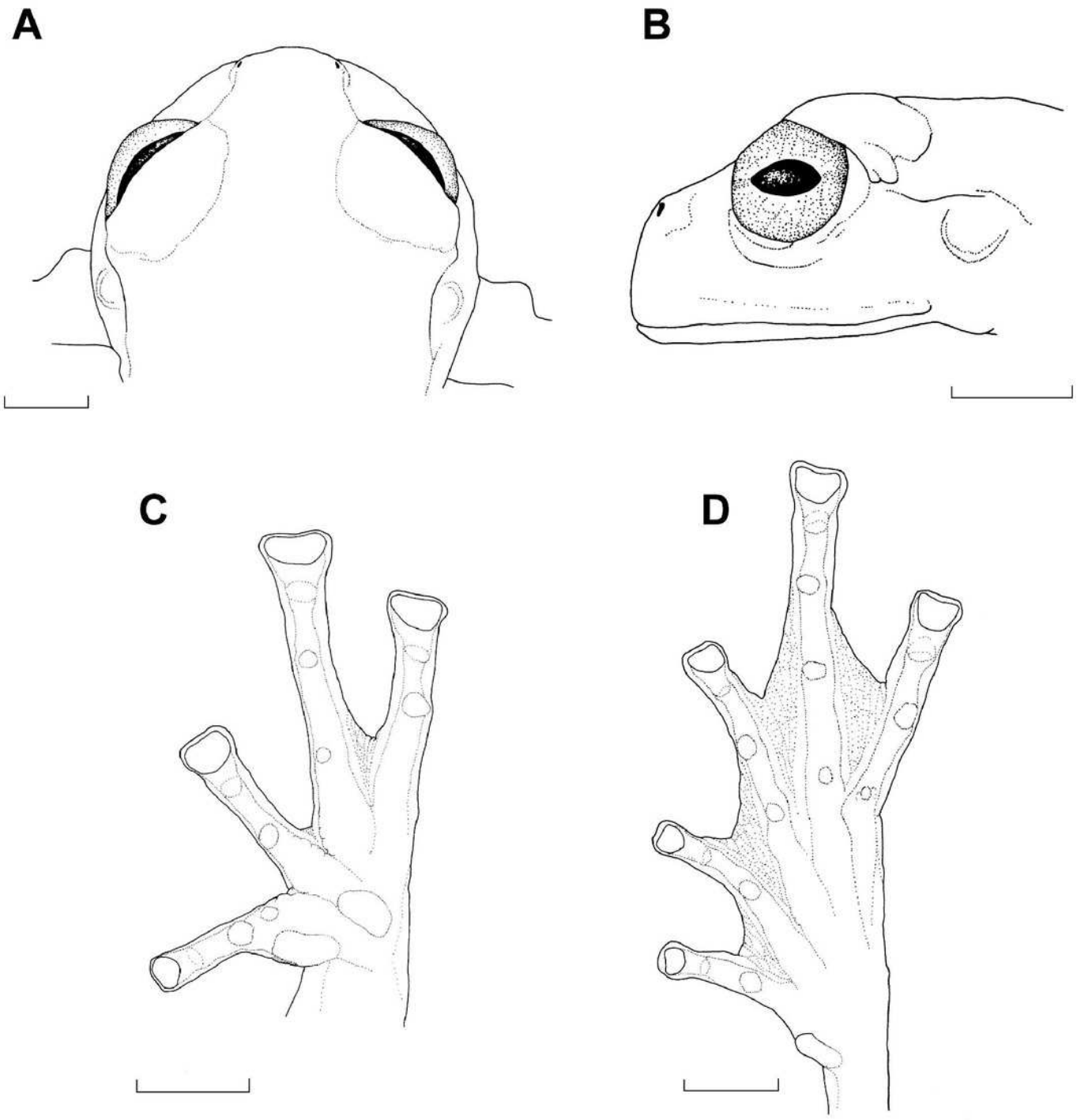
A
B
C
D

Figure 13

Cranial osteology of *Centrolene elisae* sp. nov., holotype, adult male, MZUTI 0084.

(A) Dorsal view. (B) Ventral view. (C) Frontal view. (D) Lateral view. Labels: AP = alary process of premaxilla; AS = angulosplenial; COL = columella; D = dental; EXO = exoccipital; FP = frontoparietal; MMK = mentomeckelian bone; MX = maxilla; NA = nasal; NPL = neopalatine; OC = occipital condyle; PM = premaxilla; PO = prootic; PS = parasphenoid; PT = pterygoid; QJ = quadratojugal; SQ = squamosal; SE = sphenethmoid; SM = septomaxilla; V = vomer. Images prepared by DFM.

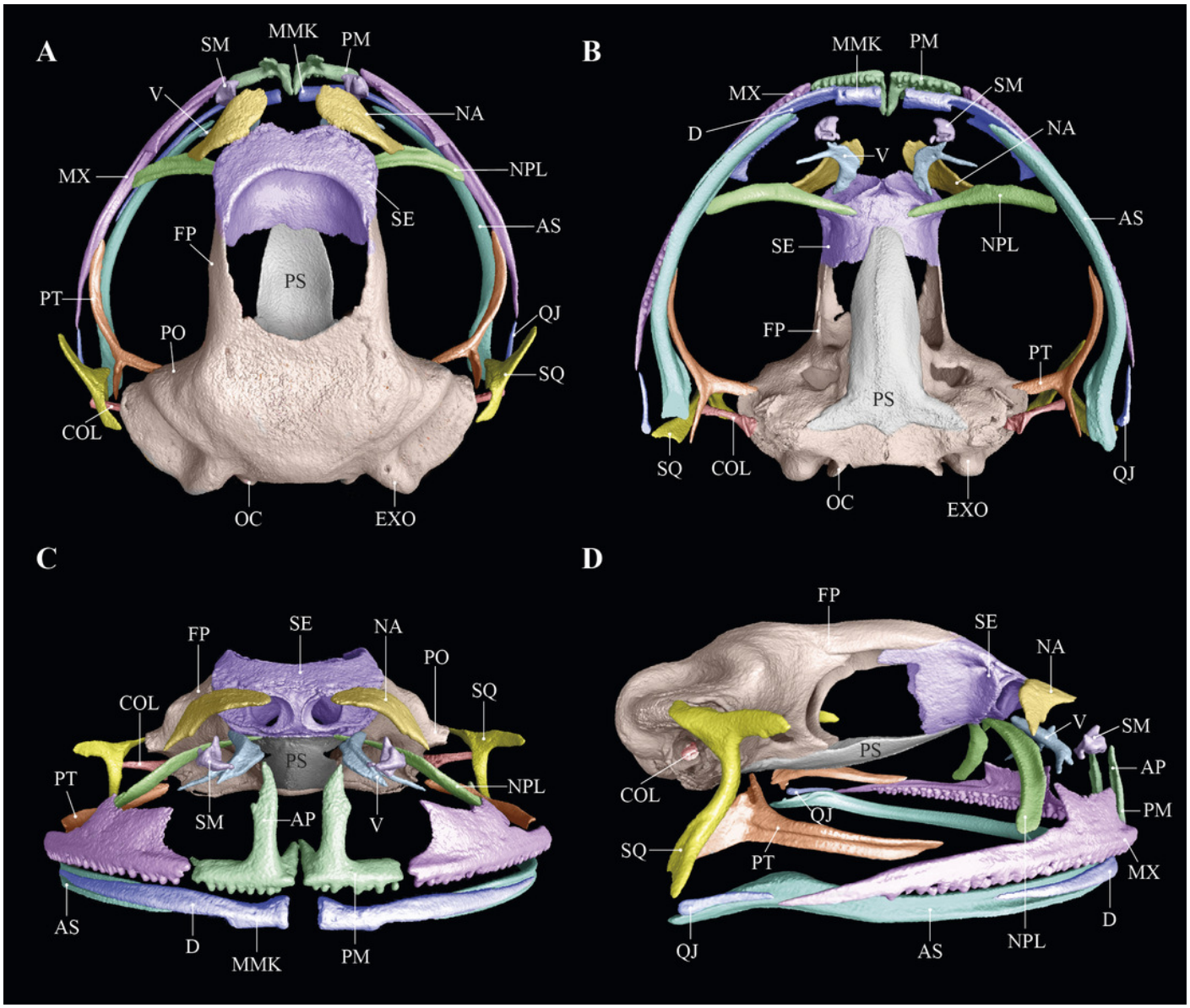
A
SM
MMK
PM
V
NA
MX
NPL
SE
AS
FP
PS
PT
PO
QJ
SQ
COL
OC
EXO
B
MMK
PM
MX
SM
D
NA
V
AS
SE
NPL
FP
PT
PS
SQ
COL
OC
EXO
QJ
C
FP
SE
NA
PO
SQ
COL
PS
PT
NPL
SM
AP
V
AS
D
MMK
PM
D
FP
SE
NA
V
SM
PS
AP
COL
PM
QJ
SQ
PT
MX
D
QJ
AS
NPL

Figure 14

Post-cranial osteology of *Centrolene elisae* sp. nov., adult male, holotype, MZUTI-0084.

(A) Forearm in ventral view. (B) Hindlimb in ventral view. (C) Pectoral girdle in ventral view. (D) Vertebral column and pelvic girdle in dorsal view. Labels: C3+C4+C5 = carpals; FB = fibulare; FM = femur; HM = humeral bone; HS = humeral spine; IE = intercalary element; MP = metacarpal process; MTC = metacarpales; MTT = metatarsals; PL = phalanges; PP = prepolex; RD = radiale; RU = radioulna; TIB = tibiale; T-SP = T-shaped phalange; T1, T2, T3 = tarsals; UL = ulnare; Y = Element Y; CC = coracoid; CLE = cleithrum; CV = clavicle; IC = ischium; IL = ilium; P–V = presacral vertebrae; PTP = posteromedial process; PUB = pubis; SC–SPS = scapula and suprascapular; S–D = sacral diapophyses; UR = urostyle. Images prepared by DFM.

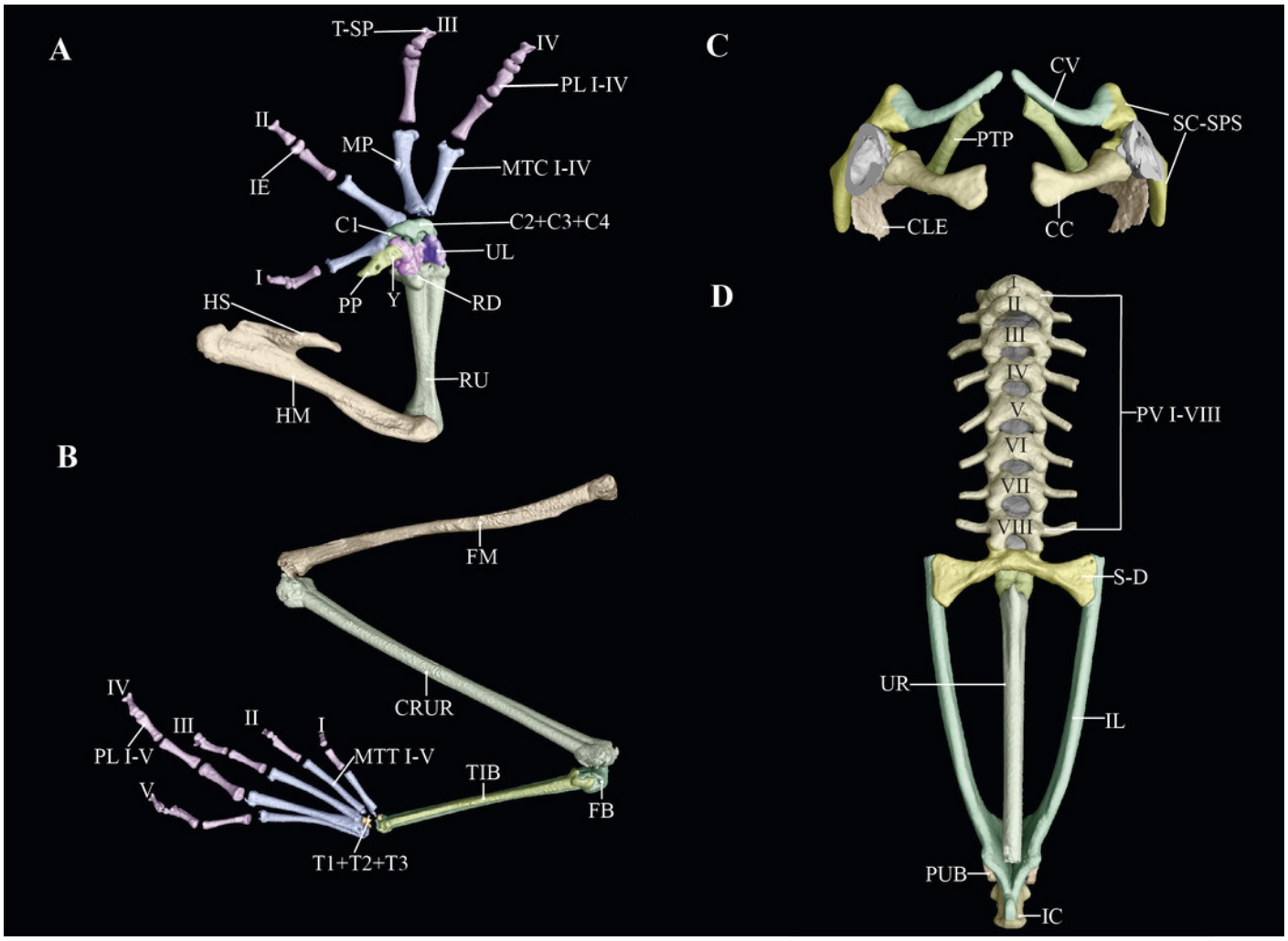
A
T-SP
III
IV
PL I-IV
II
MP
MTC I-IV
IE
C1
C2+C3+C4
UL
I
PP
Y
RD
HS
RU
HM
B
FM
CRUR
IV
III
II
I
PL I-V
MTT I-V
V
TIB
FB
T1+T2+T3
C
CV
SC-SPS
PTP
CLE
CC
D
I
II
III
IV
V
VI
VII
VIII
PV I-VIII
S-D
UR
IL
PUB
IC

Figure 15

Habitat of *Centrolene elisae* sp. nov. near the type locality.

(A-B) Yanayacu Biological Station, Napo province. (C-D) Chamanapamba reserve, Tungurahua province. Photographs by DFM. Photographs (A) by MVY, (B-D) by DFM, and (C) by JPRP.

Figure 16

Egg-clutches of *Centrolene elisae* sp. nov. from Chamanapamba reserve (ZSFQ 4428).

Photographs by DFM.

Figure 17

The new species described herein are named after Elisa Bonaccorso (left) and Marco Reyes-Puig (right).

We take great pleasure in recognizing their contributions to the understanding of neotropical biota (see the Etymology section). Photographs by JMG (A), and JPRP (B)

Figure 18

Dorsal and ventral views of the preserved holotype of *Centrolene marcoreyesi* sp. nov., adult male, ZSFQ 4418.

Photographs by AQR.

Figure 19

Centrolene marcoreyesi sp. nov. in life, paratype, MUTPL 271, adult male.

Photographs by PS.

Figure 20

Cranial osteology of *Centrolene marcoreyesi* sp. nov., holotype, adult male, ZSFQ 4418.

(A) Dorsal view. (B) Ventral view. (C) Frontal view. (D) Lateral view. Labels: AP = alary process of premaxilla; AS = angulosplenial; COL = columella; D = dental; EXO = exoccipital; FP = frontoparietal; MMK = mentomeckelian bone; MX = maxilla; NA = nasal; NPL = neopalatine; OC = occipital condyle; PM = premaxilla; PO = prootic; PS = parasphenoid; PT = pterygoid; QJ = quadratojugal; SQ = squamosal; SE = sphenethmoid; SM = septomaxilla; V = vomer. Images prepared by DFM.

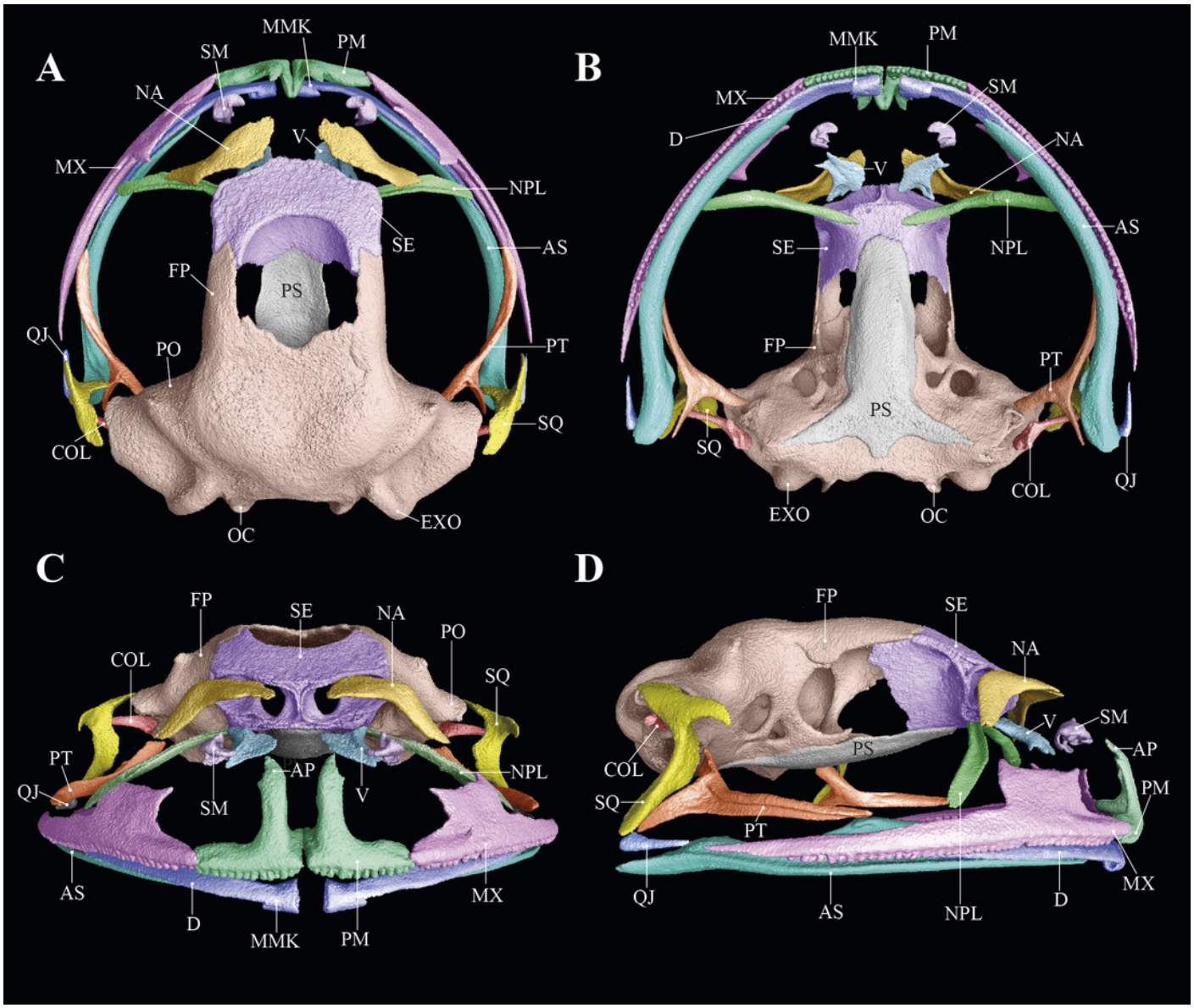
A
MMK
PM
SM
NA
V
MX
NPL
SE
AS
FP
PS
QJ
PO
PT
SQ
COL
EXO
OC
B
MMK
PM
MX
SM
D
NA
V
AS
SE
NPL
FP
PT
PS
SQ
COL
QJ
EXO
OC
C
FP
SE
NA
PO
COL
SQ
PT
AP
NPL
QJ
SM
V
AS
D
MX
MMK
PM
D
FP
SE
NA
V
SM
PS
AP
COL
PM
SQ
PT
QJ
AS
NPL
D
MX

Figure 21

Post-cranial osteology of *Centrolene marcoreyesi* sp. nov., adult male, holotype, ZSFQ 4418.

(A) Forearm in ventral view. (B) Hindlimb in ventral view. (C) Pectoral girdle in ventral view. (D) Vertebral column and pelvic girdle in dorsal view. Labels: C3+C4+C5 = carpals; FB = fibulare; FM = femur; HM = humeral bone; HS = humeral spine; IE = intercalary element; MP = metacarpal process; MTC = metacarpales; MTT = metatarsals; PL = phalanges; PP = prepolex; RD = radiale; RU = radioulna; TIB = tibiale; T-SP = T-shaped phalange; T1, T2, T3 = tarsals; UL = ulnare; Y = Element Y; CC = coracoid; CLE = cleithrum; CV = clavicle; IC = ischium; IL = ilium; P–V = presacral vertebrae; PTP = posteromedial process; PUB = pubis; SC–SPS = scapula and suprascapular; S–D = sacral diapophyses; UR = urostyle. Images prepared by DFM.

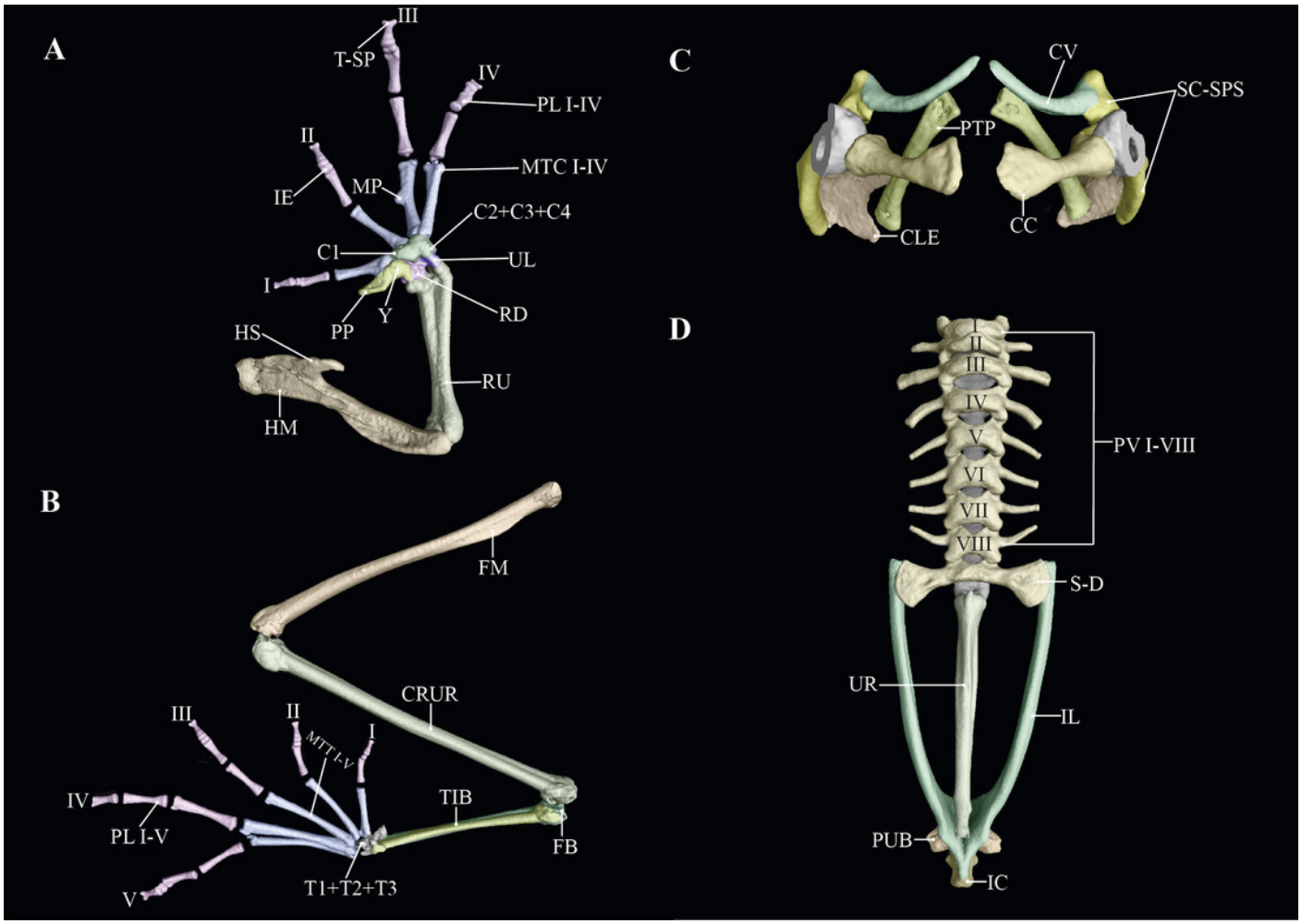
A
III
T-SP
IV
PL I-IV
II
MTC I-IV
IE
MP
C2+C3+C4
C1
UL
I
Y
RD
PP
HS
RU
HM
B
FM
CRUR
III
II
I
MTT I-V
IV
TIB
PL I-V
FB
V
T1+T2+T3
C
CV
SC-SPS
PTP
CLE
CC
D
I
II
III
IV
V
VI
VII
VIII
PV I-VIII
S-D
UR
IL
PUB
IC

Figure 22

Habitat of *Centrolene marcoreyesi* sp. nov. (MUTPL 271, 272) (A, B, C) Abra de Zamora, and (D) Guarumales (CJ 12631, CJ 11564, CJ 11364), Zamora Chinchipe province.

Photographs (A-B-C) by PS and (D) by JC.

Figure 23

Egg-clutches of *Centrolene marcoreyesi* sp. nov. from Guarumales (CJ 11564).

Photographs by JC.

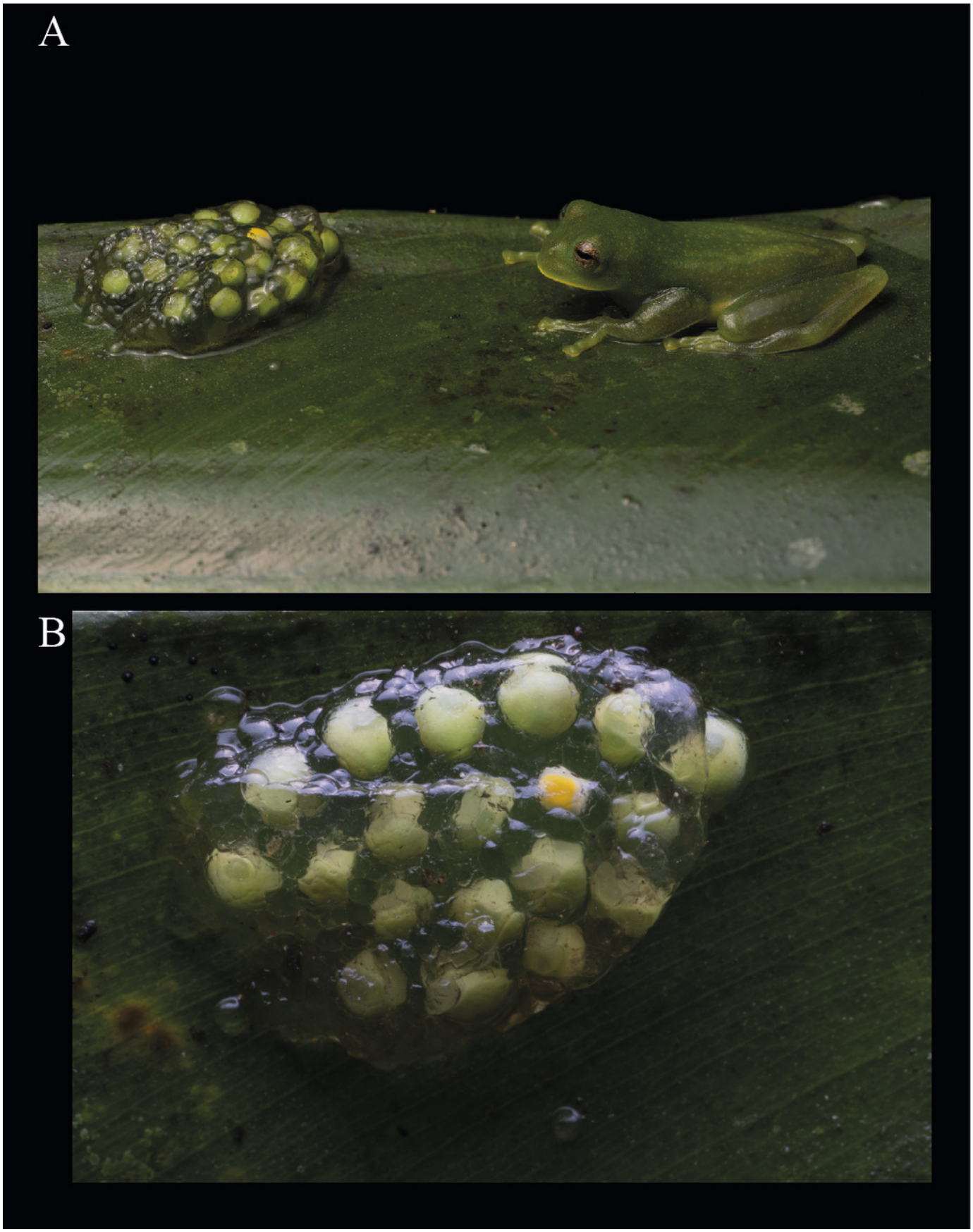
A
B

Figure 24

Ancestral ranges and rates of dispersal and vicariance under the DIVALIKE (Dispersal-vicariance) model inferred with the software BioGeoBEARS for *Centrolene* species.

Pie chart colors on the tips and nodes of the phylogeny correspond to the legend of the areas in the lower left. The new species are depicted in bold.